Lawrence Berkeley National Laboratory

Recent Work

Title

Hydrogeologic Characterization of Fractured Rock Formations: A Guide for Groundwater Remediators

Permalink

https://escholarship.org/uc/item/5m55w5gk

Author

Cohen, A.J.B.

Publication Date

1995-10-01

eScholarship.org Powered by the California Digital Library
University of California

10
4-9-96 OSD

BERKELEY LAB
ERNEST ORLANDO LAWRENCE
BERKELEY NATIONAL LABORATORY

LBL-38142/ UC-800

Hydrogeologic Characterization of Fractured Rock Formations: A Guide for Groundwater Remediators

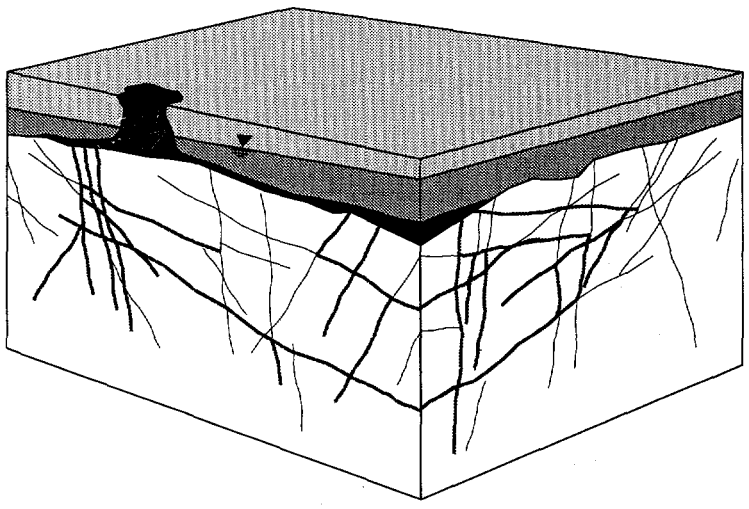

Andrew J. B. Cohen

Earth Sciences Division
Ernest Orlando Lawrence Berkeley National Laboratory
University of California
Berkeley, CA 94720

October 1995

MASTER

Prepared for the U. S. Department of Energy under Contract Number DE-AC03-76SF00098

DISTRIBUTION OF THIS DOCUMENT IS UNLIMITED

DISCLAIMER

This document was prepared as an account of work sponsored by the United States Government. While this document is believed to contain correct information, neither the United States Government nor any agency thereof, nor The Regents of the University of California, nor any of their employees, makes any warranty, express or implied, or assumes any legal responsibility for the accuracy, completeness, or usefulness of any information, apparatus, product, or process disclosed, or represents that its use would not infringe privately owned rights. Reference herein to any specific commercial product, process, or service by its trade name, trademark, manufacturer, or otherwise, does not necessarily constitute or imply its endorsement, recommendation, or favoring by the United States Government or any agency thereof, or The Regents of the University of California. The views and opinions of authors expressed herein do not necessarily state or reflect those of the United States Government or any agency thereof, or The Regents of the University of California.

Available to DOE and DOE Contractors
from the Office of Scientific and Technical Information
P.O. Box 62, Oak Ridge, TN 37831
Prices available from (615) 576-8401

Available to the public from the
National Technical Information Service
U.S. Department of Commerce
5285 Port Royal Road, Springfield, VA 22161

Ernest Orlando Lawrence Berkeley National Laboratory
is an equal opportunity employer.

LBL-38142
UC-800

HYDROGEOLOGIC CHARACTERIZATION OF FRACTURED ROCK FORMATIONS: A GUIDE FOR GROUNDWATER REMEDIATORS

Andrew J. B. Cohen

Earth Sciences Division
Ernest Orlando Lawrence Berkeley National Laboratory
University of California
Berkeley, CA 94720

October 1995

MASTER

The U. S. Environmental Protection Agency through its Office of Research and Development partially funded and collaborated in the research described here under Interagency Agreement No. DW-89935185, through U. S. Department of Energy Contract No. DE-AC03-76SF00098. This report also serves as the EPA Research Report for this work. It has been subjected to EPA agency review and approved for publication. This work was also supported by the Director, Office of Civilian Radioactive Waste Management, Office of External Relations, and was administered by the Nevada Operations Office of the U. S. Department of Energy under Contract No. DE-AC03-76SF00098.

DISTRIBUTION OF THIS DOCUMENT IS UNLIMITED

notice: The name Lawrence Berkeley National Laboratory, and the acronyms LBL and LBNL used in this report refer to the Ernest Orlando Lawrence Berkeley National Laboratory, Berkeley, CA.

ABSTRACT

A field site was developed in the foothills of the Sierra Nevada, California to develop and test a multi-disciplinary approach to the characterization of ground water flow and transport in fractured rocks. Nine boreholes were drilled into the granitic bedrock, and a wide variety of new and traditional subsurface characterization tools were implemented. The hydrogeologic structure and properties of the field site were deduced by integrating results from the various geologic, geophysical, hydrologic, and other investigative methods. The findings of this work are synthesized into this report, which is structured in a guidebook format. The applications of the new and traditional technologies, suggestions on how best to use, integrate, and analyze field data, and comparisons of the shortcoming and benefits of the different methods are presented.

Abstract iii
Acknowledgments ix

1 INTRODUCTION 1
1.1 What is Needed? 1
1.2 Intent and Organization of this Report 2

2 DIFFICULTIES ASSOCIATED WITH REMEDIATING FRACTURED ROCK AQUIFERS 4
2.1 Nature of Contaminant Fate in Fractured Media 4
2.2 Site Characterization 5
2.2.1 Plume Identification 6
2.2.2 Hydrogeologic Characterization 6
2.3 Monitoring for Remediation Performance 7
2.4 Summary 9

3 THE RAYMOND FIELD SITE 10
3.1 Site Description 10
3.1.1 General 10
3.1.2 Boreholes 10
3.1.3 Local Geologic Setting 13
3.2 Hydrogeology of the Raymond Field Site 13
3.2.1 Conceptual Model 14

4 SURFACE FRACTURE CHARACTERIZATION 16
4.1 Introduction 16
4.1.1 Approaches to Fracture Characterization 16
4.2 Regional Fracture Characterization 17
4.2.1 Regional Fracture Sets and Geologic History 17
4.2.2 Lineament Analysis 18
4.3 Site-Scale Fracture Characterization 18
4.3.1 Observations and Measurements 18
4.3.2 Visualization of Fracture Data 21
4.4 Surface Fracture Characterization at Raymond 23
4.4.1 Regional Fracture Sets and Geologic History 23
4.4.2 Site-Scale Fracture Characteristics 26
4.4.2.1 General Observations 26
4.4.2.2 Fracture Measurements 26
4.4.2.3 Results 27
4.4.2.4 Use of Surface Characterization Results in General Investigation 29
4.5 Summary 29

5 WELL DRILLING 30
5.1 Drilling Method 30
5.1.1 Air Drilling 30
5.1.2 Coring 31
5.2 Well Location 32
5.3 Drilling at Raymond 32
5.4 Comparison of Driller's Log with Geophysical Logs 33
5.5 Summary 35
5.5.1 General 35
5.5.2 Recommendations 35

6 PUMPING TESTS 36
6.1 Some Problems in the Analysis of Pumping Tests 36
6.1.1 Conceptual Considerations 36
6.1.2 Transient Response in a Fractured Aquifer 37
6.1.3 Parameters Not Representative of Region of Interest 40
6.1.4 Well Bore Storage 42
6.1.5 Apparent Anisotropy 43
6.2 Potential Negative Effects of Pumping Tests 45
6.2.1 Induced contaminant spreading to previously uncontaminated areas 45
6.3 Summary 47
6.3.1 General 47
6.3.2 Recommendations 48

7 CONVENTIONAL GEOPHYSICAL LOGGING 49

8 DETECTION AND MEASUREMENT OF SUBSURFACE FRACTURES 50
8.1 Acoustic Televiewer (ATV) Logging 50
8.1.1 Tool Description 50
8.1.2 Fracture Detection and Measurement 52
8.1.3 Extraneous Effects 53
8.1.4 Analysis of ATV Logs from Raymond 56
8.1.4.1 Identification of Fracture Sets 58
8.1.4.2 Fracture Spacing Distribution 60
8.2 Television Logging 62
8.2.1 Tool Description 62
8.2.2 Problematic Effects 62
8.2.3 Measurements and Results at Raymond 63
8.2.3.1 Fracture Observations 64
8.3 Digital Borehole Scanner 65
8.3.1 Tool Description 65
8.3.2 Fracture Detection and Measurement 65
8.3.3 Measurements and Results at Raymond 67
8.4 Borehole Core Analysis 69
8.5 Comparison of Techniques 69
8.6 Summary 73
8.6.1 General 73
8.6.2 Recommendations 73

9 BOREHOLE FLOW LOGGING 75
9.1 Impeller Flowmeter 76
9.1.1 Tool Description 76
9.1.2 Flow Measurements 78
9.1.3 Data Analysis 79
9.1.4 Validity of Analysis and Extraneous Effects 82
9.1.5 Measurements and Analysis of Results at Raymond 83
9.2 Thermal-Pulse Flowmeter 85
9.2.1 Tool description 85
9.2.2 Flow measurements 87
9.2.3 Extraneous Effects 88
9.2.4 Measurements and Analysis of Results at Raymond 89
9.3 Fluid Conductivity Logging 94
9.3.1 Tool Description 94
9.3.2 Extraneous Effects and Detection Limits 95
9.3.3 Measurements and Results at Raymond 98

9 BOREHOLE FLOW LOGGING - continued
9.4 Straddle Packer Injection Tests 101
9.4.1 Test Configuration and Methodology 101
9.4.2 Data Analysis 103
9.4.3 Problematic Effects 104
9.4.4 Measurements and Analysis of Results at Raymond 106
9.5 Comparison of Techniques 108
9.6 Summary 110
9.6.1 General 110
9.6.2 Recommendations 111

10 INTEGRATION OF GEOPHYSICAL LOGS 113
10.1 Identification of Transmissive Fractures 113
10.1.1 Heat-Pulse Flowmeter and Standard Geophysical Logs 113
10.1.2 Fluid Electrical Conductivity and Standard Geophysical Logs 118
10.1.3 Comparison of Results 118
10.2 Determination of General Hydrogeologic Structure 123
10.3 Summary 127
10.3.1 General 127

11 SEISMIC IMAGING TECHNIQUES 128
11.1 Cross-Borehole Seismic Tomography at Raymond 128
11.1.1 Methodology 128
11.1.2 Results and Conclusion 130

12 COMPUTER VISUALIZATION 132
12.1 Application to the Raymond Site Characterization 132
12.2 Conclusions 134

13 A GENERAL STRATEGY FOR HYDROGEOLOGIC CHARACTERIZATION OF FRACTURED FORMATIONS 136

References 140

ACKNOWLEDGMENTS:

Research at the Raymond Field Site was conducted by many individuals. This report and the work described in it would not have been possible without the efforts of each participant.

Kenzi Karasaki of E. O. Lawrence Berkeley National Laboratory was principal investigator of Raymond Field Site research. Barry Freifeld and Ray Solbau were instrumental in developing new hydrologic testing equipment, and conducted numerous hydrologic tests. Don Lippert, John Clyde, and Paul Cook were also critical to the site development and in conducting field tests. Peter Zawislanski conducted surface geologic investigations and constructed driller's logs. Ramsey Haught, Steve Flexser, and Ken Williams conducted cross-hole seismic tests, and Don Vasco and John Peterson analyzed test data. Bhaskar Thapa conducted digital borehole scanning. Pascual Benito helped construct report figures.

M. J. Umari and Fred Paillet and others of U. S. Geological Survey, Denver collaborated in portions of borehole geophysical studies.

Chris Doughty, Ken Grossenbacher, Chin-Fu Tsang, Preston Holland, and others of E. O. Lawrence Berkeley National Laboratory, and Douglas Heath of EPA, Boston provided critical reviews.

Funding for this work was provided by the Environmental Protection Agency under Interagency Agreement No. DW-89935185, through U. S. DOE Contract No. DE AC03-76SF00098, and by the U. S. Department of Energy, Contract No. DEAC03-76SF00098 for the Director, Office of Civilian Radioactive Waste Management, Office of External Relations, and was administered by the Nevada Operations Office, U. S. Department of Energy. Thanks are due to Steve Kraemer, the EPA project officer, and to Bob Levich of U. S. DOE for their oversight and support.

1 INTRODUCTION

This report describes tools and methodologies that can be used to characterize formation properties of saturated, fractured rock aquifers. The application of different new and traditional technologies, suggestions on how best to use, integrate, and analyze field data, and descriptions of the shortcoming and benefits of different methods is presented. This report is unique in that all of methods were applied at a single field site, which provides that best rational for making comparisons of the methods and drawing our conclusions. The report should serve as a useful guide for subsurface remediators of fractured formations.

1.1 What is Needed?

The number of contaminated fractured formations wherein contaminants are known or believed to exist is difficult to assess because site data is very scattered. A 1989 study by the EPA provides what is perhaps the most comprehensive listing of contaminated site characteristics. They surveyed 112 sites throughout the U. S. that are currently undergoing remediation and found that 15% are comprised of fractured rock formations to various degrees. This figure is a conservative estimate of the total percentage of contaminated fractured rock formations given that unconsolidated porous formations have traditionally been more targeted for cleanup. Regardless, this percentage is still very significant considering that the number of contaminated ground water sites is estimated to be between 300,000 and 400,000 (Committee on Ground Water Cleanup Alternatives, 1994). At many sites, no attempt has yet been made to investigate the fractured portions of aquifers where contaminants are known or suspected to reside (EPA, 1989).

Fundamental to every remediation effort is an understanding of the distribution of contaminants and fluid flow properties within the formation. The information gained from characterization is the basis upon which almost every decision regarding remedial action is taken, for example, the positioning of extraction and injection wells, determination of extraction rates, and maintenance of an inward hydraulic gradient at the plume boundary. The conceptual model of the site and hence the choice of a numerical model and its input parameters all stem from the information gathered and analyzed from site characterization.

Site characterization is difficult for every aquifer, but the extreme heterogeneity of fractured aquifers presents an even greater challenge. The complexity of fractured formations and hence the difficulty of characterizing them is the primary reason why the fractured portions of contaminated aquifers have not been investigated and why, at sites where remediation of fractured formations has begun, the behavior of the system is often very different than calculated. As a result, much money and effort is wasted. For a fractured system, an ideal characterization would include 1) a quantitative description of the extent, distribution, and mass of the contaminant(s); 2) the location, extent, degree of interconnectivity, and orientation of conducting fractures; 3) the distribution of the hydraulic conductivities of the fractures and rock matrix, the diffusion and adsorption characteristics of the rock matrix; and 4) the three-dimensional hydraulic head distribution within the domain of interest. Obviously, this is unrealistic. Given the degree of complexity, what we hope to extract is an understanding of those features that largely control subsurface flow, as well some quantitative evaluation of those features. As illustrated in Chapter 2, the hydrogeologic characterization is the most important component to the success of remediating fractured aquifers. A successful characterization requires a stepwise approach that integrates geologic, geophysical, and hydrologic data.

In summary, there is a clear need to address the issue of fractured rock characterization from a remediation perspective. Specifically, remediators must be made aware of new and existing site investigative tools and analysis methods and how they can best utilize and integrate different methods in order to determine the general hydrogeologic structure of fractured rock aquifers. Furthermore, they must understand the practical but essential considerations which need to be made in the characterization process.

1.2 Intent and Organization of this Report

The purpose of this report is to inform remediators about the use of a variety of hydrological and geophysical characterization tools and methodologies that can be used independently and together in an effort to characterize a fractured formation. The suggestions presented are based on conclusions drawn from a characterization effort of a saturated, fractured granitic rock aquifer in the foothills of the Sierra Nevada, California. Here, we implemented a wide variety of characterization techniques. The numerous field experiments and analyses of the different data collected has provided many insights that should greatly benefit the remediation community.

Emphasis is placed on the use of both new and traditional technologies. Descriptions of the tools and how they were used, analysis and integration of data, as well as the particular advantages and shortcoming of each method are presented. Many new tools and methods are described, such as cross-hole hydrologic imaging and digital borehole scanning. Findings obtained at other remedial sites where fractured materials are present are also referenced. Determination of subsurface flow properties is the emphasis rather than on contaminant sampling and plume delineation. However, issues regarding the effect of incorrect characterization of flow properties on contaminant behavior are addressed.

Our findings are not necessarily limited to fractured crystalline rock formations. Many may apply to fractured subsurface materials in general. No matter what remediation technology is chosen, a sufficient characterization is still a critical necessity. In this sense, this work includes information valuable to many workers in the field of subsurface flow in fractured geologic materials.

The scope of this report should be evident by viewing the table of contents. The format of the report is as follows: Firstly, an overview of the problems associated with remediating fractured aquifers is presented in order to highlight the essential difficulties. Case histories are referenced for examples. Secondly, a relatively brief overview of the characterization effort at the Raymond Field Site is presented. The tools and methods used and the model of the subsurface that resulted is described. Afterwards, each tool and method is discussed in detail. Descriptions of the tools and how they are used, the strengths and shortcoming of each, how they compare with one another, as well as how best to analyze and integrate the data collected is discussed. The stepwise approach to characterization is reflected by the order in which the methods are presented.

2 DIFFICULTIES ASSOCIATED WITH REMEDIATING FRACTURED ROCK AQUIFERS

2.1 Nature of Contaminant Fate in Fractured Media

The word fracture is used here as a collective term for several types of rock discontinuities, including joints, fissures, shear zones, and faults. The major pathways for groundwater flow and contaminant migration in crystalline rocks are through fractures. The aperture, orientation, degree to which individual fractures are mineral-filled, and the degree of fracture interconnection and spacing are the most significant factors affecting the flow characteristics within these formations. Therefore, these variables need to be considered when assessing where contaminants may reside and how they may migrate under natural or induced conditions. Additionally, because fracture apertures are stress-dependent (Gale, 1992), the extent to which contaminants can migrate may tend to be a function of depth. Since the transmissivity of a fracture is approximately proportional to its aperture cubed, the flow regime has the potential of being poorly understood even if only a few relatively large fractures are not detected. This fact emphasizes the importance of identifying those features that largely control flow. Given the degree of complexity in fractured formations, determining the general hydrologic structure of the formation can be an achievement in itself.

Because the rock matrix in crystalline rocks such as granite and gneiss have very small intergranular porosity and are generally impermeable with respect to fluids, contaminants mainly flow within the fracture network. As a result, most migrate faster and are more oddly distributed than contaminants in porous systems under comparable seepage gradients (Fortin, 1988; see, for example, McGlew and Thomas, 1984). Although the hydraulic conductivity of the rock matrix is very small, the fact that contaminants are present in a formation for considerable times before remediation practices are initiated results in the diffusion of dissolved contaminants from the fractures into the rock matrix. Adsorption within the matrix will then act to store these solutes (Mackey and Cherry, 1989).

In fractured porous media, such as fractured sandstone, the potential for storage of contaminants within the matrix is much greater than crystalline rocks. Under natural conditions the groundwater flow may be mainly through the matrix, and the fractures usually have a much smaller effect on controlling the overall transmission of

contaminants. Rather, it is the hydraulic conductivity of the matrix and the chemical retardation, adsorption, and matrix diffusion characteristics of the contaminants that control their migration and storage characteristics. The effect that these parameters have on a remediation effort is addressed by Keely (1989). Conversely, when wells are pumped during a remediation effort, the fractures may act as the primary conduits of flow, and the matrix as the primary source of contaminants. Hence, the flow characteristics within and between the fracture network and rock matrix need to be assessed.

The nature of contaminants also largely determines their migration characteristics. Contaminants exhibit different values of the characteristics described above, as well as different miscibilities and densities as compared with water. Common contaminants are industrial solvents and aromatic hydrocarbons (e.g., chlorinated solvents and creosote). These nonaqueous phase liquids (NAPL's) can be expected to migrate in unpredictable ways. Several studies have indicated that organic compounds readily migrate to the bottom of the overburden regardless of their specific gravity or solubility (Di Nitto et al., 1982). Compounds whose densities are greater than the groundwater will sink and eventually get caught in dead-end fractures and in fractures oriented perpendicular to the hydraulic gradient, as well as contaminate lower portions of the fracture network. Additionally, they have the potential of migrating in directions very different from that of the groundwater depending upon the fracture network orientation. At remediation sites in Rhode Island and Massachusetts investigators concluded that the major contaminant flow direction in the bedrock aquifer was controlled by the orientation of fractures and the slope of the bedrock surface, for example (Di Nitto et al., 1982). These behaviors, coupled with the diffusion of dissolved portions of the contaminants into the matrix will severely hamper the effectiveness of a remediation effort because little or no water will flush through the dead-end fractures or through the impervious rock matrix, both of which are likely to retain significant amounts of contaminants (Mackay and Cherry, 1989). Conditions such as these occurred at a pump-and-treat remediation effort in Quebec, Canada, for example (Martel, 1988).

2.2 Site Characterization

Site characterization is a process whereby the distribution of geologic materials and contaminants, as well as some quantitative determination of the flow properties of the formation, are determined. As described earlier, a sufficient characterization of a fractured formation, if possible, is extremely difficult, and there is no one particular

strategy. Given the degree of complexity, what we hope to extract is an understanding of those features that largely control subsurface flow, as well some quantitative evaluation of those features. We must use a stepwise approach and integrate geologic and hydrologic data.

2.2.1 Plume Identification

In order to establish the presence, concentration, and distribution of the contaminant plume or plumes, soil, surface water, and groundwater samples are collected and analyzed. A plume boundary is often defined by a lower limit concentration, but the nature of the fracture network makes it difficult to define this boundary. Contaminants may be present in areas thought to be beyond the plume boundaries because of the presence of undetected, conducting fractures. Monitoring wells are often screened at depths that are too shallow or in unsuitable locations to detect contaminants within lower portions of an aquifer. Additionally, the installation of wells used to measure the hydraulic head distribution and monitor contaminant levels may create vertical pathways along which contaminants can migrate (see Chpt 6.2), and conducting fractures may extend well below the lowest levels of wells. Even though shallow screening seems appropriate for monitoring contaminants that are less dense than the groundwater (e.g., volatile organic compounds [VOC's]), experience has shown that these contaminants are often forced lower into the aquifer as the contaminants migrate from their source (Freeze and Cheery, 1979). Therefore, shallow wells installed a distance from the source may not intersect a contaminant plume (Di Nitto et al., 1982).

Information needed in order to make a preliminary estimate of how long a remediation effort will take includes the mass of contaminants in the subsurface. However, because the outer boundaries of plumes and the formation porosity are very difficult to determine, and because concentrations vary within and between plumes, it would be difficult or impossible to determine the contaminant load in fractured systems (Mackay and Cherry, 1989).

2.2.2 Hydrogeologic Characterization

In general, the difficulty of determining the spatial distribution of flow properties in fractured formations results from their extreme degree of heterogeneity. Only one transmissive fracture may intersect a borehole along a 10 meter section, and highly transmissive fractures may simply go undetected because wells do not intersect them, for example. On the scale that is of interest, i.e., the contaminated site, there may be many

fractures, but only several dominate the flow behavior. Hence, it is necessary to identify this dominant scale structure. The tools and methods needed to characterize these features are described in this report, and they are generally more sophisticated and expensive than tools commonly used for most hydrogeological characterization efforts today. This is a simple reality, and perhaps a very practical reason why fractured rock characterization is more difficult.

Even after the important hydrologic features are identified, interpolating features between wells can be very difficult. The continuity of individual transmissive fractures may be smaller than the well spacing, discrete fractures are oriented in multiple directions, and the forces of multiple geologic events that influence fracture aperture are superimposed over the complex three-dimensional fracture network. In this sense, the truth may be that with such high degree of spatial heterogeneity, many boreholes may be necessary.

Identifying the general structure of the formation is critical, since it is the basis for developing the conceptual model of the subsurface. The conceptual model determines how future tests are conducted and analyzed, and what kind of numerical model is constructed. A particular difficulty is the determination of flow properties such as transmissivity and storativity by various borehole testing techniques. Determination of these parameters requires the use of analytical solutions. Since these solutions describe the behavior of idealized formations, they are themselves models, and application of an appropriate model and an understanding of its underlying assumptions and limitations is greatly needed if a meaningful description of the formation properties is sought. Without a proper conceptual model of the subsurface and full understanding of the analytical model used to analyze a test, the derived parameters may not be representative of the region of interest. This is a crucial point which is highlighted in this report. Examples will show the possible errors that can be made by employing unjustified analysis methods because necessary tools were not implemented and an improper conceptual model resulted. Failure to recognize this fact translates directly to lost money and effort.

2.3 Monitoring for Remediation Performance

Data also needs to be collected during the remediation phase to evaluate the effectiveness of the scheme, and hence to make adjustments accordingly. In order to make sure that the plume does not spread once pumping is initiated, it is usually required that the hydraulic gradient be maintained in the direction of the pump well, and that this

gradient persists at least to the periphery of the contaminant plume undergoing pump-and-treat remediation. To ensure that this criterion is met, an array of piezometers needs to be installed between each pair of adjacent pumping or injection wells in such a way that the water pressure surface can be determined. Because the locations of conducting fractures is not fully known, because horizontal and vertical velocity divides exist between wells (Keely, 1989), and because non-connecting pathways might have pressures that are more dependent upon local rock stresses rather than on hydrostatic ones, it may be difficult to establish local gradient control with installed piezometers. Hence, many piezometric levels at many different locations and elevations in the rock may be necessary to establish the true 3-dimensional head distribution.

For fractured aquifer cleanup, it will be difficult to define and possibly meet the criteria which indicate that the contaminant concentrations have been reduced to acceptable levels. Even though the range of aperture sizes of the conductive fractures may only vary over a few orders of magnitude, the fact that the conductivity of a fracture is proportional to its aperture cubed results in a conductivity distribution that can vary over many more orders of magnitude. Therefore, levels of contamination measured at monitoring wells may be dramatically reduced in a moderate period of time because the larger fractures are subject to a faster withdrawal of contaminants. However, contaminants may still be present in the less conductive fissures, and depending upon the percentage of the system these pathways comprise, it could mean that considerable levels of contaminants are still present. Additionally, contaminants will reside in dead-end fractures and within the rock matrix. These factors could cause a remediation effort to be continued indefinitely because the contaminants are extracted from these zones very slowly, but at a rate sufficient enough to keep the concentration at monitoring wells above the target level. Conversely, if the zones of significant storage do not respond quickly enough, premature halting of the remediation process may ensue because of the apparent reduction of the contaminants to a target level (Keely, 1989). Figure 2.1 illustrates some problematic factors associated with remediating fractured formations.

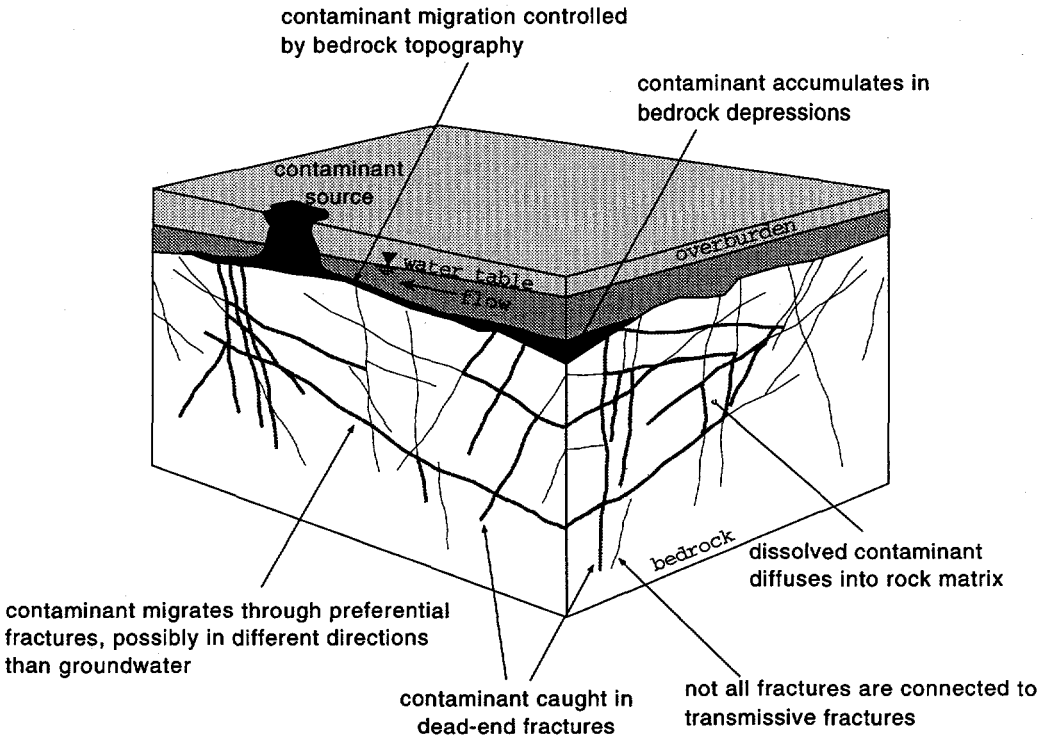

Figure 2.1. Problematic factors of contaminant behavior in fractured formations.

2.4 Summary

The forgoing discussion makes it clear that the success of a remediation effort in a fractured formation is mostly a function of the degree to which we understand the complexity of the subsurface. Even if hydrologic containment is the only realistic solution for extensively contaminated fracture rock environments (Committee on Ground Water Cleanup Alternatives, 1994), proper hydrogeologic characterization is still a critical necessity. This report should provide the remediation community with the knowledge needed to attain this goal.

3 THE RAYMOND FIELD SITE

3.1 Site Description

3.1.1 General

The work described here was conducted at the Raymond Field Site, which is operated by Lawrence Berkeley National Laboratory and the U. S. Geological Survey, under the sponsorship of Office of Civilian Radioactive Waste Management of the Department of Energy, and the U. S. Environmental Protection Agency. No ground water contamination is present at the site. Rather, the site was established to develop and test a multi-disciplinary approach to the characterization of ground water flow and transport in fractured rocks. Research began in 1992 and is ongoing.

The site is situated in the western foothills of the central Sierra Nevada, California, approximately 60 km (37 mi) south of Yosemite Valley and about 5 km (3 mi) southeast the town of Raymond (Figure 4.3, Chpt 4). This site was selected in part because it is both easily accessible and yet relatively isolated. Therefore, there is freedom to carry out different types of experiments without interfering with other activities.

The local relief is subdued, with altitude ranging from 245 to 610 m (800 to 2000 ft) above mean sea level. The bedrock is overlain by a thin layer of soil and regolith which is approximately 8 m thick near the well field. Bedrock is exposed in frequent outcroppings along hillsides and in stream beds, and in several nearby quarries. Annual precipitation varies widely from year to year, but it is on the order of 50 cm/yr (20 in/yr). More than 75 percent of the precipitation falls in the winter (Mitten *et al.*, 1970). The potentiometric surface is generally shallow, and during the period of this study it ranged from about 5 m to 1 m (15 to 3 ft) below ground surface. The surrounding area is dissected by several ephemeral streams, and groundwater flow is generally to the west (Mitten *et al.*, 1970).

3.1.2 Boreholes

Nine vertical boreholes were drilled between March and May, 1992 with an air-percussion rotary drill. They are arranged in a triangular pattern and are spaced no more than 61 m (200 ft) apart (Figure 3.1), and range in depth between 75 to 90 m (245 to 295 ft). Given the shallow depth of regolith and soil, it is believed that the wells are situated

in the granodiorite. However, it is not yet known whether or not the tonalite intersects the wells at greater depths, mainly because borehole core samples are not available. Tonalite was not observed in the cuttings from borehole drilling, although no chemical or petrographic analysis of the cuttings were performed. No intact core samples were collected. Cuttings were usually powdered or finely crushed. The maximum relative difference in surface elevation between the wells is less than 2.5 m (8 ft). Driller's logs indicate that relatively unweathered granitic rock is located beneath less than 8 m (25 ft) of soil and regolith. Steel casings were installed in each hole to a depth between 7 to 15 meters below ground surface, and the lower part of each borehole was left unscreened and uncased. All wells were grouted around casing except 0-0, SE-1, and SW-1. Table 3.1 lists the borehole specifications. Wells SE-2 and SW-2 were originally drilled as 17 cm diameter wells, but were later increased to 25 cm.

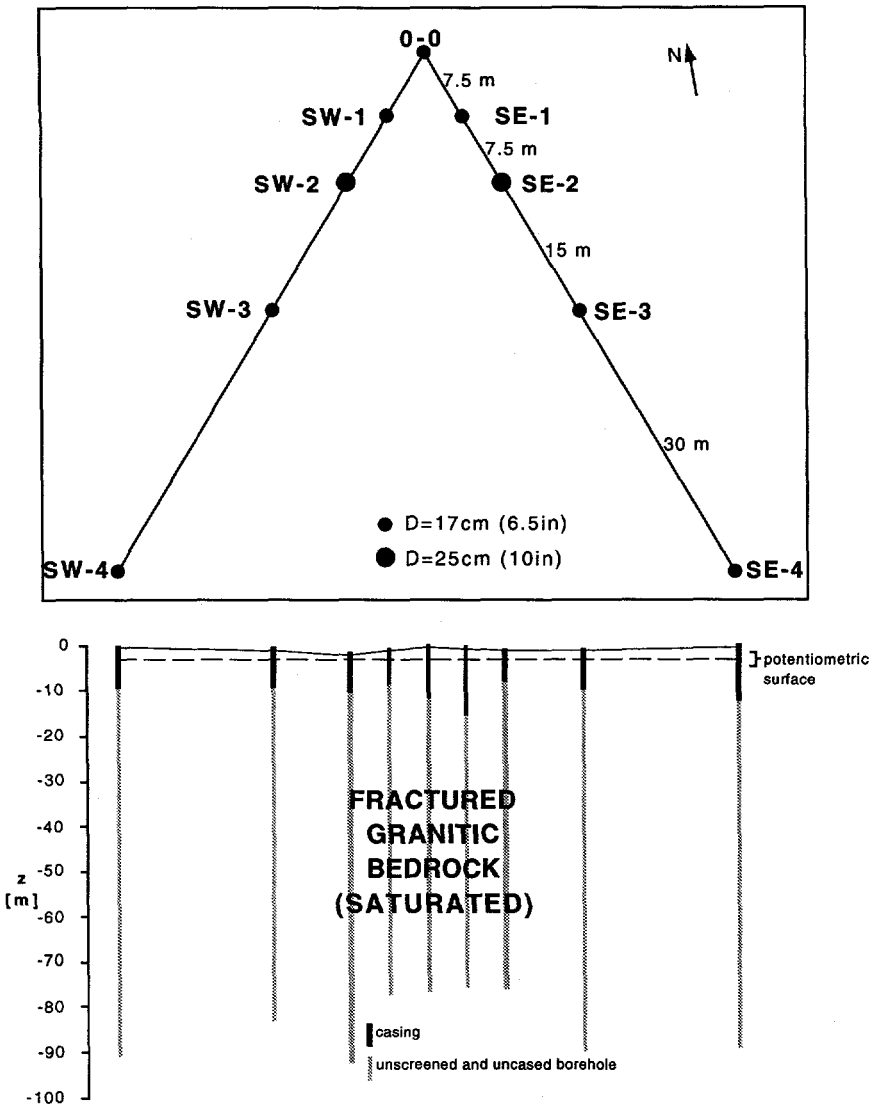

Figure 3.1. Plan and cross-sectional view of boreholes at the Raymond Field Site.

Table 3.1. Borehole specifications.

Borehole	Total Depth [m]	Casing Depth [m]	Casing Diameter [m]	Nominal Uncased Borehole Diameter [m]	Elev. of top of casing relative to 0-0 [m]
0-0	76.2	12.2	0.168	0.17	
SE-1	74.7	15.2	0.168	0.17	-0.384
SE-2	74.4	7.3	0.254	0.25	-1.049
SE-3	88.4	8.1	0.254	0.17	-0.989
SE-4	88.1	11.6	0.254	0.16	-0.250
SW-1	76.2	7.9	0.168	0.17	-0.732
SW-2	89.9	9.0	0.254	0.25	-2.014
SW-3	82.0	7.9	0.254	0.17	-0.839
SW-4	90.1	8.7	0.254	0.17	-0.263

3.1.3 Local Geologic Setting

The local and regional geology is described in detail in Chapter 4.4.

3.2 Hydrogeology of the Raymond Field Site

The hydrogeology of the site was investigated by implementing and integrating many different characterization tools and methodologies. The remaining chapters describe the different characterization stages in detail.

The nature of fracturing was investigated via inspection of aerial photographs and extensive surface outcrop mapping, and by subsurface fracture measurements from acoustic televiewer (ATV), digital borehole scanner, and by fish-eye lens down-hole camera logs. Borehole geophysical measurements were made and correlated with one another and with various hydrologic tests. These measurements included conventional geophysical logs such as electrical resistivity, caliper, and gamma logs, and also more sophisticated cross-hole seismic and radar tomography surveys. Thermal-pulse flowmeter and spinner-type flowmeter measurements, borehole fluid logging, a sophisticated suite of injection profiling tests, and ordinary open-hole slug and pumping tests and pumping tests with packers comprised the hydrologic measurements. Determination of fluid flow properties and the general hydrologic structure of the subsurface was made from the integration of the hydrologic tests and geophysical logs. Seismologic and hydrologic data inversions aided in the determination of the subsurface hydrologic structure and property distribution.

Various tracer tests using both conservative and reactive tracers were carried out. These included radially convergent and partially recirculating tests using bromide and lithium. A sophisticated automated data acquisition system was used to collect and monitor test data and to control test parameters. Some tests utilized over 30 inflatable packer and pressure transducers. Visualization software was used to further our understanding of the subsurface structure by integrating various field data, and a detailed 3-D model of the subsurface was constructed.

This section briefly summarizes the site hydrogeology in order to provide the reader with a proper mental picture of the site upon which to view the application of the tools and methodologies described in later sections. The conceptual model of the site subsurface is based on the integration of all work conducted at the site.

tools and methodologies described in later sections. The conceptual model of the site subsurface is based on the integration of all work conducted at the site.

3.2.1 Conceptual Model

Measurement of fractures from acoustic borehole televiewer logs revealed that there are at least three sets of fractures: two nearly orthogonal and subvertical fracture sets, and another that dips westwardly and subparallel to the topographic surface. The two subvertical sets are tectonic fractures, a conclusion supported by surface outcrop mapping and the correlation of their various properties with the regional geology and geologic history. Surface mapping revealed that subhorizontal unloading fractures, and pegmatitic and aplitic dikes of various orientations and dip comprise the general group of fractures that are westwardly dipping.

Results from the various flow logs and injection profiling tests indicate that although there are hundreds of fractures intersecting each well, there are only several distinct hydraulically conductive fractures in each. Many of the transmissive fractures are subhorizontal and westwardly dipping, and a few are subvertical or of different orientation. Most occur within or near one of two zones of relatively low electrical resistivity and increased borehole diameter, both indications of altered rock. These zones dip gently to the west and are separated by about 25 meters. Fractures of minimal transmissivities occur in other portions of the well. The conceptual model of the aquifer is comprised of two subhorizontal and hydraulically conductive fracture zones that behave as confined units imbedded within a relatively impermeable rock matrix (Figure 3.2). Results from cross-hole seismic surveys support this model.

Pressure transients observed during standard open-hole pumping tests show no signs of dual-porosity behavior, and it is concluded that the rock-matrix does not significantly store or transmit water. This is consistent with the fact that the bedrock is composed of unweathered granite and with the results from the various hydraulic tests described above in which flow was found to be confined to discrete fractures. Results from pumping tests performed with numerous inflatable packers situated between conductive fracture zones in observation wells indicate that the two fracture zones are hydraulically connected, although weakly. Results from a sophisticated hydrologic imaging survey support this model in general, and also reveal the locations of relatively high and low transmissivity (Cook, 1995).

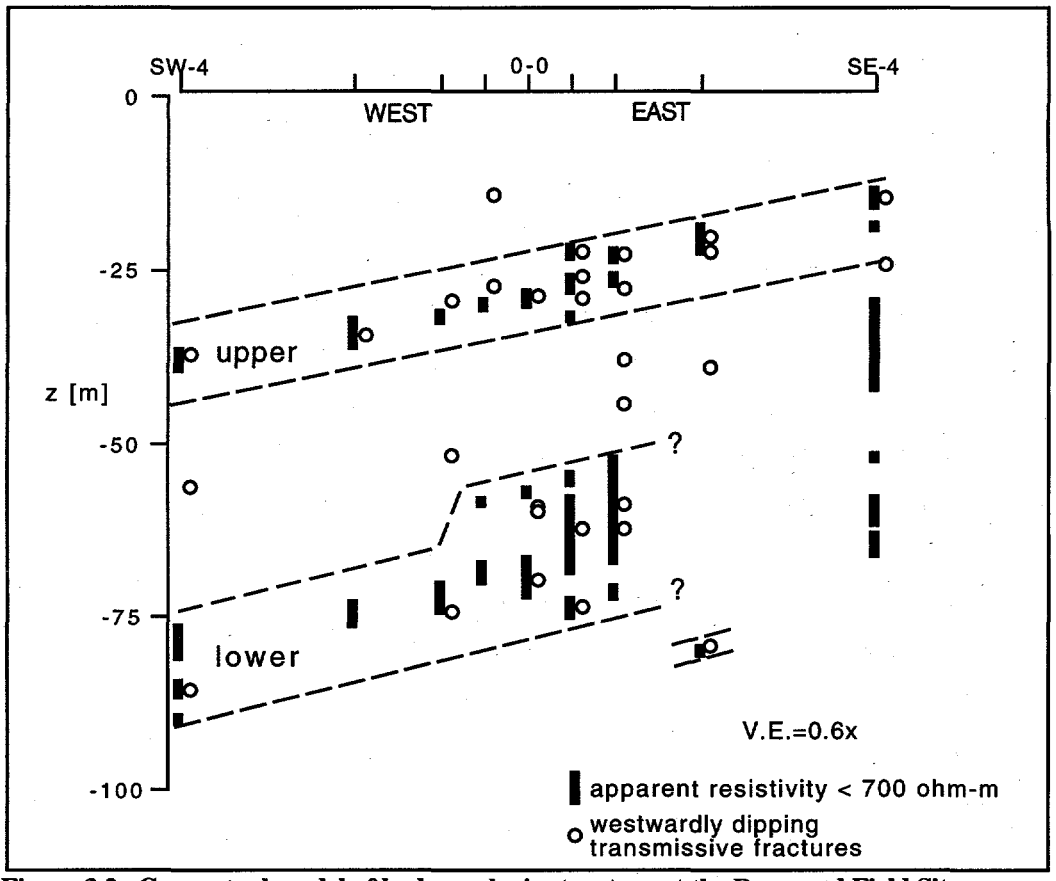

Figure 3.2. Conceptual model of hydrogeologic structure at the Raymond Field Site.

4 SURFACE FRACTURE CHARACTERIZATION

4.1 Introduction

Observation and measurement of surface geologic features is a standard and usually initial investigative phase in any subsurface characterization effort. A non-intrusive, relatively low cost surface study combined with previous documented geologic studies can provide a means to determine the dominant types and orientations of fracture sets present, as well as their physical properties, spatial distribution, and probable modes of genesis. Surface fracture characterization therefore provides an understanding of the fundamental geological characteristics of the site which ultimately control subsurface flow. However, surface fracture characterization does not provide the necessary answers needed to deduce subsurface flow characteristics. The relative ease and low cost of performing surface characterization and the pertinent information that it reveals makes it a practical necessity, but it is not a substitute for borehole studies. For example, most of the fractures observable at the surface may not be significant hydrologically, dominant conductive fractures in the subsurface are not typically observable on the surface, or only limited fractures may be observable at the surface simply because few bedrock outcrops are present. Surface characterization should be viewed as a part of the larger characterization effort in which each phase is integrated with others.

4.1.1 Approaches to Fracture Characterization

Two common approaches to characterizing surface fractures are referred to here as the engineering and geologic approach. A good example of the engineering approach is that taken by rock engineers who are mainly interested in relating fracture properties to rock strength and stability. Fracture measurements are mainly used to determine fracture geometry and spacing characteristics. Statistical parameters which are thought to describe bulk characteristics of the rock mass are derived from fracture measurements of surface exposures. These include the Rock Quality Designation (RQD) and other discontinuity frequency and orientation statistics (see, e.g., Priest, 1993). Grossenbacher et al. (1995) developed a new method to characterize fracture traces on outcrops with irregular surfaces. Very detailed measurements of surface fractures and their statistics have been used to construct statistically equivalent fracture networks for fluid-flow modeling in fracture networks.

The focus of the geologic approach is on the identification of fracture sets based on their orientations and other physical attributes, and on using these characteristics to deduce their probable modes of genesis and their potential for being important hydrologically. This information is used during initial characterization stages to assess where wells should be drilled or where contaminants are likely to migrate, for example, and during later phases of the study in combination with subsurface geophysical data. Descriptive statistics of fracture spacing and orientation are also considered, but generally in a qualitative manner. They may be used to make educated speculations when interpolating features at depth. Constructing fracture network models to simulate subsurface flow based solely on surface fracture statistics is probably inappropriate. The fact of the matter is not all fractures are important hydrologically, and the properties of surface fractures can deviate significantly from those at depth because of weathering processes. The hydrologically important fractures can only be determined by various borehole geophysical and hydrologic tests. Perhaps fracture statistics may be used in a quantitative manner in later stages of characterization such as sophisticated modeling, but only after a conceptual model of the site is developed from borehole geophysical and hydrologic data. Our recommendation is to use surface fracture observations in combination with borehole data to develop a conceptual model of the site. This is no more than recommending that a scientific approach be taken. The geologic approach is illustrated in this report.

4.2 Regional Fracture Characterization

4.2.1 Regional Fracture Sets and Geologic History

Prior to the investigation of fractures at the site, an appreciation for the regional geologic history, the characteristics of the fracture systems present, and the processes responsible for their formation is necessary. Since the fractures found at the site are likely to be part of the larger, regional system, such an understanding may provide clues as to what properties a particular fracture or fracture set might possess, and/or the relationships which can be expected to be seen or to which special attention should be devoted. The word fracture is used here as a collective term for all types of discontinuities including joints, fissures, shear zones, and faults. Topographic and geologic maps are certainly needed, and are generally available from the U. S. Geological Survey, U. S. Forest Service, U. S. Army Corps of Engineers, and various state agencies. Books and journal articles describing the geologic properties and history in the area of interest are especially helpful. Aerial photos are useful for identifying fracture-related

features, as described below. Information regarding areas photographed is available from the National Cartographic Information Center.

4.2.2 Lineament Analysis

Fracture traces and lineaments are surface expressions of joints, zones of joint concentration, or faults (Lattman and Matzka, 1961), and are generally identified via the analysis of aerial photographs. Surface expressions may reveal the orientations of features at depth. Because groundwater flow preferentially follows the most permeable pathways, fracture trace analysis can be used to determine locations for monitoring wells. High yielding wells have successfully been located using this method (Lattman and Matzka, 1961). In fact, the placement of the well field at Raymond was chosen in part because of the numerous tectonic fracture outcroppings located in the stream gully to the northeast, which are observable on aerial photos and in surface mapping. Shortcomings of the method result from the fact that only a relatively small portion of the conducting fractures are expressed on the surface, and because they often can cross folds and faults, or have different orientations than the faults at depth. Additionally, linear features of human origin such as fences, cow paths, roads, and power lines can easily be misidentified as natural linear features (Lattman and Matzka, 1961), and fracture zones can be easily eroded and lose their linear character. Therefore, field checks are necessary after linear features are identified on aerial photographs. Inadequate assessment of surface fractures has led to the installation of bedrock wells in areas that are not in the proper location for detecting contamination (Di Nitto *et al.*, 1982).

4.3 Site-Scale Fracture Characterization

Local fracture characterization refers to the measurement and description of physical fracture properties near the well field. The regional fracture structure may not reflect the smaller-scale geologic features which significantly influence the site hydrogeology.

4.3.1 Observations and Measurements

The following is a list of some measurements that can be made on rock outcrops. Not all may be appropriate or useful for a particular field investigation.

orientation

Orientation is the most common and familiar fracture measurement. A Brunton compass is used to measure the strike, dip and dip direction of a fracture (Compton, 1985).. Orientation is a dominant variable used to define a particular fracture set, although other fracture characteristics need to be considered since different fracture sets may have similar orientations. An obvious problem is that subhorizontal fractures are underrepresented at the surface, although subhorizontal fractures resulting from unloading may be dominant transmissive features at depth.

mineralization and alteration

Observation of fracture mineralization and alteration provides a secondary means for classifying fracture sets. Primary mineralization in fractures is related to their infilling shortly after formation. For example, quartzo-feldspathic dikes such as pegmatites and aplites commonly fill fractures shortly after they formed during the emplacement and cooling of the magma. Fracture alteration may be mechanical or hydrologic. Infill banding can result from lateral offset due to microfaulting. Ferric hydroxide staining is an indication of fluid flow, which may be recent or associated with the original emplacement of dikes. Successive geologic events can lead to alteration of a previously non-transmissive fracture. For example, mineral filled fractures may become fractured during a later tectonic event because they represent planes of weakness in the rock. Mineralization and alteration can indicate fracture origin and subsequent geologic processes and may directly indicate fluid flow. Mineralization, alteration, and orientation are probably sufficient to define particular fracture sets.

aperture / thickness

Aperture measurement seems particularly appealing since fracture transmissivity is related to aperture. However, weathering processes erode fractures and reduced stresses near the surface and may cause previously sealed fractured to open. Therefore, fracture apertures at the surface are poorly related to apertures at depth. The aperture of open fractures can be measured with an automotive feeler gauge or a metric scale if the aperture is large. A feeler gauge is a tool consisting of several metal blades of known thicknesses, ranging from 50 μm to 1 mm. Thickness of mineralized fractures can be useful characteristic in distinguishing dike sets from one another.

trace length and planarity

Trace length refers to the horizontal or vertical extent of fracture traces observable on an outcrop. The fact that fracture traces may exceed the dimensions of the outcrop makes accurate measurements problematic, although general characteristics of different sets may be deduced (Najita, et al., 1993). Fracture planarity refers to the degree a fracture deviates from an ideal plane. Trace length and planarity of fractures may be useful when evaluating the confidence of extrapolating a known transmissive fracture in a borehole to an adjacent borehole.

fracture spacing

The perpendicular distance between fracture traces of the same set can be used as a measure of fracture spacing. The observed spacing is actually an apparent spacing because fractures are not generally oriented perpendicular to the outcrop surface. The relevance of fracture spacing statistics are discussed in Chapter 6.

fracture connectivity

Fracture connectivity ultimately determines if a fracture is significant hydrologically since a fracture is only transmissive if it is connected to other transmissive fractures. Barton and Larson (1985) identify surface fractures as either abutting, cross-cutting, or blind. Figure 4.1 shows these fracture types. In a region subjected to several geologic events, it is likely that cross-cutting fractures are the norm. Regardless, whether or not fractures intersect one another has little bearing on site hydrology if none are transmissive.

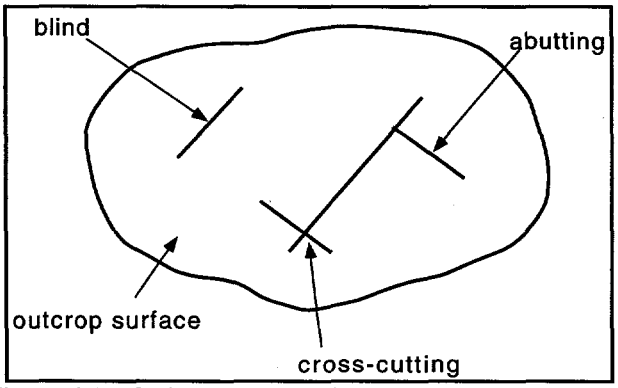

Figure 4.1. Various modes of fracture trace connections.

surface roughness

Fracture surface roughness is an important factor in geomechanical studies since it affects the shear strength of adjoining blocks. However, like the other fracture specific properties observed at the surface, its bearing on the overall site hydrogeology is questionable. Like the other fracture properties, we recommend that surface roughness be used for delineating fracture sets and gaining insights into their general characteristics. On a microscale, surface roughness plays a major role in subsurface flow since the asperity distribution in a fracture plane influences fluid channeling and hence contaminant dispersion (Tsang et al., 1991). Roughness on exposed fracture surfaces is measured with a contour gauge, which is a 15 cm long device consisting of approximately 150 millimeter-wide pins. The pins are held together by two metal plates, such that when the gauge is pressed against a fracture surface, the pins adjust to and retain the shape of the surface. Roughness is characterized by comparing the profile with a set of standardized roughness profiles (Barton and Choubey, 1977), or by subjecting samples to microscopic analysis.

4.3.2 Visualization of Fracture Data

Rose diagrams, stereonets, and histograms are three common graphical techniques used to represent fracture data. An example of each using hypothetical data is shown in Figure 4.2. The histogram can be used to show the distribution of a particular fracture property observed within the whole or part of the data set. For example, spacing distribution of fractures within particular fracture sets is often represented with a histogram. The histogram shown shows the frequency of fracture strike azimuths of a hypothetical data set. A rose diagram is a specialized histogram often used to represent the distribution of fracture strike azimuth. It provides an easy means to view the general orientation distribution since the data are plotted in an angular fashion. The length of each pie segment is proportional to the number of fractures that have strikes within a particular angle interval. The shortcoming of the rose diagram is that it does not show the three-dimensional nature of fracture orientation data. The stereonet is the optimal way to display fracture orientation data because it shows both the dip azimuth and the dip angle of individual fractures. An equal area, lower hemisphere, polar projection stereonet of the hypothetical data set is shown in Figure 4.2. For the sake of clarity, the lines of longitude and latitude that normally appear on a stereonet have been omitted. Each point on the stereonet represents the intersection of the pole of a fracture plane surface that

passes through the center of a sphere with the surface of the lower hemisphere. The stereonet shows the intersection as if the surface of the lower hemisphere is viewed from the top of the upper hemisphere. For example, the cluster of points on the western edge of the stereonet represent fractures that dip steeply to the east, and the cluster at the bottom represents fractures that dip steeply to the north. A horizontal fracture would be represented by a point in the center of the stereonet.

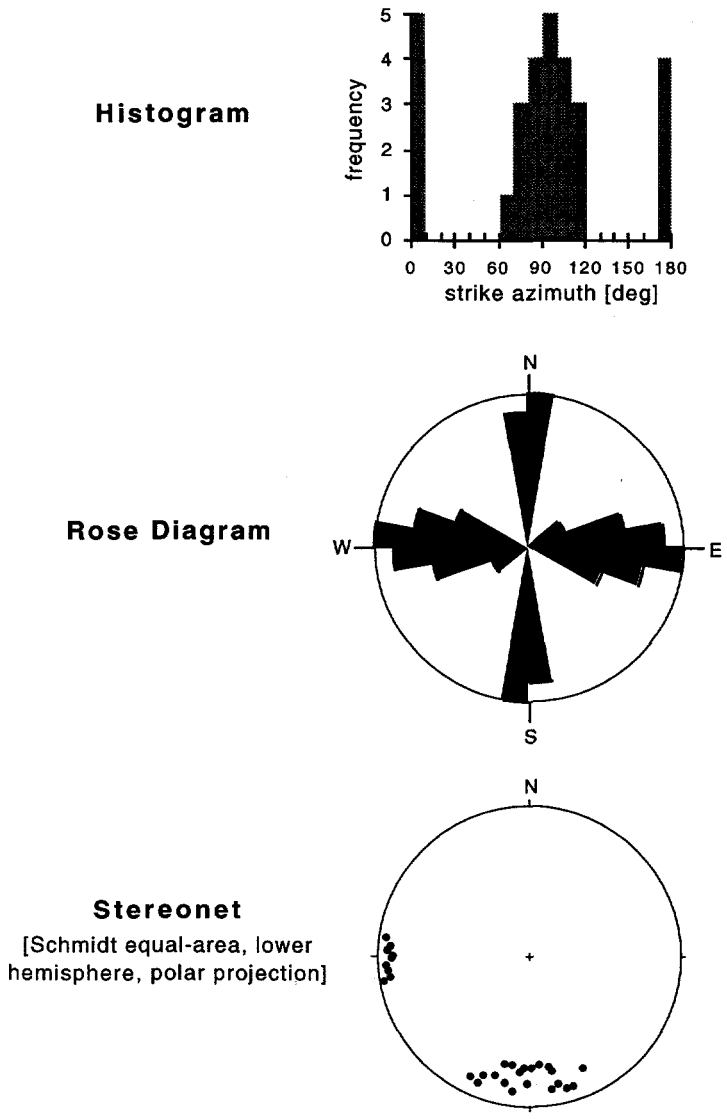

Figure 4.2. Histogram, rose diagram, and stereonet of hypothetical fracture data. Two fracture sets are present: a set that dips steeply to the north and one that dips steeply to the east.

4.4 Surface Fracture Characterization at Raymond

4.4.1 Regional Fracture Sets and Geologic History

In general, three different systems of fractures are prevalent throughout the Sierra Nevada: two nearly vertical dipping sets that strike almost orthogonal to one another in a northeasterly and northwesterly direction, and a relatively shallow and young subhorizontal set that produces the sheet-like structure typical on many of the high ridges in the Sierran interior (Norris and Webb, 1976). Because these fractures crosscut the subvertical joints, do not contain hydrothermal deposits, are oriented subparallel to the topographic surface and are found at depths ranging from meters to no more than several hundreds of meters, there is little doubt that they are unloading fractures which resulted from pressure relief due to surface erosion (Segall and Pollard, 1983a,b; Billings, 1972). In contrast, the processes responsible for the formation of the near vertical fractures has been difficult to decipher. Cohen (1993) summarizes the different works and hypotheses regarding the geologic history associated with these fractures. It has long been acknowledged that they formed in response to tectonic forces. The rectilinear arrangement of near vertical fractures is a characteristic indicative of a tectonic origin (Chernyshev and Dearman, 1991). Additionally, many of the fractures are strike-slip faults, and the direction of compressive stresses inferred from their arrangement is consistent with plate tectonic theories regarding the geologic history of western North America (Dott and Batten, 1988). These fractures have varying infilling and deformational characteristics as a result of different episodes of tectonic activity throughout the Sierra (Martel *et al.*, 1988). Lockwood and Moore (1979) observed that the tectonic fractures dip steeply in either direction perpendicular to their strike.

Prominent lineaments observable on aerial photographs display the large-scale rectilinear arrangement and orientations of the two near-vertical sets. The lineaments are commonly marked by brush and trees or narrow depressions of extensively weathered angular blocks of rock. The depressions often serve as channels for surface water and are expressed on topographic maps.

Two plutonic rock masses of the larger Sierra batholith comprise the bedrock in the vicinity of the site (Figure 4.3). The granodiorite of Knowles is a light-gray, equigranular, and medium-grained rock. It is generally spatially isotropic with respect to mineral composition and texture, and foliations are generally not observed. Because of these characteristics the rock has been extensively quarried and widely used as a building

stone in some of the large cities of California. The Raymond Quarry is located approximately 2.5 km north of the site and is active. An inactive quarry is located just south of the site and another is located 1.5 km to the northwest. The tonalite of Blue Canyon near the site is a medium-grained, dark gray rock with conspicuous hornblende prisms, and it is generally well foliated. The emplacement of granodiorite followed the tonalite, as indicated by their respective ages of 111 and 114 million years (Bateman and Sawka, 1981).

The outcrop of tonalite just west of the field site is shown to be approximately 0.3 mi (0.5 km) from the well field. Recent field mapping has revealed that the contact is actually on the order of 0.2 km west of the well field and that a tonalite subunit lies between the tonalite and granodiorite (K. Grossenbacher, LBL, oral comm., 1995). However, the general orientation of contact is the same as that shown in Figure 4.3. Given the shallow depth of regolith and soil at the site (see Chpt 3), it is believed that the wells are situated in the granodiorite. Tonalite was not observed in the cuttings from borehole drilling, although no chemical or petrographic analyses of the cuttings were performed.

Huber (1987) observed that the spacing of joints in plutonic rocks in Yosemite National Park is related to composition and texture of the rocks. Generally, rocks with relatively low silica content (e.g. tonalite and diorite) or those that are finer grained have more closely spaced joints than the more siliceous (e.g. granite and granodiorite) or coarser grained rocks. The fact that the site is located very close to the contact between the tonalite and granodiorite may therefore influence its hydrogeologic structure.

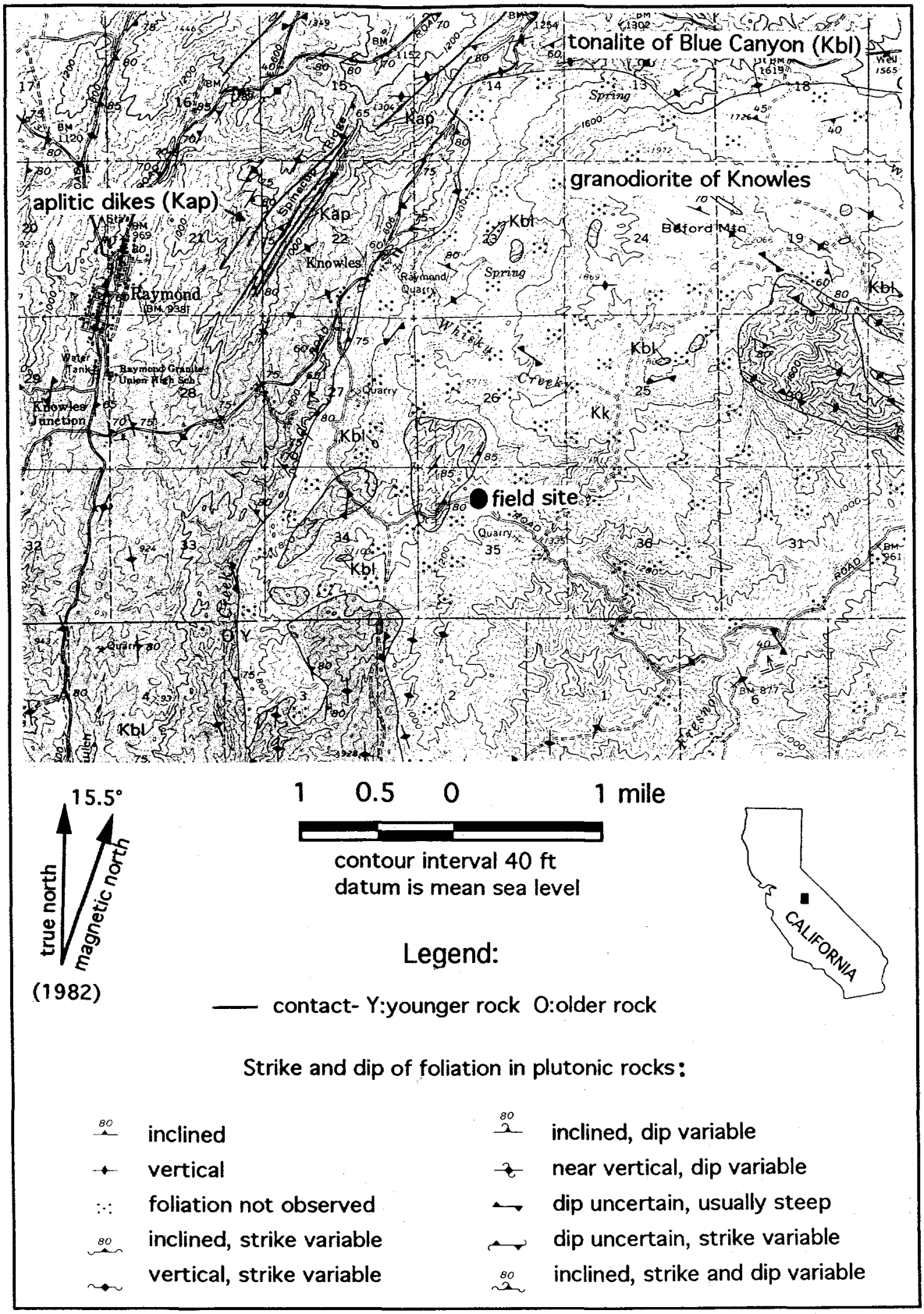

Figure 4.3. Regional geologic map (modified from Bateman *et al.*, 1982, Geologic map of the Raymond quadrangle, Madera and Mariposa counties, California).

4.4.2 Site-Scale Fracture Characteristics

4.4.2.1 General Observations

There are numerous surface exposures of bedrock surrounding the site. In general, surface expressions of the regional fracture sets are present, along with other fracture types. There is no apparent systematic fracture structure. The spatial distribution of fracture properties in general is highly heterogeneous on the scale of the well field. As expected, outcrops are most prominent along creek beds and along road cuts. This presents the possibility of sample bias in that fractures and dikes at high angles to the road or creek will be better exposed than those at low angles. For example, the subvertical tectonic fractures are more prominent than the subhorizontal unloading fractures in the vicinity of the well field. They exhibit the typical angular outcropping behavior described above, but some are also observed to be sealed. Laterally continuous unloading fractures subparallel to the surface are very obvious at the abandoned quarry to the south, but in the immediate vicinity of the well field they mainly comprise the surfaces of exposures, such as the tops of the angular block in stream gullies. Pegmatitic and aplitic dikes are frequently exposed in the outcrops. Some pegmatite dikes are fractured and exhibit ferric oxide staining.

4.4.2.2 Fracture Measurements

Observations and measurements were made by several Raymond Project participants. Many measurements of fracture orientation, trace length, spacing, weathering, secondary mineralization, and relative displacement were made. Measurements of fracture aperture, roughness, and planarity were measured on some fractures. Detailed measurements of fracture spacing were made at nine outcrops, and a large fracture pavement was mapped.

The measurements of fracture orientation, trace length, spacing, weathering, secondary mineralization, and relative displacement described here were made by Peter Zawislanski of Lawrence Berkeley National Laboratory. The results of the other field efforts are in progress and are not yet available. Fractures exposed on outcrops in the area within a 200 to 300 meter radius from well 0-0 were measured. In total, 471 measurements were made. In the case of a clearly defined fracture set, at least three orientations on three different fractures were measured when possible. Exposed fracture planes, fractures within rock, and dikes were measured.

4.4.2.3 Results

subvertical and subhorizontal fractures

A stereonet projection of all mapped fractures excluding dikes is shown in Figure 4.4. For the sake of clarity, the lines of longitude and latitude that normally appear on a stereonet have been omitted. The density of the plotted data is also shown and allows visual determination of the central tendency of strike and dip of the sets. There are three distinct sets of fractures present: two orthogonal and subvertical sets, and a subhorizontal set. The subhorizontal set dips slightly to the west at about 5°. The two subvertical sets strike at N30W and N60E. Their dips fall primarily within the range of 75° to 90°. The other fractures may be outliers or belong to less prominent fracture sets.

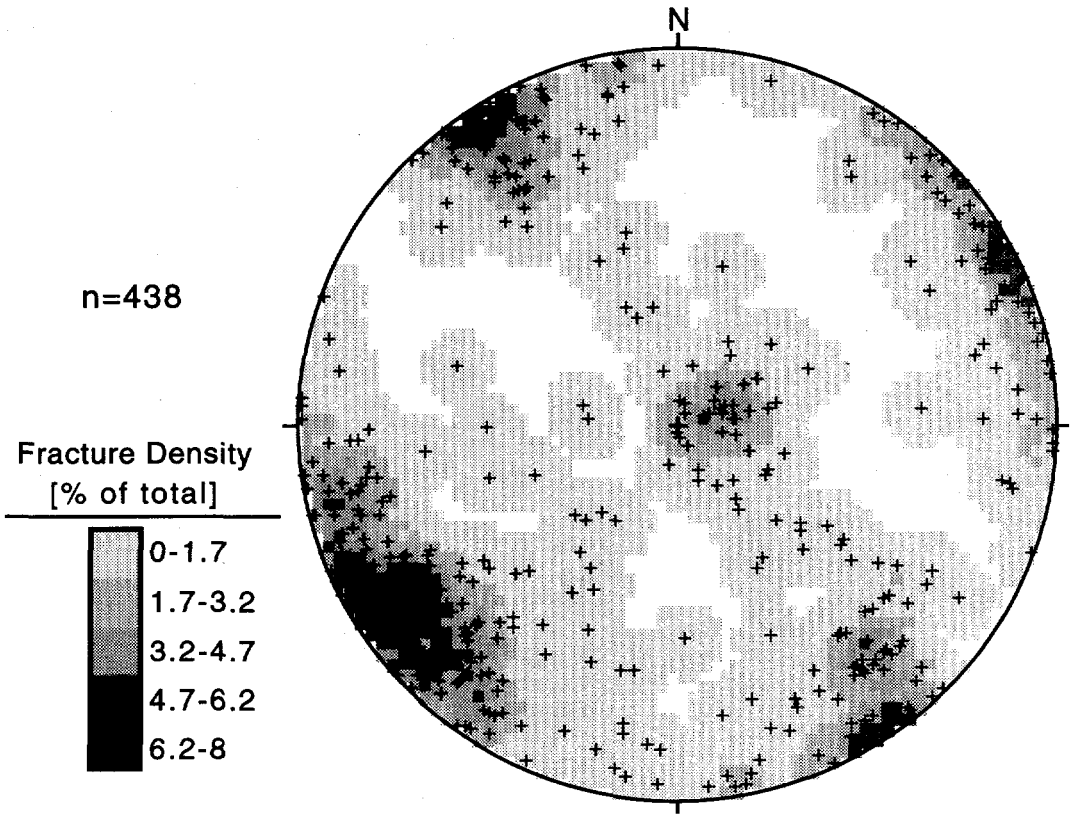

Figure 4.4. Density plot stereonet of mapped surface fractures (Schmidt equal-area, lower hemisphere, polar projection). North is 1982 true north.

The orientations and characteristics of the subvertical fractures coincide with the dominant regional set, and they are therefore considered tectonic fractures. The dip of the subhorizontal fractures is approximately equal to the regional slope of 4°, so it is reasonable to conclude that these are unloading fractures.

The subvertical tectonic fractures have trace lengths on the order of several meters, and the northeasterly striking set shows a greater percentage of blind fractures. Not enough trace length measurements of the unloading fractures were made to suggest any general statistics. The spacing of the tectonic fractures is irregular. Some are only a few centimeters apart, while others are spaced by tens of meters. Most tectonic fractures do not show signs of secondary mineralization. Weathering was prominent on exposed fracture planes.

Pegmatite and Aplite Dikes

Many aplite and pegmatite dikes are exposed in the vicinity of the well field. They vary in thickness from 1-40 cm. Pegmatite dikes were measured around the site, as these were more easily traced than the smaller aplite dikes. The exposed continuity of pegmatitic dikes is much larger than that of the tectonic or unloading fractures in the vicinity of the well field. The average continuity of pegmatitic dikes is on the order of 10 m, with some extending 30 meters or more. Pegmatites on the order of 10's of centimeters wide are generally not fractured. Smaller pegmatites with thicknesses on the order of centimeters were often observed to contain a discontinuous open fracture near the center and signs of fluid flow. Often, this fracture jaggedly subparallels the pegmatite-host rock contact. This corresponds to high values of surface fracture roughness. Pegmatites at the surface show signs of preferential fracturing and are associated with fluid flow. The large pegmatites often form the surface of an outcrop, for example. At the abandoned quarry to the northwest, a subhorizontal pegmatite has an open fracture in its center, and seepage stains appear under the fracture.

The contact between the host rock and the pegmatite dikes does not have chilled margins, which suggests they were emplaced while the pluton was still hot. This is consistent with the observation that the dikes are routinely cut by the two sets of subvertical, conjugate fractures, generally with very little to no displacement, thereby indicating they are older than the tectonic fractures. One possibility is that the dikes filled cooling fractures that formed near the contact between the tonalite and the granodiorite.

The distribution of pegmatite dikes is shown on a stereonet projection in Figure 4.5. Two sets are apparent. They are oriented nearly orthogonal to one another and dip to the northwest and northeast with dips between 20°and 60°.

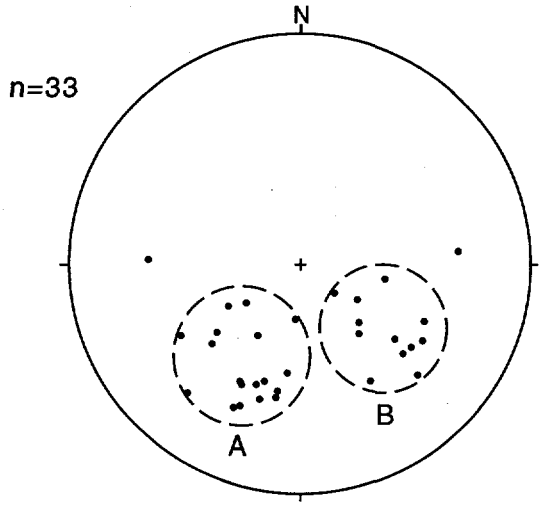

central tendency of dip:

SET	DIRECTION	ANGLE
A	N35E	45°
B	N50W	40°

Figure 4.5. Stereonet of mapped pegmatitic dikes (Schmidt equal-area, lower hemisphere, polar projection). North is 1982 true north.

4.4.2.4 Use of Surface Characterization Results in General Investigation

Surface fracture characterization at Raymond provided information useful to other phases of the site hydrogeologic characterization. The decision to situate the well field at its present location was based on the observation that this area in dissected by several streams gullies that exhibit a high degree of tectonic fracturing. The geophysical logs described in Chapter 10 revealed that a transmissive zone was associated with pegmatite dikes in the upper portion of the wells. The observation that pegmatite dikes at the surface are laterally continuous for tens of meters and are often fractured and exhibit signs of fluid flow provided support for our inference that these intervals are portions of a continuous band of fracturing associated with a pegmatite (Chpt 3.2; 10). Similarly, tectonic fractures were observed to be planar and laterally extensive, which justified the use of extrapolating these fractures linearly to other boreholes as a means of hypothesis testing (Chpt 11).

4.5 Summary

This chapter described some methods to characterize surface fractures and described the methodology and findings at the Raymond Field Site. Regional characterization and site specific fracture measurements were discussed. Subvertical tectonic fractures and subhorizontal fractures were observed and are part of the regional fracture sets. In addition, two sets of pegmatite dikes are also present.

5 WELL DRILLING

This chapter describes air drilling methods, with special emphasis on the air-percussion method. Air drilling is the most appropriate method for installation of wells in crystalline bedrock in terms of its relative cost, penetration rate, and potential to yield relevant hydrogeologic information. Observation of drill cuttings, drilling rate, and flow out of the borehole during drilling may be used to infer lithology and the location of transmissive fractures, for example. After a brief description of the drilling method and its advantages, the results of its application at the Raymond Field Site are presented and compared to geophysical logs in order to illustrate how careful logging during drilling can optimize the hydrologic characterization process.

5.1 Drilling Method

5.1.1 Air Drilling

Driscoll (1986) describes different drilling techniques as they apply to ground water investigations. For air drilling systems, either a direct rotary or down-the-hole hammer (percussion) method can be used. In both methods, compressed air is forced down the drill pipe and through small holes at the bottom of the drill bit. The cuttings beneath the drill bit are lifted to the surface in the passage around the drill pipe by the uphole flow of air, and they collect at the surface around the borehole. The direct rotary method utilizes roller cone bits which rotate as the entire string of drill pipe is rotated from the drill rig. In the down-the-hole or percussion method a pneumatic hammer at the end of the drill pipe rapidly strikes the rock while the drill pipe is slowly rotated. The hammer is constructed from alloy steel equipped with very hard tungsten-carbide inserts which are sharp or hemispherical (button inserts). Because the cuttings are continually being blown up the well, the air hammer always strikes a clean surface. Therefore, it is very efficient. Adding a small amount of water or water and surfactant solution can help increase the lifting capacity of the air and suppress dust at the surface. Driscoll (1986) suggests the down-the-hole hammer is the best choice for crystalline rock formations. Six inch and 6.5 inch hammer bits are most commonly used (Driscoll, 1986). Air-drilling is only applicable in partially to fully consolidated rock, so more conventional drilling methods such as standard mud-rotary drilling would be used if weathered rock or unconsolidated materials overlie the bedrock. Once the competent bedrock is reached, the upper portion may be cased and then air-drilling can continue for the remaining

depths which are left uncased. Some air-drill rigs are also equipped with a mud pump in addition to the air compressor.

The advantage of using air-drilling methods in crystalline formations extends beyond their high rate of penetration. Careful observation during drilling and a descriptive log can provide very valuable hydrogeologic information. Of great significance is the fact that the depth of transmissive fractures may be observable, because water will be brought to the surface with the cuttings when such fractures are encountered. Flow can be measured with a bucket at the surface, and changes in flow with depth may indicate that the drill bit encountered another transmissive fracture or fracture zone. In addition, the flow measured at the total depth may be used as a relative measure of well yield. This information can be used to assess which wells are relatively high yielding, and which therefore are the best candidates for pumping during pumping tests or borehole flow profiling tests, for example. Paillet (1994) compared driller's reports of the Raymond wells with results from pumping tests and found that the observed flow during drilling correlates with the productivity of the wells.

Examination of cuttings and measurement of drilling rate also provides information. Cuttings may show secondary mineralization such as ferric staining, which may indicate the presence of fluids. Observation of cutting mineralogy in general and changes in drilling rate correspond to changes in lithology. At depths where a zone of alteration and fractures occur, drilling rate increases. If a fracture or fracture zone is very large and degraded, the drill bit may in fact drop down to where the rock is again competent. Cuttings produced by the hammer method are finely ground particles, whereas larger cuttings or chips are produced when drilling through a fracture. Mineralization and alteration can be identified by changes in color and consistency of the cuttings. It may be possible to collect water samples as different transmissive fractures are encountered to assess which may contain contaminants. No settling pond needs to be constructed for the borehole slurry fluids used during other common types of drilling methods. An example application of careful logging is given below.

5.1.2 Coring

Coring is described in section 8.4

5.2 Well Location

The extreme heterogeneity of many fractured formations makes optimal well placement very difficult. The fact of the matter is that well placement adjacent to a high producing well may be essentially dry, and a considerable amount of trial and error may ensue. This was the case at a remediation site in New Hampshire, for example (Buckley, et al., 1985). Surface fracture characterization may provide some clues, such as where lineaments and regions of intense fracturing are located. This is described in Chapter 4. Certainly, the contaminant source location and general direction of ground water flow are important considerations. Nearby wells and driller's reports may provide information regarding general groundwater flow direction, typical well yields, and depth below which little flow is observed. This may help define maximum drilling depths, although there is always the likely possibility that transmissive fractures are located beneath the wells.

5.3 Drilling at Raymond

Nine vertical boreholes were drilled at Raymond using the down-the-hole hammer technique described above. Eight inch and 12 inch carbide-tungsten button bits were used in the upper portions of the wells where casing and grouting were to be used, and 6-in bits were used to drill the remaining borehole which was left uncased. The specifications of the wells are described in Chapter 3. Water was occasionally injected via the drill rod in order to suppress dust and help bring cuttings to the surface. Lithological determination was made by a geologist using the cuttings which were usually powdered or finely crushed. Tonalite was not observed in the cuttings from borehole drilling, although no chemical or petrographic analysis of the cuttings were performed. Samples were taken when changes in lithology were noted. The location of some fractures could be identified by a combination of drill behavior and cuttings. Fractures or joints on sub-centimeter scale probably went unnoticed during drilling. Drilling rate was measured by observing the descent of the drill pipe over measured time intervals. Where changes in discharge were observed, a bucket and stopwatch were used to measure the flow. A funnel was placed over the well and diverted water into the bucket. (Zawislanski, 1992; Zawislanski, oral comm., 1995).

5.4 Comparison of Driller's Log with Geophysical Logs

Figure 5.1 shows the geologists' log of well SW-3 and the corresponding normal resistivity, caliper, and acoustic televiewer logs. The transmissive fractures identified using heat-pulse flowmeter and other geophysical logs are shown with an arrow adjacent to the acoustic televiewer (ATV) log. The principles of these logs are described in Chapters 8 and 9. Low resistivity is typical of zones of hydrologic alteration where clay and ferric staining are present. Caliper logs indicate changes in borehole diameter associated with fractures or fracture zones. The ATV provides a image of the borehole wall and shows the locations of fractures. The driller's log indicates the first flow encountered is at 96 feet, which is in accordance with the geophysical logs. Above that depth, only dry cuttings came to the surface. Flow was recorded at the subsequent depths for the purpose of taking incremental measurements, or when flow appeared to change. The change in flow at 146' is not corroborated by geophysical tests. It may be the result of decreased flow from the 96 feet fracture or a measurement error. The change in flow to 2.5 gpm at about 220 feet is in accordance with geophysical measurements.

Not all transmissive intervals were identified by the logger, although regions of intense fracturing were noted. Note that the increased drilling rates correspond to the regions of closely spaced fractures and zones of low resistivity. The logs collected at Raymond are especially detailed and generally much more thorough than those collected by driller's logs. The logger noted fractures and described alteration and other fracture-specific properties. Careful logging during drilling obviously provides valuable information relevant to the characterization effort.

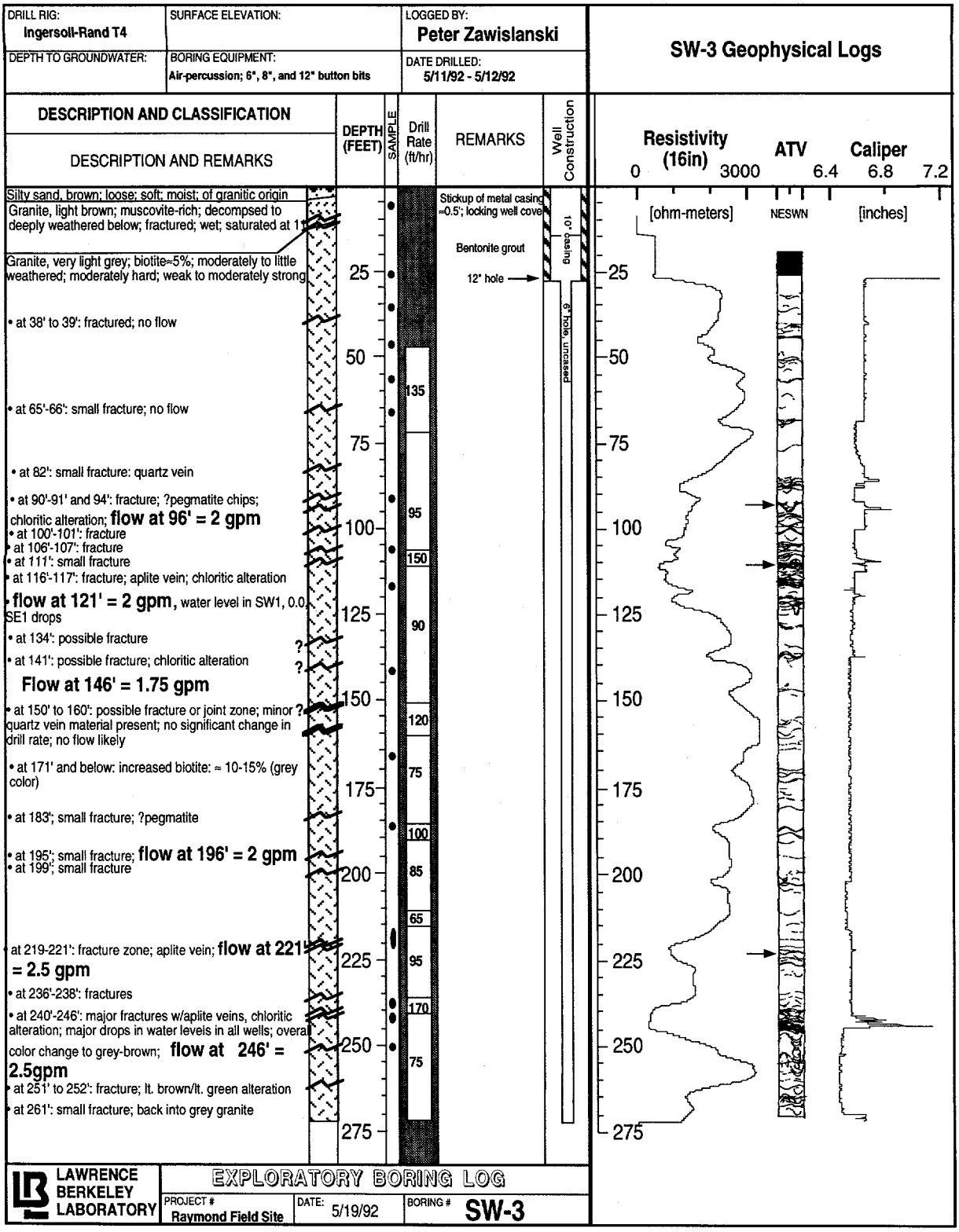

Figure 5.1. Comparison of geologists' log and geophysical logs of well SW-3. Arrows adjacent to ATV log represent transmissive fractures.

5.5 Summary

5.5.1 General

Air drilling is an excellent choice for drilling boreholes in fractured bedrock formations. The fast penetration rate, coupled with the fact that the locations of transmissive or potentially transmissive intervals, and an indication of the productivity of the well is attainable, make it the best choice for drilling in fractured crystalline formations. The rate of penetration offers an obvious cost advantage over other methods, but a greater savings is probably due to the increased information gained concerning fluid bearing zones.

5.5.2 Recommendations

• Wells in crystalline formation should generally be drilled using the air-percussion or direct air rotary method. Weathered overburden should be cased and the remaining hole left uncased. This permits use of fractured detection and measurement techniques (Chapter 8), and in general there is no reason to case if the rock is competent enough.

• Cuttings, drilling rate, and flow rate from the borehole should be carefully monitored during drilling.

• Wells with the highest discharge observed during drilling should be used first when conducting pumping tests, borehole flowmeter tests, etc.

6 PUMPING TESTS

Pumping tests are one of the most commonly employed methods to determine hydrologic properties of aquifers. The tests usually take the form of pumping a single well and recording the transient pressure response in the pumped well and in neighboring wells. Combined with other geologic data, the results can indicate the general hydrologic behavior of the aquifer, for example, whether it is unconfined, confined, or double-porosity. Analysis of the results can yield estimates of bulk characteristics such as transmissivity, storativity, and anisotropy. Pumping tests with multiple observation wells are commonly employed since they are relatively simple to conduct with the equipment of today's hydrogeologic investigative teams. However, it appears that they are relied upon too heavily in characterization efforts of contaminated aquifers. For example, long-duration pumping tests (e.g., tens of hours to days) are common but unjustified; the storage and/or treatment of the large volume of water discharged during the test is costly, analysis of the tests can easily yield parameter values that are not representative of the region of interest, and they can induce contaminant migration to previously uncontaminated areas.

The purpose of this chapter is not to describe how to conduct and analyze pumping tests per say; that is a science in itself and books are devoted to the subject (e.g., Matthews and Russell, 1967; Kruseman and de Ridder, 1990). Rather, several subtleties which can have a profound impact on the interpretation of pressure transients in fractured media are highlighted. Here we consider constant rate pumping tests conducted in open boreholes. Test results obtained at the Raymond Field Site are used to illustrate the concepts described.

6.1 Some Problems in the Analysis of Pumping Tests

6.1.1 Conceptual Considerations

Conceptually, one must appreciate what is being measured during a pumping test. Flow toward a pump well is a diffusive process that occurs over an ever-increasing volume with time. Therefore, pressure transients and the parameters derived from them represent spatially averaged, effective properties in some way. In general, the observed transient is a function of the duration of the test, the distance away from the pump well, and the formation properties, which include the type and scale of heterogeneities present.

There is no single, correct analytic model for tests conducted in fractured formations. Intuitively it may seem that the Theis solution, which is for a homogeneous and porous confined aquifer, is inappropriate. Solutions to other, more sophisticated models may be appropriate. The double-porosity aquifer concept proposed by Warren and Root (1963) or Bourdet and Gringarten (1980), or models that account for various discrete fracture geometries are several examples. However, fractured formations can behave in a manner predicted by the Theis solution under certain conditions. This is shown below. More recent models have been proposed (e.g. Barker, 1988), but it is not yet clear what the derived parameters represent.

The way in which drawdown data is analyzed, such as the choice of analytical model solution used and the portion of the data used to match the solution, can have a profound effect on the calculated parameter values. An inappropriate model may be used because different heterogeneities can produce similar pressure transients, for example. This non-uniqueness can lead one to formulate an incorrect conceptual model of the aquifer and derive irrelevant parameter values. This is especially so today given the use of computer software routines that automatically fit analytical solutions to field data. Two examples of non-uniqueness are the similarity between the transient response of a double-porosity and unconfined aquifer, and the apparent anisotropy which can result from local heterogeneities. Usage of any model requires that other hydrogeologic information warrants its use.

An important fact described in a following section is that pressure transients may represent average properties that are not related to the region of interest. For example, mid to late-time pressure transients in an observation well may be completely independent of the formation properties between the pumping and observation well, and well bore storage effects may mask the signature effect of important heterogeneities that would otherwise be reflected in early-time data.

In summary, there are numerous considerations which need to be made prior to conducting and analyzing pumping tests. The concepts described above must be understood in order to reduce the potential for misinterpreting test results. A discussion illustrating some of the potential problems is given in the following sections.

6.1.2 Transient Response in a Fractured Aquifer

Figure 6.1 schematically shows several different heterogeneous fractured rock aquifers. Each Figure represents a portion of infinite aquifer, and the four points

represent a hypothetical well field. Figure 6.1A represents a well fractured porous media that may be conceptualized as the well known double-porosity continuum usually attributed to Warren and Root (1963). Here the porous matrix provides the bulk fluid storage while the flow towards the pump well is restricted to the fractures. The characteristic pumping response of these systems is an early time transient exhibiting Theis curve behavior, followed by a transitional period, then again followed by a late time Theis behavior. The early and late time transient is dominated by the fracture properties, and the transitional period is a function of the matrix storativity. However, a well located at a distance from the pump well may show no signs of the early or transitional transient period, and well bore storage effects can completely mask the early time behavior in the pump well (Bourdet and Gringarten, 1980). Therefore, the observed transient behavior may not reveal the fundamental structure of the aquifer, and the transmissivity obtained from standard curve fitting would unknowingly represent a bulk transmissivity which is not representative of some average property of the whole formation. The double-porosity model is not well suited for a site like Raymond, in which flow is confined to discrete fractures within a granitic rock matrix that is essentially impermeable.

Figure 6.1B represents a homogeneous porous aquifer with several high conductivity fractures that do not intersect the wells. In this case, it is most likely that the presence of the fractures will not have a detectable effect on the transient behavior. The pressure transients would behave as that of a homogeneous medium, and the derived parameters would not reflect the presence or properties of the very high conductivity pathways which contaminants are likely to follow. The pressure transients would be noticeably influenced if the wells intersected the fractures, however. Butler and Liu (1993) discuss the problem of detecting heterogeneities from pressure transients.

Figure 6.1C represents a discretely fractured crystalline aquifer like that at Raymond. Flow is confined to conductive fractures and essentially no flow is through the matrix. Early time transients will be dominated by near-well fracture geometry and flow properties, but the late-time transient may be fitted to a Theis curve if the degree of fracture interconnection is large enough relative to area perturbed by the test (Karasaki, 1987). This can occur because at late times fluid is being released from storage at distances far from the well, and flow toward the well is generally radial over the region. Depending on the scale of heterogeneities and the distance between the pumping and observation well, the pressure transient may not deviate significantly from the Theis curve at any observable time during the test.

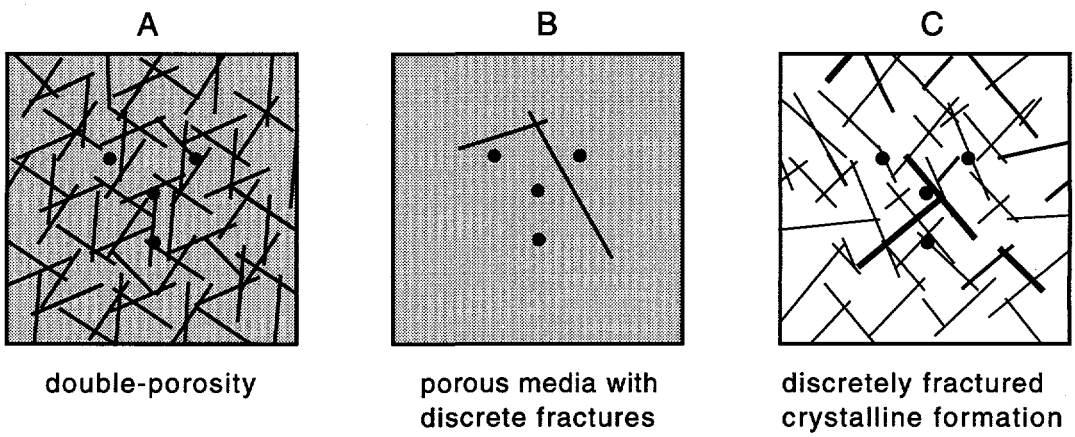

Figure 6.1. Schematic of different heterogeneous fractured rock aquifers.

Here we present an example of a transient response in the discretely fractured formation at Raymond. More detailed discussion of pumping tests and their analysis is presented in Cohen (1993). Well SW-3 was pumped at a constant rate and the transient water level responses in several adjacent wells were recorded. High precision pressure transducers were used to measure drawdown. The transducers can detect water level changes on the order of 0.1 mm, and measurements were recorded as often as every 10 seconds by an automated data acquisition system. Well SW-4 responded in an ideal confined aquifer manner, that is, a Theis curve can be matched to the transient almost exactly (Figure 6.2). This observation, coupled with the apparent density of fracturing in the subsurface (Figure 8.5), might reasonably lead one to conclude that the aquifer is sufficiently fractured and therefore can be modeled as an equivalent porous medium on the scale of the well field. Furthermore, the parameters obtained from curve fitting may be thought to represent the average properties within the well field. Both of these conclusions are incorrect, however. We now know that most wells intersect only several conducting fractures, and that some wells are connected by conductive fractures with transmissivities orders of magnitude greater than the value obtained from curve fitting. This example highlights the importance of implementing fracture flow profiling techniques to determine which fractures are actually conductive.(Chpt 9 & 10).

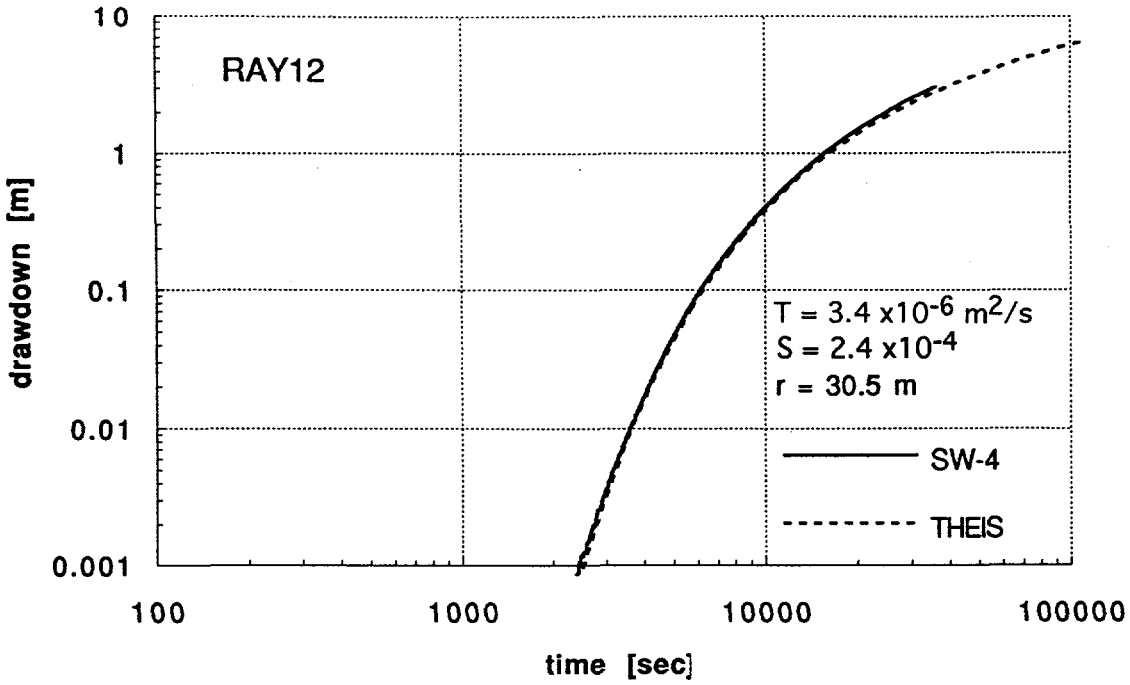

Figure 6.2. Theis curve match to drawdown in well SW-4 during constant pumping in well 0-0.

The important point in the above discussion is that in the limit of long pumping times, several kinds of fractured formations behave as ideal, confined aquifers. In some cases, depending on the scale of heterogeneities present and the distance to the observation well, nearly all of the transient may be fitted by a Theis curve. However, this does not mean the aquifer is indeed definable as some equivalent porous medium. Equally important is the fact that the parameters derived from fitting the Theis curve to the data can yield parameters that are not relevant to the area of interest. This is especially so when the data is analyzed using the semilog approach which only emphasizes the late-time data. The importance of recognizing this fact becomes obvious when one considers that estimation of capture zones are made using the derived transmissivity values. This problem and the relevance of the parameters derived in the above example are addressed in the following section.

6.1.3 Parameters Not Representative of Region of Interest

For a well in an ideal confined aquifer with uniform properties and infinite extent, the drawdown plots as a straight line on a semilog plot of drawdown vs. time (Cooper-Jacob plot), and this slope is not affected by duration of the test. In an aquifer

with a heterogeneous distribution of properties, however, the shape of the drawdown curve may have different slopes at different times, and therefore the drawdown behavior is partly dependent on the duration of pumping (Streltsova and McKinley, 1984). For example, in an ideal composite aquifer, in which a well pumps at a constant rate within the inner circular region of differing hydraulic diffusivity (*T/S*) than the outer, infinite region, the semilog drawdown plot exhibits two slopes. Figure 6.3 illustrates the case in which the transmissivity of the outer region is less than the inner region, but both regions have the same storativity. The first slope is inversely proportional to the transmissivity in the inner region, and the second slope is inversely proportional to the transmissivity in the outer region. The shape and duration of the transitional period depends on the ratio of inner and outer properties. Depending on this ratio and the location of the observation well, the semilog plot slope may not show any sign of a dual-slope characteristic. Regardless, in the limit of late pumping times the semilog slope becomes a function of the transmissivity in the outer region only, regardless of where the observation well is located.

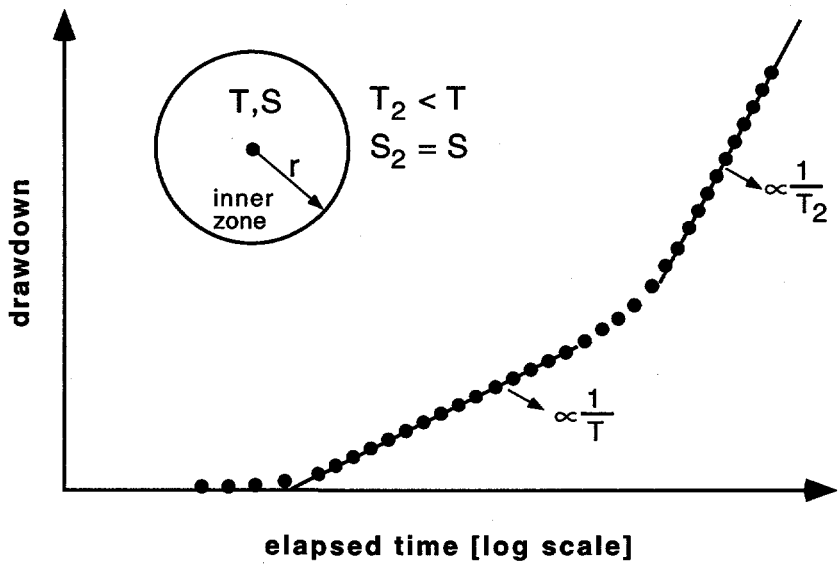

Figure 6.3. Transient response in pump well in an ideal composite aquifer.

The composite model is an idealized case, but its general behavior can be extended to other more realistic heterogeneities, and the dependence of the transient on properties further and further from the pump well applies to heterogeneous formations in general (Streltsova and McKinly, 1984). We now know, for example, through various hydrologic tests conducted at Raymond, that a fracture zone with a transmissivity of at

least two orders of magnitude greater than that shown in Figure 6.2 exists between well 0-0 to SE-3 (Chpt 9.4.4; Figure 9.17). In essence, the aquifer behaved as an effective composite system during the pumping test, but because well SW-4 is not situated adjacent to the inner region of greater transmissivity, its transient is mostly a function of spatially averaged properties outside of this inner region.

6.1.4 Well Bore Storage

The concept of well bore storage and its signature effect on the pressure transients in the pumped well is generally well known. It is briefly reviewed here because fractured formations generally have low storativities which magnifies well bore storage effects.

Because of the fluid stored in an open well, more water will be removed from the well than from the formation at early time periods following the initiation of pumping. Typically, well bore storage effects are identified as a unit slope at early times on a log-log plot of drawdown vs. time (Figure 6.4, inset). This behavior is easily recognized. Strictly speaking, however, a unit slope occurs only during the period when 100% of the pumped water is coming from the well bore. This period may not be recognized, either because it is of short duration, because the frequency of data measurements is not rapid enough, because of other early-time disturbances such as pump rate variations, or because of a combination of the above. In these cases, it may not be evident that well bore storage effects are still significant, even though the pressure transient in the pumped well is significantly influenced by well bore storage for a period extending 1 to 1.5 log cycles of time after the drawdown curve begins to deviate from the unit slope (Earlougher, 1977). Figure 6.4 shows that the pressure transient during well bore storage periods can appear as a straight line on a semi-log drawdown plot, and can mistakenly be used to calculate a fictitious transmissivity which will be less than that of the formation. A model that accounts for well bore storage effects may be used to analyze the data (e.g., Papadapolus and Cooper, 1967; Novakowski, 1990).

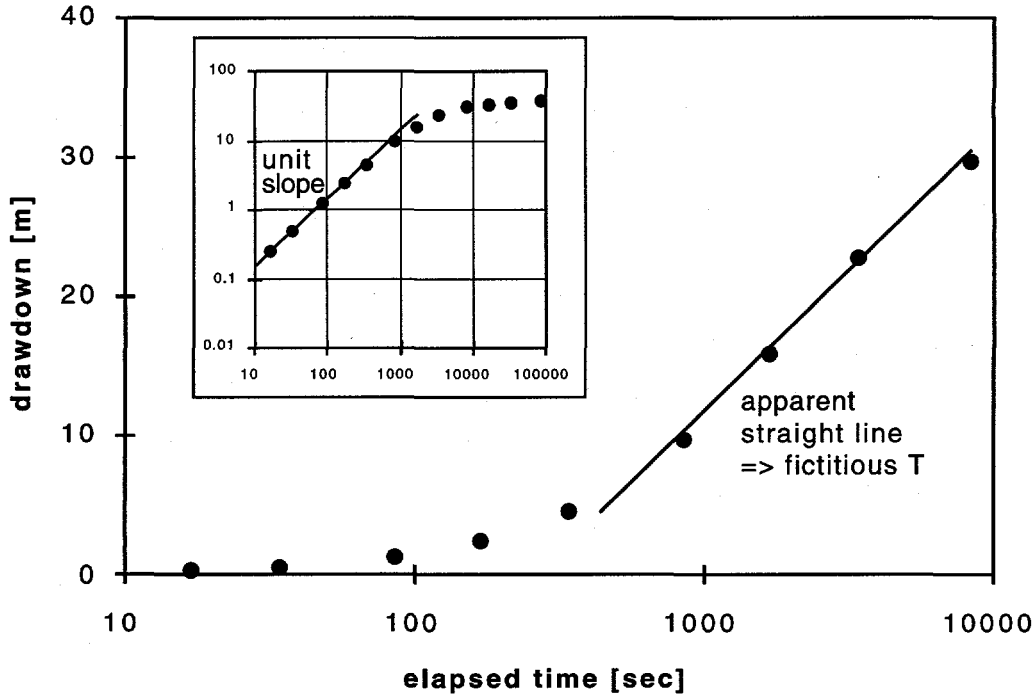

Figure 6.4. Well bore storage effect on drawdown transient.

If the unit slope behavior is not evident, one useful way to assess if well bore storage effects are still significant is to calculate the percentage of water withdrawn from the wellbore over a given flow period. This can be determined using water level decline over a specified time period, the cross-sectional area of well bore, and the pumping rate. A plot of percentage withdrawn with time can then be computed using the drawdown data.

Even if an analytic solution which accounts for well bore storage is used to analyze the drawdown, a significant problem is its masking effect of near-well heterogeneities. One way to avoid well bore storage effects is to pack-off the pump well with an inflatable packer above the pump. However, this requires some sophisticated equipment.

6.1.5 Apparent Anisotropy

Several methods have been developed to determine anisotropic properties of aquifers from transient drawdown measurements during pumping tests (e.g., Papadopulos, 1965; Hantush, 1966; Hantush and Thomas, 1966). These are the most commonly employed methods to determine the principle directions of anisotropy and/or

the tensoral transmissivity values, and they are developed for confined, horizontal aquifers. Fractured crystalline formations can behave as confined, equivalent homogeneous aquifers, as illustrated above. It may be tempting to analyze the pressure transients from pumping tests conducted in a fractured formation for properties of anisotropy, since the notion of a fracture network may seem corollary to that of anisotropy, and especially since both surface and subsurface fracture mapping yields obvious principle fracture orientations. However, the general fracture patterns present at the surface may not be ubiquitously connected in the subsurface over the scale of investigation, and there may be several dominant fractures controlling the hydrologic behavior that are not present at land surface. For example, surface and subsurface fracture mapping at Raymond showed very clearly that in general there are northeasterly and southeasterly dipping subvertical fracture sets, but subsequent hydrologic testing revealed that these are not the most hydrologically significant fracture sets throughout the well field. Furthermore, local subsurface heterogeneities can produce what appears to be anisotropic behavior, as illustrated below.

In an ideal confined and horizontal aquifer exhibiting anisotropy in the horizontal plane, the equipotentials around a fully penetrating pump well are elliptical rather than concentric. The late-time pressure transients in different observation wells located at different angular positions from the pump well have the same slope but different magnitudes when plotted on a distance-normalized semi-log drawdown plot. In essence, analysis of the slopes of these drawdowns and their x-intercepts forms the basis of determining the principle directions of anisotropy and their respective transmissivity values.

Figure 6.5a shows a hypothetical transmissivity distribution and the location of several wells within a portion of an aquifer. The wells are located at the same radial distance from the pump well to simplify this illustration, but the results can be extended for the case of different distances. Figure 6.5b schematically shows the general transient responses at these wells when the center well is pumped. Because of the greater hydraulic connection between the pump well and well #2 than between the pump well and the other wells, well #2 has the greatest drawdown. This high transmissivity zone may represent a region of relatively high fracture density, or the effective property produced by the presence of a single, high conductivity fracture, for example. Conversely, well #1 has the least drawdown because of the lower transmissivity region surrounding it. As the Figure shows, the local heterogeneities within the well field produce what appears to be anisotropic behavior. Although anisotropic properties could

be calculated from such data, the parameters would be erroneous and misleading. Karasaki (1987) numerically simulated constant rate injection into a heterogeneous fracture network and showed that the transients in arbitrarily chosen observation wells show apparent anisotropic behavior even though the system is not anisotropic. One has to have ample evidence of anisotropy, and generally should have more than three observation wells.

In general, the effects of local heterogeneities in producing seemingly anisotropic behavior will be lessened as the distance between pumping and observation wells increases.

6.2 Potential Negative Effects of Pumping Tests

6.2.1 Induced contaminant spreading to previously uncontaminated areas

Installation of wells introduces new transport pathways since the well itself has an extremely high effective transmissivity and because it can connect conductive fracture zones that were previously unconnected. Hence, contaminants may migrate in new ways, especially during pumping. Figure 6.6 illustrates potential migration of contaminants to previously uncontaminated regions. The Figure shows a schematic cross section of the formation at Raymond in the region of wells SW-1, 0-0, and SE-1. The general transmissivity distribution in each fracture zone is based on hydrologic test results. The flow pattern shown was actually observed when well 0-0 was pumped during an impeller flowmeter survey. It is quite apparent that if contaminants were originally present in the high conductivity region of the upper fracture zone around well SW-1, contaminants would migrate to the lower fracture zone during pumping because of the short-circuiting effect of the boreholes. Williams and Conger (1990) found that wells may have served as short-circuits for contaminants in a fractured bedrock aquifer.

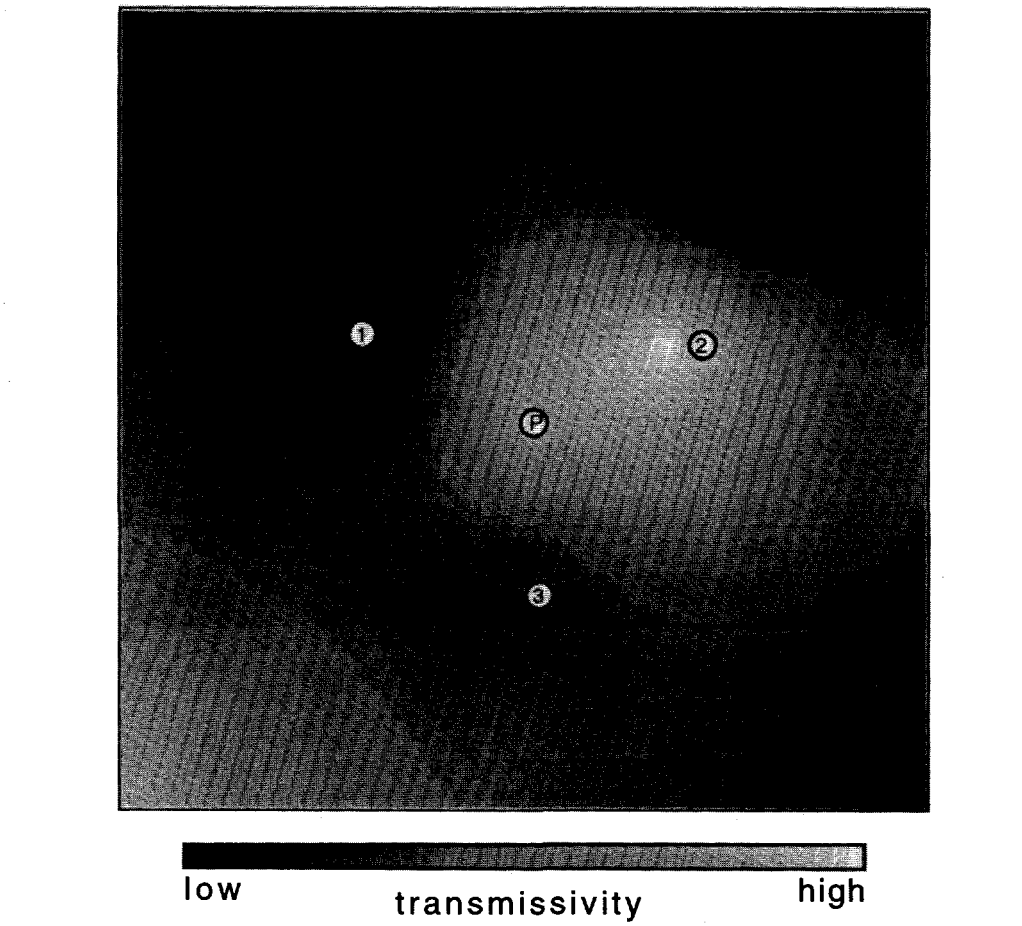

Figure 6.5. a) hypothetical transmissivity distribution and well field. p=constant rate pump well; b) transient response in observation wells.

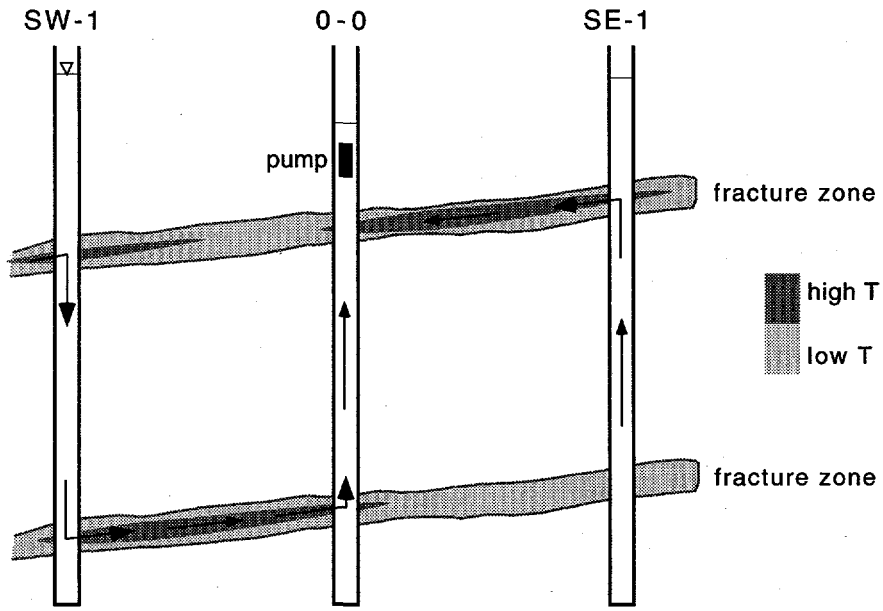

Figure 6.6. Flow pattern observed in wells during flowmeter test at the Raymond Field Site.

6.3 Summary

6.3.1 General

The purpose of this chapter was to highlight several problems associated with implementation and analysis of pumping tests in fractured formations. We showed that the drawdown transient in different fractured systems can behave in a manner describable by the Theis or Cooper-Jacob solutions, but that such behavior does not necessarily indicate the aquifer is an equivalent porous medium. Irrelevant parameter values can be derived from analysis of drawdown transients, and analysis of late-time drawdown may be essentially unrelated to the region of the aquifer that is of interest. Well bore storage can mask the effects of important heterogeneities, and semilog analysis of drawdown in the pump well will lead to underestimates of transmissivity. Local transmissivity heterogeneities can produce apparent anisotropic behavior in the drawdown responses in observation wells. The installation of wells can connect previously unconnected fractures and create short-circuit pathways. Pumping of wells can further initiate transport of contaminants to previously uncontaminated areas. The following recommendations are made based on the problems.

6.3.2 Recommendations

Given the inherent difficulties associated with pumping tests in fractured formations described in this chapter, we recommend the following:

• In order to maximize the information necessary for characterization and minimize cost and the potentially negative effects of pumping, pumping tests should *not* be conducted as tests in and of themselves. Other hydrologic tests which are necessary in characterizing a fractured formation yield more valuable information, and can simultaneously provide pressure transients amenable to standard pumping test analysis. For example, impeller flow meter profiling allows one to determine which fractures are conductive, and pressure transducers can be installed in wells during the test to measure pressure transients (see Chapter 9). Implementation of the proper drilling method can provide information regarding which well(s) are best suited for pumping.

• Pumping of wells during any type of test should be minimized in duration, and efforts should be made to analyze the entire pressure transient rather than resort to late-time data analysis only.

7 CONVENTIONAL GEOPHYSICAL LOGGING

The term conventional geophysical logging is used here to refer to logging methods other than the kinds described in chapters 8 and 9. Conventional logs include caliper, fluid temperature, fluid conductivity, and lateral logs; electric logging (e.g., spontaneous potential, single-point resistance, normal-resistivity, and focused resistivity); nuclear logging (e.g., gamma, gamma-spectrometry, gamma-gamma, and neutron). A very comprehensive review of the principles and uses of these and other downhole geophysical logging techniques used in groundwater investigations is given by Keys (1989). A discussion of the conventional geophysical logging performed at Raymond and their use in the characterization process in described in Chapter 10. The use of conventional geophysical logs at other sites for the purpose of hydrogeologic characterization is described by Paillet (1991), Williams and Conger (1990), and Jones and others (1985), for example.

8 DETECTION AND MEASUREMENT OF SUBSURFACE FRACTURES

Measurement of subsurface fracture properties is an essential component of the characterization process. Standard geophysical logs, packer injection tests, and various borehole flow detection techniques, for example, are most useful when combined with knowledge of the locations and orientations of particular fractures intersecting boreholes. When this information is used together, the geophysical and hydrologic properties of individual fractures and fracture zones can be determined. Analysis of these properties from multiple boreholes may then enable one to deduce the general subsurface hydrogeologic structure.

We implemented several subsurface fracture mapping/sampling tools at Raymond. Acoustic Televiewer (ATV) logs were collected in all nine wells. These logs provide images of the borehole wall, and were used to make quantitative measurements of fracture locations and orientation. Seven wells were probed with a digital borehole scanner. This tool provides high resolution optical, color images of the borehole wall, thereby enabling detailed measurement of fractures, identification of fracture mineralization, and other microscale properties. Television camera logs were used to visually evaluate sections of interest in boreholes, but no quantitative measurements were made. Lastly, fracture properties were measured from the cored portion of a newly drilled well.

8.1 Acoustic Televiewer (ATV) Logging

Detailed mapping of individual subsurface fractures in all nine wells was performed using acoustic televiewer logs. The orientation, dip, and apparent apertures of fractures were measured. The logs were collected in August, 1992 by the U. S. Geological Survey of Denver, Colorado. Several distinct fracture sets were identified from the analysis of fracture measurements.

8.1.1 Tool Description

An acoustic borehole televiewer (ATV) produces an image of the acoustic reflectivity of a borehole wall. Figure 8.1 shows a schematic of the logging system. As the probe is pulled up the borehole, a piezoelectric transducer is rotated at 3 revolutions per second, and it is pulsed between 800 and 2000 times per second. The emitted acoustic energy is reflected from the borehole wall and received by the same transducer,

which sends the signal to an oscilloscope at land surface. When the transducer rotates past magnetic north, a flux-gate magnetometer signals a sweep on the oscilloscope. Therefore, a complete 360° rotation of the transducer is represented by a complete scanline across the oscilloscope screen. Because the amplitude of the reflected acoustic signal will be lower where discontinuities and irregular surfaces are present, and because the brightness of the oscilloscope trace is proportional to this amplitude, fractures and other openings will appear as dark areas on the oscilloscope screen. Since the tool is moved vertically simultaneously with transducer rotation, a spiral strip of the borehole wall is probed, and a fracture plane that intersects the borehole at an angle other than 90° will ideally produce a sinusoidal image on the oscilloscope screen (Zemanek *et al.*, 1969; Keys, 1990). The rate of ascent of the probe in this study was 5 feet per minute, and all nine wells were logged in three days. A Polaroid camera was used to record the oscilloscope image, and the photographs were taped together to form a continuous log. A method to digitize the measurements has recently been developed (Barton, 1988). Figure 8.2 shows a portion of the ATV log of well 0-0.

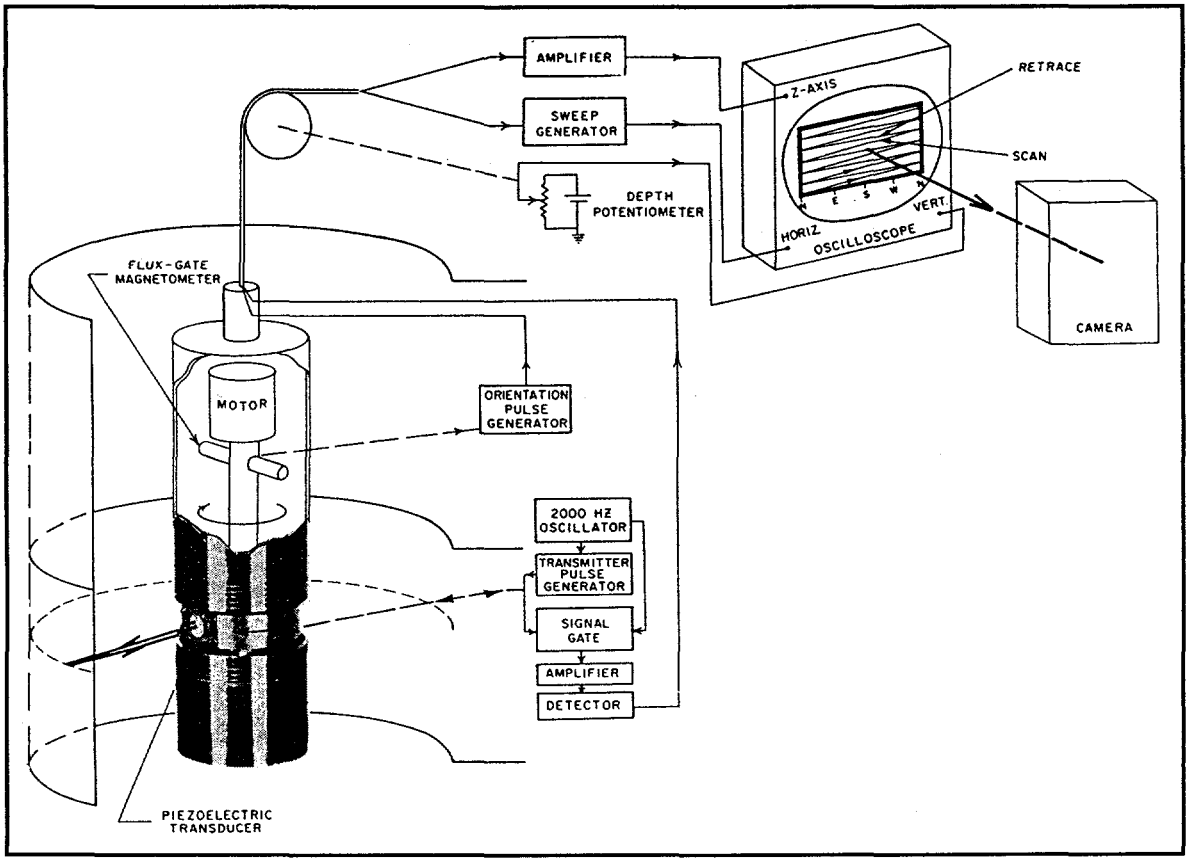

Figure 8.1. Schematic of ATV logging system (from Zemanek *et al.*, 1969). Reprinted with permission from the Society of Petroleum Engineers.

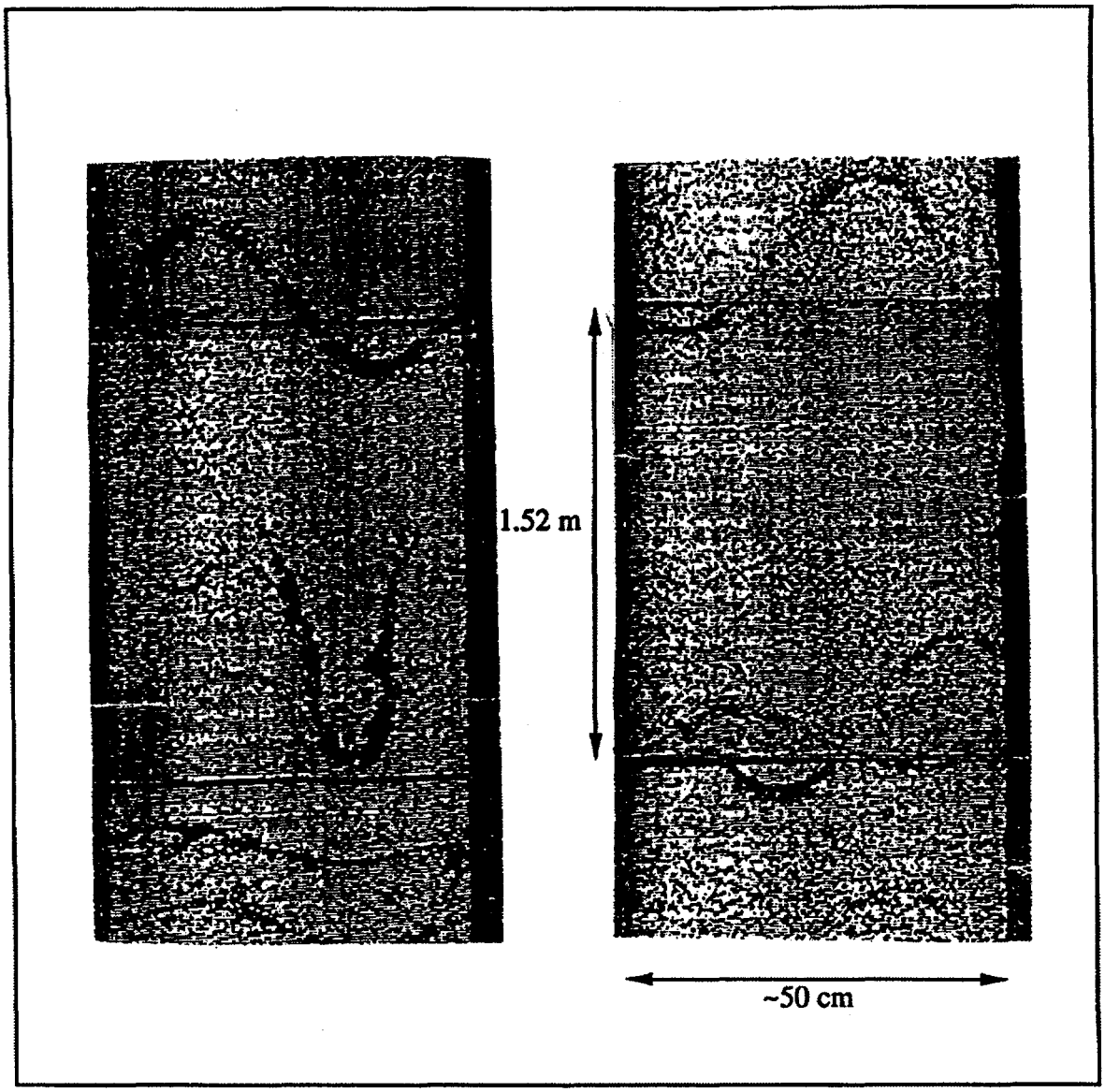

Figure 8.2. Portion of ATV image from well 0-0.

8.1.2 Fracture Detection and Measurement

Under ideal conditions the sensitivity of the ATV is great enough to detect open fractures in crystalline rocks with apertures greater than 1mm (Davison *et al.*, 1982) . Closed or completely filled fractures are not detected unless there is a difference between the acoustic reflectivity of their infilling and that of the intact borehole wall. Because the instrument measures reflected acoustic energy, the instrument can be used in clear or murky water, although image resolution is slightly better in clear water.

The determination of fracture dip and azimuth of individual fractures from the ATV log is relatively straightforward (Figure 8.3). The dip angle is simply the arc tangent of H/D. Since the edges of the oscilloscope image represent magnetic north, a 360° scale constructed to fit the width of the image can be used to determine the dip azimuth. Similarly, a scale constructed to fit the actual 5 ft borehole length represented by each oscilloscope image can be constructed.

An approximate aperture of the fracture can be calculated by measuring the thickness of the fracture trace and then correcting for the fracture dip angle. However, because of fracture alteration due to drilling, the accuracy of the calculated aperture is very questionable.

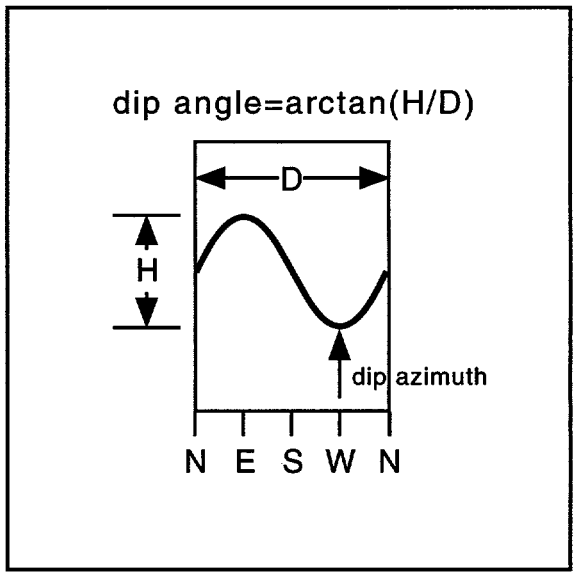

Figure 8.3. Determination of dip angle and azimuth of fracture from the ATV log. D = diameter of borehole.

8.1.3 Extraneous Effects

Measurements may be problematic because the fractures are inevitably disturbed by the drilling process and/or because fractures intersecting the borehole wall do not always form a sinusoidal image. Figure 8.4 illustrates how these conditions are manifested on the ATV log. Gouging of fracture infilling during drilling can result in an apparently open fracture on the ATV log. This can give the appearance that there are many transmissive fractures, when in reality only several are indeed conductive. Other filled and resilient fractures may go undetected (Figure 8.4 A, B). Concentration of stress at the fracture-borehole intersection during the passage of the drill bit often causes the

rock adjacent to fractures to break out. This in turn increases the apparent thickness of the fracture on the ATV log (Paillet *et al.*, 1985). Thin wedges of rock situated between closely spaced subparallel fractures that are either open or mineral filled can be broken out to give the appearance of a single large, open, and nearly horizontal fracture zone, the orientation and dip of which cannot be easily determined (Figure 8.4 C). For nearly vertical fractures, chips of rock are frequently broken out near the upper and lower fracture-borehole intersection. This gives the appearance that the fracture is more steeply dipping (Figure 8.4 D). Vertical deviation of the borehole can further complicate feature determination (Fig 8.4 E), but is easily correctable if borehole deviation logs are obtained. Also, magnetic field variations must be accounted for if the study site is situated in a region where the magnetic field has a strong vertical component (Keys, 1990).

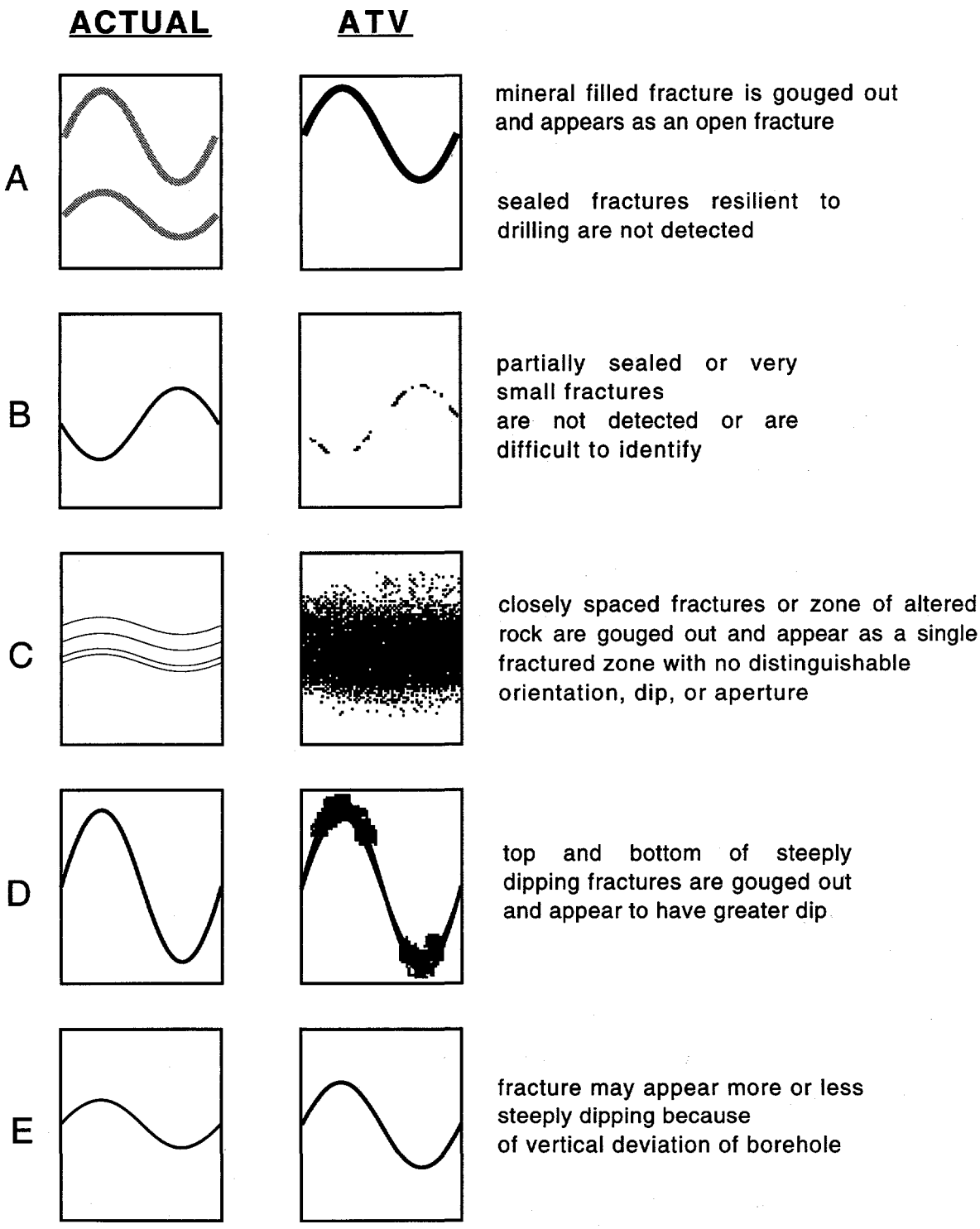

Figure 8.4. Effects of drilling and fracture type on fracture detection from ATV logs.

8.1.4 Analysis of ATV Logs from Raymond

ATV logs show that the number of fractures intersecting each well ranges between 70 and 200. Figure 8.5 shows the ATV logs of all nine wells. These are reduced images of individual sketches made from the ATV oscilloscope as the wells were logged (Paillet, U.S.G.S., Denver, 1992). Actual measurements were made from the oscilloscope photos, as described above. The logs reveal that the bedrock is intensely fractured. Without any knowledge of the hydraulic conductivity profile in each well, an initial and logical conceptual model of the aquifer might be that it behaves as an equivalent porous medium as a result of the intense fracturing. As it will be shown, only several fractures are indeed fluid conducting, thereby illustrating the importance of integrating various geophysical data to meaningfully characterize the subsurface.

Prior to fracture measurements, the detectability of the ATV was checked by carefully comparing the television camera log and the ATV log of well 0-0. All fractures visually observable were found to be recorded by the ATV. Using the Polaroid pictures of the oscilloscope, four measurements were taken of each fracture trace:

1) the elevation of the middle of the trace at its minimum depth,

2) the elevation of the middle of the trace at its maximum depth,

3) the dip direction, and

4) an average apparent aperture thickness, taken as an approximate average over the entire trace.

The logs from all nine wells were analyzed. For the sake of brevity, only the results from wells 0-0, SE-1, and SW-1 will be described here. The general methods and conclusion described pertain to all the data.

Measurements were made in English units since the photographs were marked at 5 ft intervals. Measurements 1 and 2 were taken with a standard ruler with markings every 1/10 inch. Because the vertical scale of the photos is 2.5 in/5 ft, a 0.20 ft elevation difference in the borehole measures as 0.10 inches on the photo. Interpolations were made to the nearest 0.05 in. (0.1 ft). A 360° scale with markings every 10° was used to measure the dip angle to the nearest 10°. To determine the dip angle as it is shown in Figure 8.3, H was taken as the difference between measurements 1 and 2. The nominal

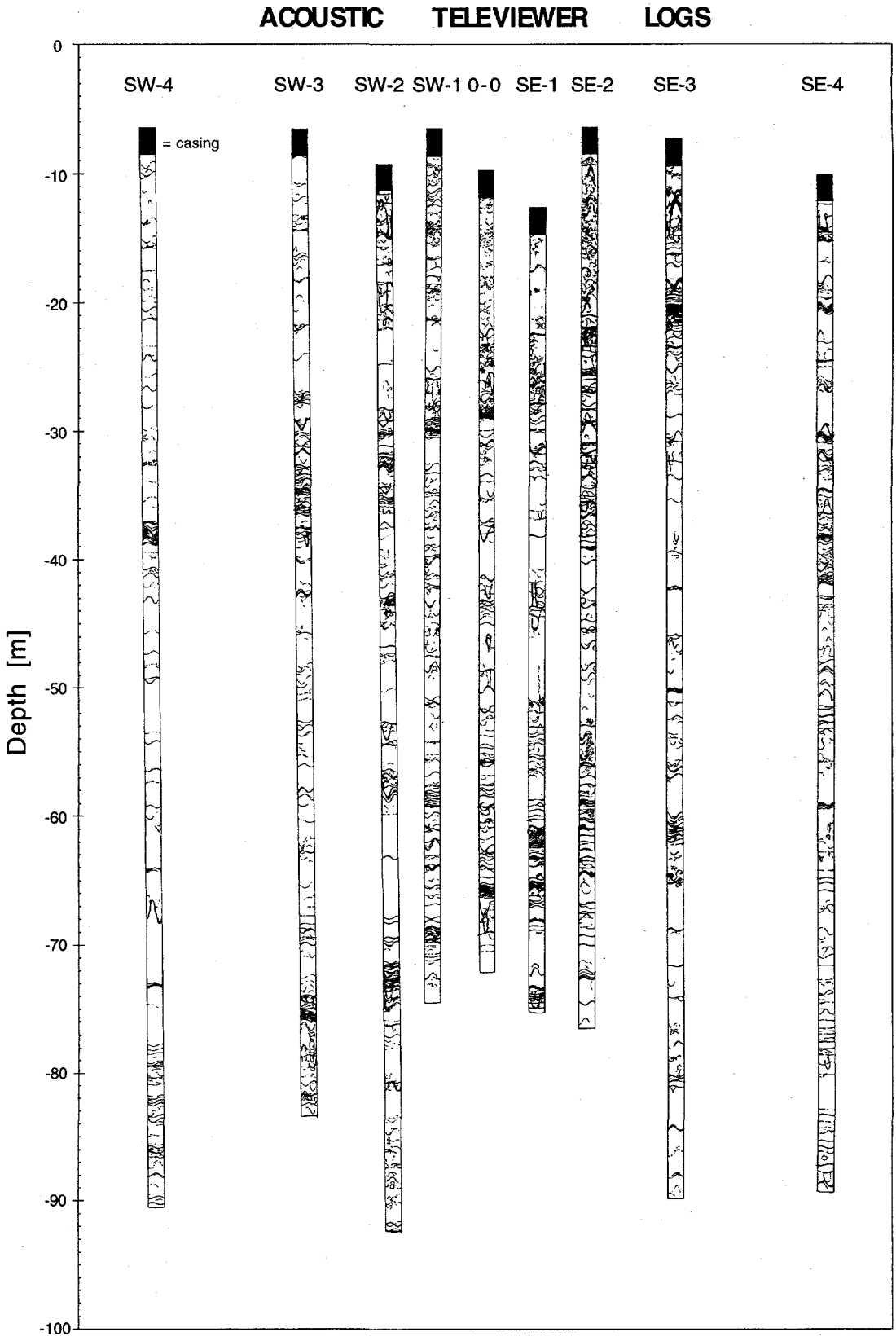

Figure 8.5. Acoustic Televiewer logs of all nine wells.

borehole diameter of the well was used for D. Geophysical logs indicate that all the boreholes at the site are essentially vertical and that the three boreholes investigated here deviate less than 3° from the vertical. No correction was made for this deviation, since the purpose of measuring the fractures was to examine the overall general structure, and since the relative errors associated with the measurements are of the same order as the deviation.

The above calculations were not possible for all fractures, however. Only one or two of the measurements were obtainable on traces that were not continuous across the entire borehole wall, for example. Several vertical fractures intersected the wells, and these do not show up as sinusoidal images on the ATV log. These fractures pierce the borehole over a short distance and therefore appear as oval traces with a major axis in the vertical direction. The azimuth of this axis was taken as the dip azimuth of these fractures. In addition, no fracture properties could be measured in the highly altered fracture zones that appear as large horizontal fractures, as described in section 8.1.3. Only an approximate thickness of these zones could be measured.

8.1.4.1 Identification of Fracture Sets

The ATV logs show that a combined total of approximately 210 fractures intersect wells 0-0, SE-1, and SW-1. The fracture traces that were not continuous across the entire televiewer image were difficult or impossible to measure with confidence. Therefore, only the measurements of the 181 continuous fracture traces constitute the fracture database from which the following analyses are based. It should be noted that the incomplete traces did not appear to be of fractures with distinctly different characteristics. They often paralleled other fracture traces, for example, but simply were not distinct enough to measure.

A density contoured stereonet projection of the mapped fractures in the three wells is shown in Figure 8.6. A stereonet is a convenient way to display fracture orientation data because it shows both the dip azimuth and angle of individual fractures. The principles of the stereonet are described in section 4.3.2. For the sake of clarity, the lines of longitude and latitude that normally appear on a stereonet have been omitted. The stereonet clearly shows that there are two nearly orthogonal, nearly vertical sets, as well as a set that dips to the west.

Measurements of the large, seemingly horizontal altered zones are not included in Figure 8.6. Inclusion of these fractures on the stereonet would give the appearance that many more horizontal fractures are present.

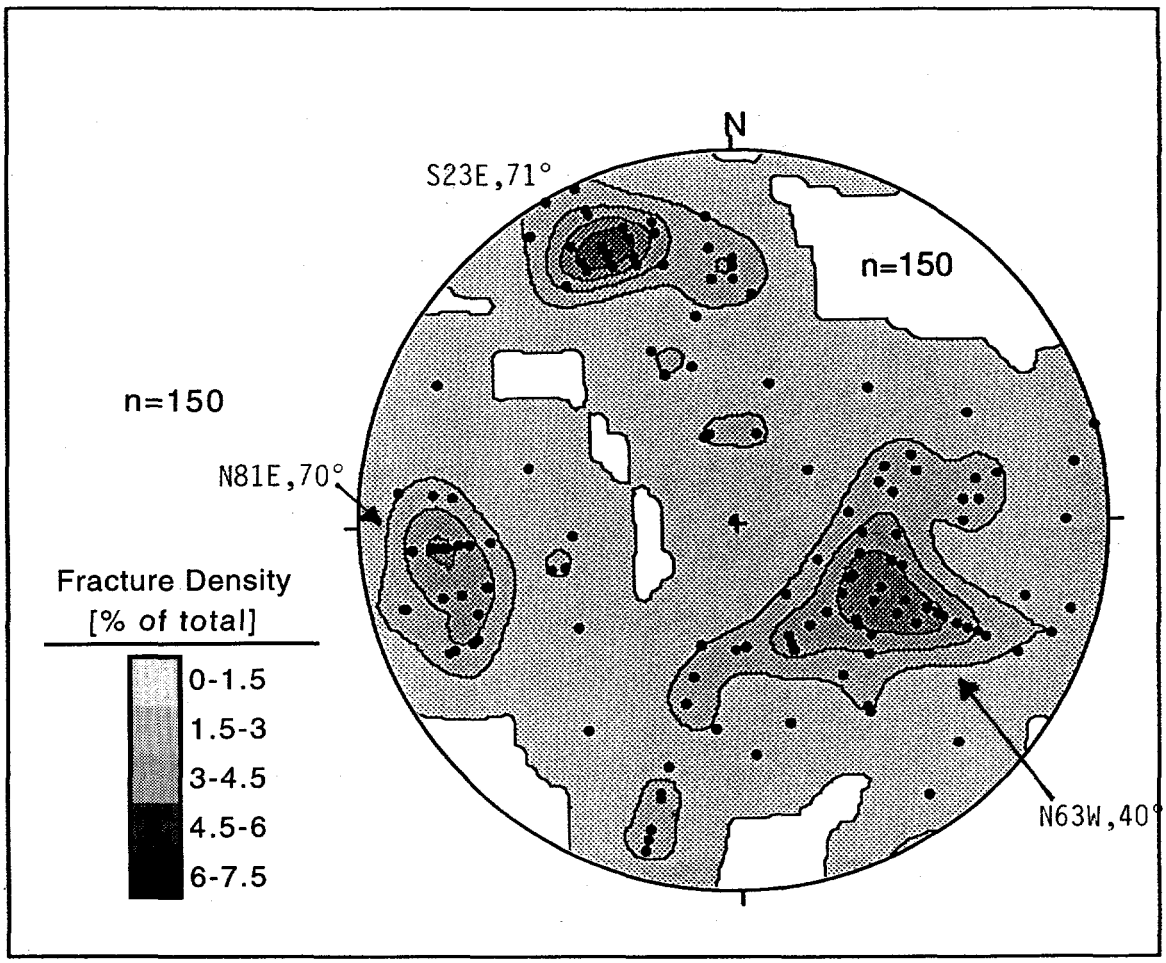

Figure 8.6. Density plot stereonet of mapped fractures from wells 0-0, SE-1, and SW-1 (Schmidt equal-area, lower hemisphere, polar projection). North is 1982 true north. Central tendency of dip direction and angle shown for each set.

The two subvertical and orthogonal fracture sets are tectonic fractures. This conclusion is based on their similarity to the two major tectonic fracture sets prevalent throughout the Sierra Nevada (section 4.4). It is not yet clear why the borehole-mapped subvertical fractures fall on only one side of the vertical as compared to surface mapping (section 4.4).

The westwardly dipping set is comprised of several different fracture types not discernible on the ATV logs. Detailed surface mapping, inspection of television logs, and correlation between ATV logs and geophysical logs reveal that within this general set

there are unloading fractures, pegmatitic dikes, and other types whose origins are not yet known.

8.1.4.2 Fracture Spacing Distribution

The spacing distribution of fractures measured from the ATV logs of wells 0-0, SE-1, and SW-1 is shown in Figure 8.7a. The data include all continuous fracture traces, including the seemingly horizontal and altered zones. The data appear to be distributed log normally (Figure 8.7b). Analyses used to examine the spatial structure of hydrogeologic data rely on measured statistical parameters of distributions such as these. However, considerable caution must be exerted before using these parameters to describe hydrogeologic properties, as described below.

Priest and Hudson (1976) concluded that unless there is a large predominance of evenly spaced fractures, any combination of evenly spaced, clustered or randomly positioned fractures will lead to a negative exponential spacing distribution. Such a combination would result, for example, when several different fracture sets are present or when fractures resulting from different tectonic events overlap one another (Chernyshev and Dearman, 1991). The distribution shown in Figure 8.7 contrasts these findings, but is not surprising. The fracture spacing distribution appears lognormal because very small fractures are not detected, thereby resulting in an underestimate of the number of smaller spacings between adjacent fractures (Chernyshev and Dearman, 1991). Effects such as this introduce errors into calculated statistical parameters. However, a more fundamental issue is whether or not it is appropriate to use fracture distributions such as spacing and aperture to infer hydrologic properties of the aquifer. Several investigators have attempted to correlate the spacing distribution of subsurface fractures with hydraulic conductivity in granitic rock with very little or no success (e.g. Jones *et al.*, 1986; Carlsson and Olsson, 1981). This results from the fact that fractures are highly disturbed during drilling and from the consistent finding that only a small fraction of the many fractures intersecting a well conduct fluid (e.g., Paillet, 1991). As shown subsequently, this also proved to be the case at the Raymond site. In light of these observations, it is generally inappropriate to use statistical descriptions of fracture orientation, spacing, and aperture based on ATV logs alone as a means to infer hydrologic properties. Meaningful analyses can be formulated if this data is coupled with fracture specific geophysical and hydrologic data.

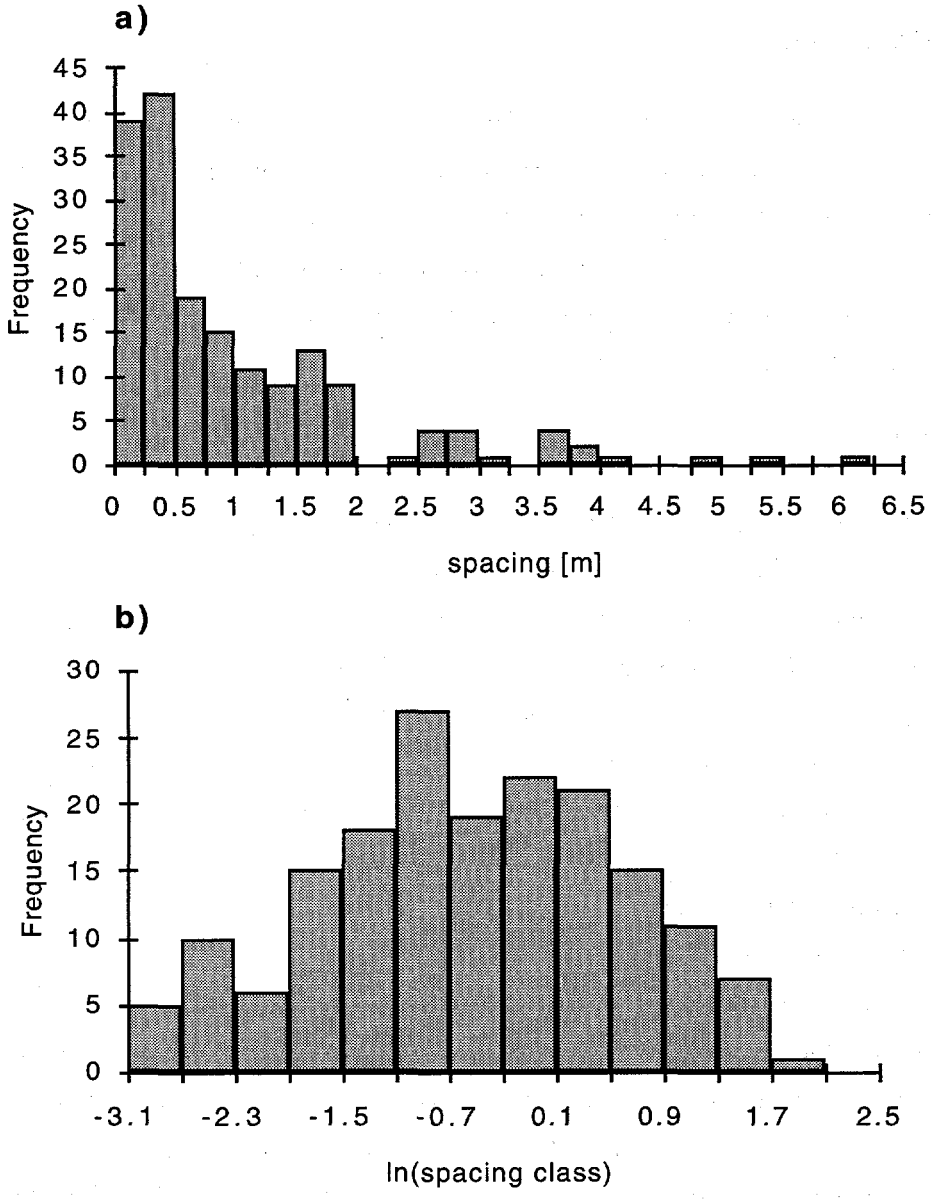

Figure 8.7. Fracture spacing histograms of all continuous fracture traces from ATV logs of wells 0-0, SE-1, and SW-1. a) frequency vs. spacing, b) frequency vs. log spacing.

8.2 Television Logging

Television logs were collected in all nine wells by a local contractor shortly after drilling. Images were recorded on standard VHS tape as the instrument was lowered down each borehole. Although no quantitative measurements were possible with the chosen type of video logger used, the images proved very valuable because they provide a means to visually examine fracture properties which are otherwise measured indirectly by the ATV and other geophysical logs.

8.2.1 Tool Description

Downhole cameras have been used for several decades primarily to diagnose problematic water wells, such as checking screen conditions and detecting casing deterioration, mineral deposition, or bacterial growth. The ease of video recording and various improvements over the past 20 years make them useful tools for formation characterization. Several different models are available through local logging companies. The more sophisticated versions include color cameras with remote focus and remote iris that allow optimum downhole viewing, cameras with rotating heads or lenses which allow close-up, straight-on views of the borehole wall, well screen, or casing (Katz, 1993). Some very recent versions provide images that are ready for computer processing to create conic sections. Color cameras are available in diameters as small as 4.1 cm (1-5/8 in.). Typically, the survey is viewed live at the job site on a TV monitor and is recorded on videotape for later viewing. The depth of measurement is encoded on the recorded video image. The most common version has a fish-eye lens oriented downward and an illuminating light centered in front of a camera mounted on the tip of a weighted logger cable, which is lowered either by an automatic winch or manually. This tool yields a color, 360° image of the borehole. This version was used to log the wells at Raymond.

8.2.2 Problematic Effects

An obvious requirement for effective camera logging is that the well water must be clear. Usually the water is murky after drilling, so the well must be pumped in order to remove residue and allow clean formation water to fill the borehole. Therefore, this problem is usually easily correctable. Potential problems with the more sophisticated versions are not described here.

8.2.3 Measurements and Results at Raymond

The standard fish-eye lens downhole camera as described above was used to log all nine wells at Raymond. The overall diameter of the tool was 3 in, and was equipped with remote iris and focus control. The color video image was recorded on standard VHS tape, and the depth of images was encoded in the corner of the image. A sample of the images is shown in Figure 8.8. Because these are black-and-white reproductions of the actual video, details such as discoloration on the borehole wall can not be seen. The light mounted in front of the camera is at the center of the image.

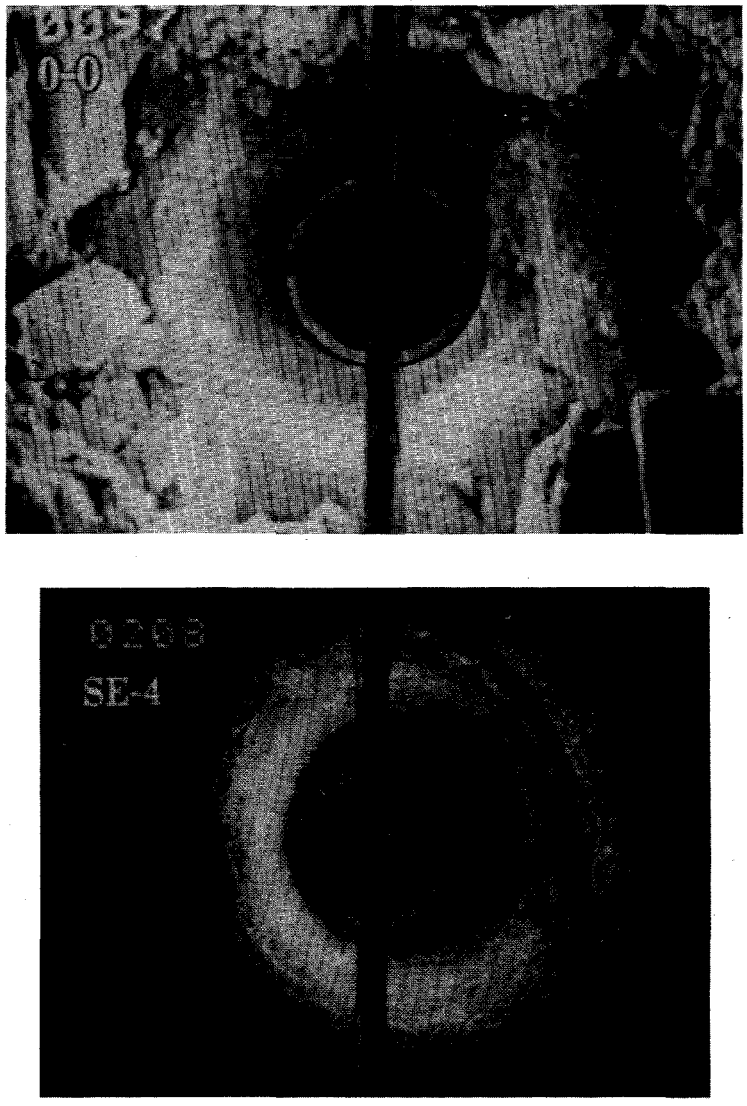

Figure 8.8. Television camera log images of wells 0-0 and SE-4. Actual video is in full color, and some resolution was lost in processing the video to obtain these images.

8.2.3.1 Fracture Observations

The television logs had several, very useful applications. Firstly, various pertinent information not observable on the ATV logs was obtainable. In some cases it was possible to see whether or not particular fractures were infilled or not, thereby reducing the seemingly enormous number of possibly conductive fractures seen on the ATV logs. Areas of discoloration around individual fractures could be seen, and therefore helped locate fractures that might be hydrologically altered and warrant future investigation. The location of many pegmatite dikes were identified because their large, reflective crystals were easily recognizable on the image. Peaks on natural gamma logs were believed to be associated with pegmatitic dikes. The television logs validated our inferences, and thereby allowed us to confidently identify where pegmatites were located based on geophysical logs alone. This was very valuable because we later found that these dikes were one of the significant conductive fracture sets. In addition, and as described in section 8.1, the television log was used to verify the ATV log. For these reasons, the television logs were a very valuable addition to the collection of geophysical logs.

On a more basic level, the visual images provided by the logs were invaluable in terms of providing a mental image of what the general interior of the borehole looks like. Seeing what blow-out zones, undisturbed zones, and discrete fractures *actually* look like is helpful when planning future borehole tests, and in developing one's conceptual model of the subsurface.

The possibility of using the television images to further divide the fracture sets measured from the ATV logs into more detailed sets with differing properties was explored. The television log of well 0-0 was carefully examined and qualitative properties of individual fractures was recorded. These included whether or not the fracture was open or mineral filled, and a qualitative assessment of degree of alteration. This was a very tedious and time consuming task which involved the repeated rewinding and forwarding of the video tape to view individual fractures. Dikes could be identified, but only in a few cases could we definitively conclude if they were fractured or not. It is more feasible to inspect particular fractures of interest after standard geophysical and flow logs are conducted.

8.3 Digital Borehole Scanner

The digital borehole scanner (DBS) is a new logging tool which provides optical, true color images of a borehole wall. The digitally recorded data yields very high resolution images, thereby enabling detailed measurement of fractures, identification of fracture mineralization, and other microscale properties not observable with other instruments. Seven wells at Raymond were logged with a DBS between March and April, 1995. The tool was developed by Core Corporation, Japan, and is now being tested and further developed at Lawrence Berkeley National Laboratory. Reference to Core Corporation does not imply any endorsement by the authors or by the agencies that funding this work..

8.3.1 Tool Description

The DBS produces a digital, unrolled color image of the borehole wall. Figure 8.9 shows a schematic of the logging system. The primary components are the white light source, rotating mirror, magnetic compass or gyroscope, and photoelectric transformer. The mirror rotates at 3000 rpm, simultaneously illuminating the borehole wall and directing the reflected light through a lens and into a photoelectric transformer. The mirrored section is encased in clear glass. The transformer measures the intensity of the red, blue, and green light wavelengths and converts them to digital form. The data stream passes through an azimuth gauge and is marked at the point corresponding to north. The controller receives the oriented reflectance data and scanner depth data, which comes from the depth gauge. Presently, the minimum depth increment the gauge can detect is 0.1 mm. The combined data is stored on digital tape. A scrolling, unrolled image of the borehole wall is also simultaneously recorded on video tape and displayed on a TV monitor (Thapa, 1994).

8.3.2 Fracture Detection and Measurement

Both water filled and dry boreholes can be scanned with the DBS. The water must be clear in order to obtain images, so the borehole generally needs to be pumped after drilling to remove suspended particulates. Plans are underway to equip the instrument with an infrared light source. This will enable scanning in murky water (Thapa, 1994).

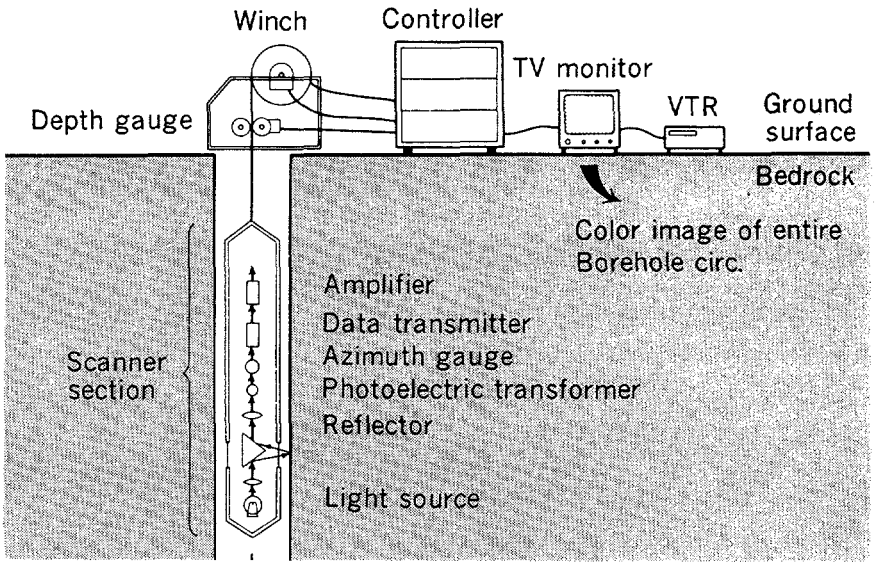

Figure 8.9. Schematic of Digital Borehole Scanner System.

Since the tool records high resolution color images, mineral filled fractures, open fractures, and zones of discoloration due to rock alteration by fluids can be detected. Fracture features are easier to detect in lighter color rocks such as granites and gneisses than in darker colored rocks such as shale. Software accompanying the tool enables quick measurement of fracture properties from the 2-D image of the borehole wall. Optical lenses in the tool have focal ranges of several centimeters, so even fracture properties in gouged and altered zones often can be detected and measured. This contrasts ATV logs, which can not detect individual fractures in zones where the borehole has been heavily disturbed by drilling. Lenses for different sized boreholes are available and interchangeable. Currently, lenses for borehole diameters between 6 and 30 cm are available. The maximum vertical resolution of the DBS is 0.001 mm, but depends on the logging rate. Horizontal resolution depends on the diameter of the borehole. For the 17 cm diameter wells at Raymond, the horizontal resolution was about 0.5 mm. In general, the extremely high resolution color capabilities of the instrument can yield borehole images that are comparable to close-up photos of actual core. The following section shows a DBS image from a section of well at Raymond.

The high resolution recording results in a very large data set for each well. For the logging and image recording method used for the Raymond study, for example, one probed meter of the borehole required about 7 megabytes of storage space. Data is stored on a digital audio tape (DAT). A personal computer is used for data processing and image analysis (Thapa, 1994).

In general, the digital borehole scanner can provide borehole images with resolutions comparable to actual cores. The tool may therefore replace acoustic televiewer logging, television logging, and expensive coring. Improvements which allow fast detection and measurement of fracture properties, as well as other geophysical properties is imminent. For example, a method to automatically scan the borehole data and detect and measure fracture orientations is being developed at LBL; image detection techniques may be used to identify hydraulically altered fractures, and measurement of a greater portion of the light spectrum may enable detection of fluid specific properties and mineral composition of rock. Measurement of infrared absorption may enable detection of organic contaminants, for example. In summary, the current capabilities of the digital borehole scanner and near future advancements in the tool design, data processing, and the application of image analysis techniques make the DBS the logging tool of the future.

8.3.3 Measurements and Results at Raymond

All wells except SE-2 and SW-2 were scanned with the DBS. Each borehole took approximately 3 hours to log. A pair of centralizers were mounted at both ends of the measurement section. The logging rate was slow enough to maintain the maximum vertical resolution of 0.1 mm. Horizontal resolution is approximately 0.5 mm. The scanned wells have nominal borehole radii of 8.5 cm, and the lenses used had a focal range between 7.5 and 10 cm.

Figure 8.10 shows the unrolled digital image of well SE-1, for example. Note that discrete open fractures, dikes, and rock discoloration are clearly noticeable. The vertical line in the images is the small shadow created by a small necessary wire within the light source. It does not effect image quality.

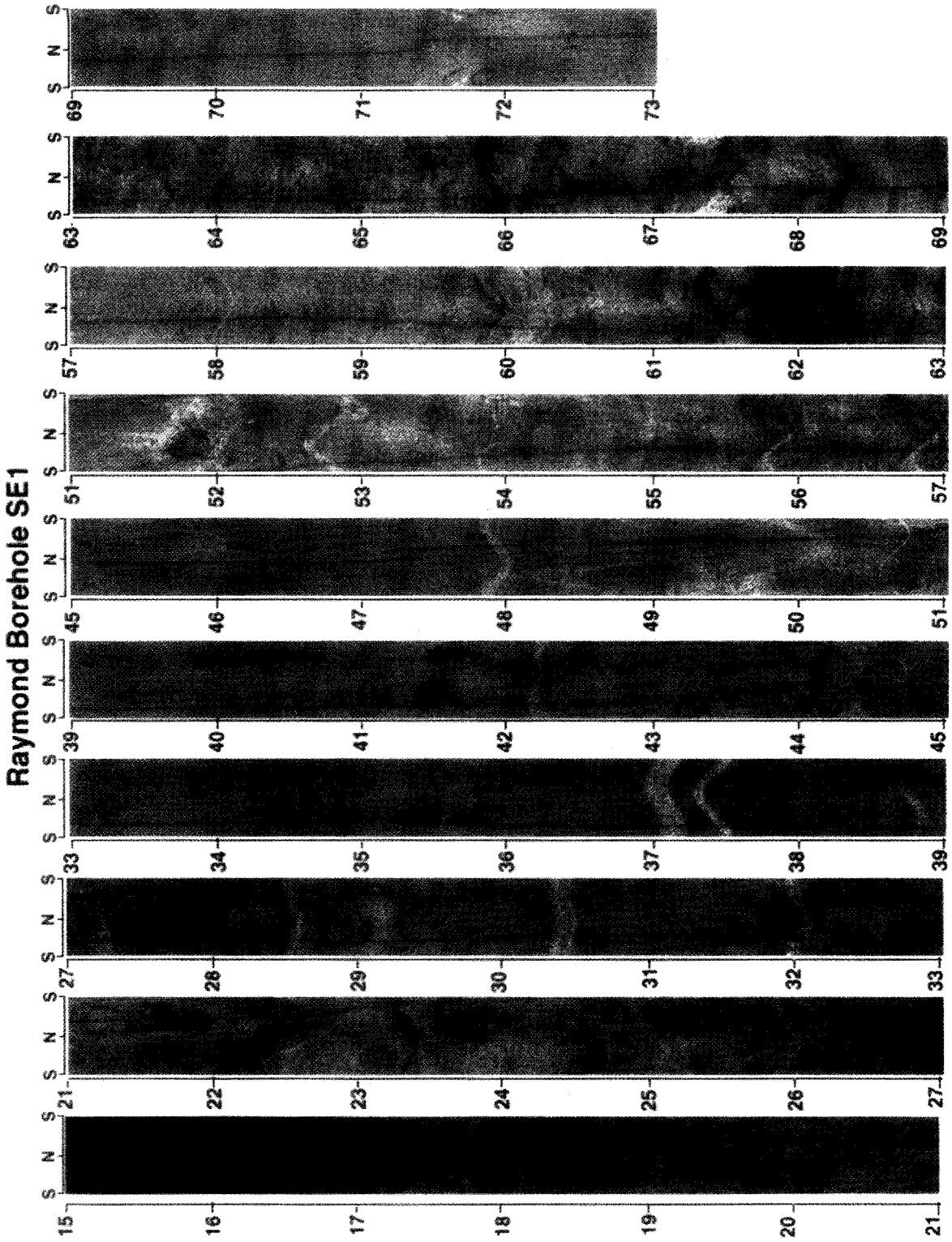

Figure 8.10. Digital Borehole Scanner image of well SE-1.

We found that a very important capability of the DBS is its ability to scan regions of the borehole that have been highly disturbed by drilling. The highly transmissive fracture zone near 30m in well 0-0 was substantially enlarged and disturbed during drilling. This is the same zone that appears in Figure 8.8. Because of this damage, the acoustic energy emitted from the ATV was substantially attenuated and scattered, and the ATV image is therefore completely black; the fracture properties of the individual constituent fractures can not be measured. In contrast, the image from the digital borehole scanner reveals that the zone is comprised of at least two fractures. The orientation and dip of the fractures were measured and used to determine where they might intersect the other wells. This information, coupled with standard geophysical and flow logs enabled us to determine how the fractures were connected to other wells. This is described in section 10. Given that many of the more hydrologically significant fractures are usually altered and therefore easily disturbed during drilling, the capability of the DBS to detect the individual fractures within these zones is very valuable.

8.4 Borehole Core Analysis

No cores were obtained prior to the completion of this document. However, work at other sites may provide some general guidelines. Within the granitic rock at the Whiteshell Research Area in Canada, Paillet (1991) found that ATV logs consistently detected all fractures listed as permeable or possibly permeable by the core logger, for example, and the combination of ATV, television, and conventional geophysical logging at Raymond provided more than sufficient data needed to deduce fracture characteristics. Coring is probably unnecessary for most field applications, especially considering its expense.

8.5 Comparison of Techniques

All of the techniques enable detection and measurement of fractures to varying degrees and at varying costs. The advantages and disadvantages of each technique are described below.

DOWNHOLE TELEVISION CAMERA:

advantages:	disadvantages:
• most local contractors offer the service at relatively inexpensive rates. Least expensive method.	• very difficult to measure fracture properties from common tool version. Newer models may enable easier measurement.
• logs are stored on video tape, which make data easily accessible.	• visibility is reduced or is zero in murky well water.
• enables qualitative look at fracture properties such as alteration and infilling.	• detection of fractures may be more difficult in dark rocks.
• provides one with a mental image of the borehole and its features. This is useful for planning of future tests and in developing a conceptual model of the subsurface.	
• can be used in water filled and dry portions of the well.	

ACOUSTIC TELEVIEWER (ATV):

advantages:	disadvantages:
• fracture orientation and dip are easily measured manually.	• because of drilling effects, sealed fractures and dikes get gouged and appear as open fractures. Hence, there appears to be many more open fractures than there are.
• complete log of well is in the form of a strip of photographs. Therefore the data is easily accessible and manageable.	• individual fractures within intensely altered and broken-out zones cannot be detected. This is important, since flow is usually associated with these zones.
• quantitative data set of fractures properties provides a means to determine geophysical and flow properties of fractures using other logs.	• can not directly observe fracture infilling and alteration.
• tool can be used in clear or murky water.	• can only be used in water filled portion of well.
• detection of fractures is not affected by color of rock.	

DIGITAL BOREHOLE SCANNER (DBS):

advantages:	disadvantages:
• provides high resolution color images which enable detection and measurement of fracture properties, identification of mineralization, and other microscale properties.	• very large disk storage space and significant data processing efforts are currently needed. However, advancements in data manipulation and faster computers will make this a logging tool that can replace television, ATV, and core logs.
• can be used in water filled and dry portions of the well.	• detection of fractures may be more difficult in dark rocks.
• quantitative data set of fracture properties provides a means to determine geophysical and flow properties of fractures using other logs.	• expensive method; currently in research and development stage.
• can detect fractures in altered and break-out zones.	
• provides information gained from ATV, downhole camera, and cores, and at higher resolution.	
• digital data storage enables computer-aided image analysis techniques to be performed.	
• data is also stored on videotape, thereby providing same benefits as television camera but at much higher resolution.	

CORE ANALYSIS:

advantages:	disadvantages:
• provides direct observation of fracture properties and measurement of fractures	• most expensive and time consuming method
• lab tests can be performed	• sample disturbance can result in fracture orientation measurement errors
• real samples	• not economically or time feasible for all the boreholes usually needed in a remediation/characterization effort.
• usually can see if particular fractures are open or infilled	• cores have to be physically stored in storage room
	• may mistake drilling-induced fractures for in-situ fractures

8.6 Summary

8.6.1 General

The acoustic televiewer, television camera, and digital borehole scanner were used at the Raymond site to detect and measure fractures intersecting boreholes. The orientation and dip of individual fractures was calculated from measured fracture traces made from acoustic televiewer logs. Three general fracture sets were identified from these measurements. The measurements also provided a fracture database which was used throughout the study. Fracture-specific hydrologic and geophysical properties were determined by comparing the results to various hydrologic and geophysical logs. This is described in later sections. Downhole television camera logs provided color videotapes of the interior of each borehole. Quantitative measurements were not possible, but the logs enabled us to view particular fractures of interest, and in some cases determine if they were infilled or hydrologically altered. Very importantly, the television logs revealed that many of the fractures identified by the ATV were indeed infilled. The digital borehole scanner provided high resolution color images of the borehole wall. Not only were many more fractures detected compared to the ATV logs, but infilling, alteration, and fracture properties within highly altered zones were measurable. Measurements from the images and development of an automated fracture detection and measurement algorithm is underway.

8.6.2 Recommendations

The identification and measurement of fractures intersecting boreholes is an absolute necessity. Besides its use in determining the general fracture trends or sets, a database of fracture locations and orientations in boreholes enables one to determine fracture-specific geophysical properties because it can be compared with standard geophysical and flow logs, for example. The combination of a flow meter log and an acoustic televiewer log may enable determination of the particular hydraulically conductive fractures, and its measured orientation and dip may be used to determine which fracture set it belongs to and where it may intersect other wells.

Although the digital borehole scanner provides the most and highest resolution data, its current expense makes logging by other methods more feasible. However, given the capabilities of the tool and imminent reductions in its cost, it will be the best tool for use in the near future. At present, acoustic televiewer and television logs used together

provide very useful fracture data, especially when coupled with standard geophysical logs. Fractures can be easily mapped from the ATV logs, and television logs can be used to check if particular fractures are altered and infilled. We found that the ATV is most useful for identifying the location of fractures and determining their orientation, rather than for measurements of individual fracture properties, such as aperture or roughness. The determination of orientation and dip of individual fractures was very useful for later use, when the data was integrated with visualization software and measured fractures were extrapolated to see where they might intersect other boreholes. Most of the information gained from coring is obtainable through the combined data from the ATV, television, and standard geophysical logs, which are more economical and timely.

The large data set resulting from the fracture measurements makes a statistical analysis of spatial properties very tempting. However, because of the effects of drilling on the appearance of individual fractures and on the fact that only several of the many fractures detected conduct fluid, statistical descriptions of fracture aperture and spacing, for example, based on ATV data alone should not be used to estimate general hydrologic properties.

9 BOREHOLE FLOW LOGGING

The term borehole flow logging refers to various logging techniques with which hydraulically conductive intervals in the borehole can be identified. The techniques described here also enable calculation of the transmissivities of particular intervals. Flow logging is a critical component of the characterization process. There often appears to be hundreds of fractures intersecting a borehole, and flow logging provides a means to identify only the relatively few which are in fact conductive. Results from borehole logs are best when integrated with other geophysical logs. For example, properties of the conductive fractures measured from other geophysical logs, such as their orientation, electrical resistivity, or gamma activity can be used to assess which fractures in different wells are interconnected throughout the well field. Flow logging therefore provides a means for determining the hydrologic structure of the aquifer and the potential contaminant pathways.

Four different flow logging techniques were implemented at the Raymond site. Impeller flowmeter profiling was performed in three wells. All nine wells were profiled with a thermal-pulse flowmeter. Fluid conductivity logging was performed in seven wells, and straddle-packer injection tests were conducted in all nine wells. This chapter describes the different tools and methodologies and their applications at Raymond. A comparison of the results from each method is presented, followed by a summary of the advantages and disadvantages of each tool/method and recommendations on how to best use and integrate them.

Paillet et al. (1994) describe other instruments such as the electromagnetic, laser doppler, and acoustic doppler flowmeter. Molz and Young (1993) describe the application of the electromagnetic flowmeter in a fractured rock aquifer.

9.1 Impeller Flowmeter

Impeller flowmeter tests were conducted in wells 0-0, SE-1, and SW-1 between October 23 and November 6, 1992. Water was pumped from the upper portion of a well and the vertical flow at different depths was simultaneously measured. This procedure was repeated in each well. The flow entering the well between particular depth intervals was determined from the variations in vertical flow with depth. A quantitative estimate of the transmissivity of different depth intervals was determined based on the calculated inflows and the observed pressure transients produced by pumping.

9.1.1 Tool Description

The impeller flowmeter is a relatively simple tool that can measure vertical flow in a well bore or screened interval. The tool has been used for several decades in the petroleum industry, and is the oldest of the flowmeter methods described in this report. Several studies describe its application to groundwater studies. Molz et al. (1989) describe its use in a stratified, porous aquifer, and compare the results to slug tests. Several models are commercially available, each with different sensitivities and detection limits.

Figure 9.1 shows a schematic of the impeller flowmeter used in this study. The tool is composed of an impeller-type flowmeter mounted above a hollow shaft that passes through the center of an inflatable packer. Older models utilize a centralizer rather than a packer. When the assembly is inflated at depth beneath an active pump, upward flow is forced through the flowmeter. The shaft of the impeller is mounted in an oil suspension with bearings, and two magnets are mounted to the impeller shaft. The rotating magnets activate a sealed reed switch mounted adjacent to the shaft, and an electric signal is sent through a logging cable to a surface display where readings are obtained in revolutions per minute. Some flowmeters are equipped with different rotation sensors, such as a Hall effect sensor or optical encoder. Some recent models have installed jeweled bearings that further reduce friction on the shaft, thereby reducing the stall velocity of the instrument and increasing its sensitivity (Paillet, et al., 1994). Flow rates are determined with a calibration curve obtained in the laboratory or field. Models equipped with the packer assembly are generally better, since a single calibration curve can be used for different diameter boreholes, and especially since all of the flowing water is forced through the measurement section. For flowmeters equipped without a packer, separate calibration curves must be obtained for different borehole diameters. Another option is to use a

funnel which is fitted in place of the centralizer or packer. Most versions only measure flow magnitude, not direction.

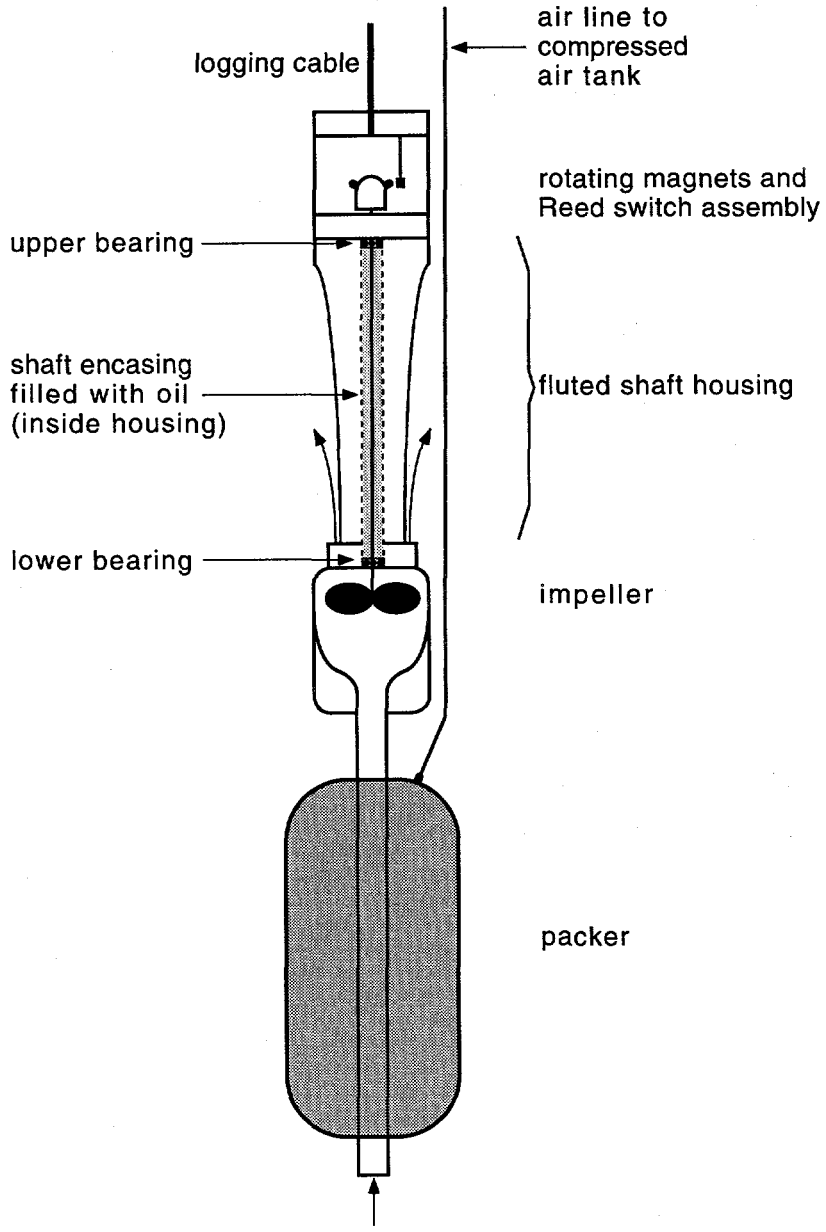

Figure 9.1. Schematic of impeller flowmeter.

Impeller flowmeters typically have minimum detection limits (referred to as stall velocity and starting velocity) greater than other instruments, such as the thermal-pulse and fluid conductivity methods. However, their range is much greater than the others, and this makes them well suited for high velocity borehole conditions. The stall velocities of the most commonly used impeller flowmeters are on the order of 0.05 m/s

(~5 ft/min) (Keys, 1990), but recently developed versions can measure velocities less than the thermal-pulse (reference). These are generally research tools and are not yet commercially available. The impeller flowmeter used in this study was originally developed at Lawrence Berkeley National Laboratory for use in geothermal wells in which very high velocities, temperatures and potentials for mechanical corrosion of the instrument are present. The instrument was therefore not developed for very low flow detection which is necessary in fractured formations. The minimum measurable flow is approximately 4 L/min. Rehfeldt et al. (1989) used an impeller flowmeter that measures flows approximately 1/10 this amount.

9.1.2 Flow Measurements

A schematic of a test configuration is shown in Figure 9.2. Near the top portion of the uncased wellbore, water is pumped at a constant rate to the surface via a downhole-submersible pump. A pressure transducer is situated above the pump, and the flowmeter-packer assembly several meters below it. The packer is inflated at this initially shallow depth and the pump is turned on. After the flow through the packer stabilizes, it is deflated, lowered to another depth, and inflated again. A measurement is taken and the procedure is repeated successively at different depths. The flow rate is determined from a calibration curve. The flow entering the well bore within particular depth intervals is simply the difference in flow measured at two depths. Figure 9.3 shows an example profile of measurements and calculated inflows.

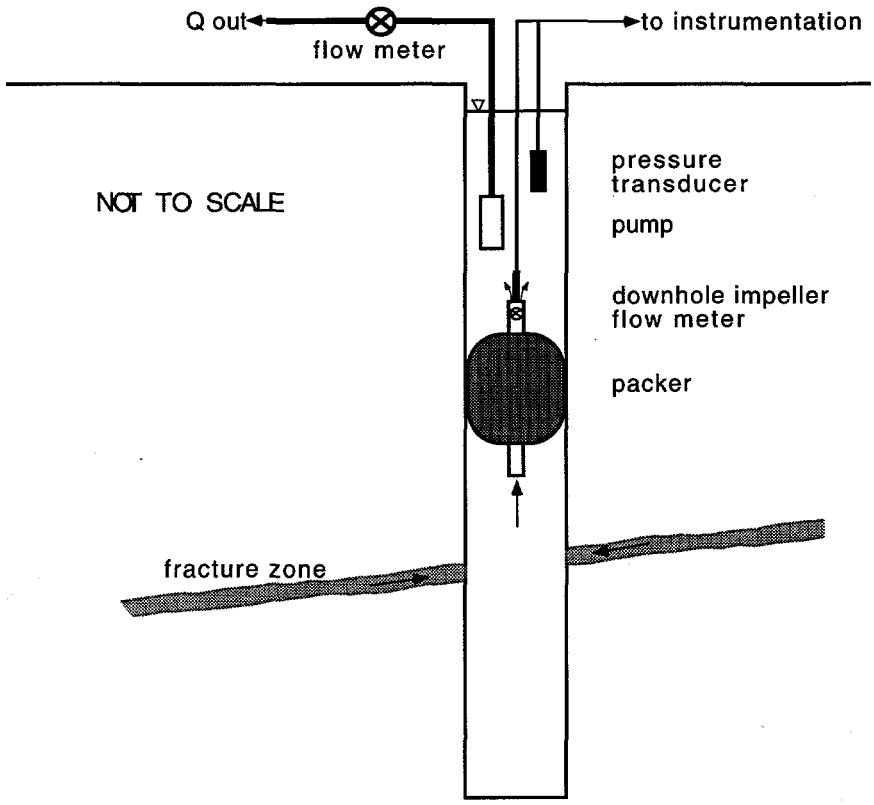

Figure 9.2. Schematic of impeller flowmeter test configuration.

9.1.3 Data Analysis

Flow measurements with depth can be used to identify the locations of conducting intervals and their contribution to total flow. These calculations are straightforward, as shown in Figure 9.3. A quantitative estimate of the transmissivity of different depth intervals can be determined based on the calculated inflows and the observed pressure transients produced by pumping.

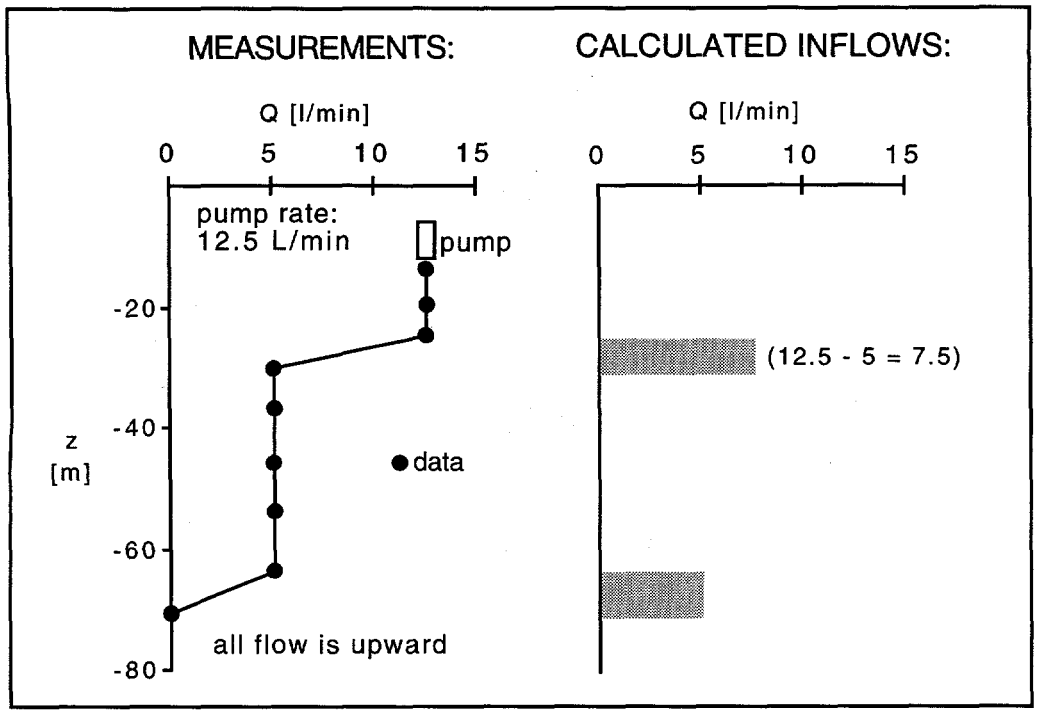

Figure 9.3. Example flow profile and calculation of wellbore inflows.

In an ideal confined aquifer, in which the pump well penetrates the entire aquifer thickness, water flows horizontally towards the well. After a relatively short time of pumping, drawdown in the pump well can be expressed by the Cooper-Jacob equation:

$$s_{(r_w,t)} = \frac{2.3Q}{4\pi T}\log_{10}\frac{2.25Tt}{r_w^{\,2}S} \tag{9.1}$$

where s is the drawdown, Q is the total pumped discharge, T and S are the aquifer transmissivity and storativity, respectively, t is the time since pumping began, and r_w is the well radius. When $4Tt / Sr_w^{\,2} \geq 100$, the error in using (9.1) rather than the complete Theis formula is less than 0.3% (de Marsily, 1986). Taking the derivative of s with respect to r_w in (9.1) reveals that the hydraulic gradient near the well is constant in time. For this reason, a semi-steady state condition is said to exist near the pump well when (9.1) becomes applicable (Matthews and Russell, 1967). Javandel and Witherspoon (1969) studied the transient pressure behavior in multilayered aquifers in which the permeability contrasts between the horizontal layers differed by several orders of magnitude. They found that cross-flow between layers occurs at early times following the initiation of constant rate pumping, and that the degree of this cross-flow and its duration depends on the degree of permeability contrast. At large times, there is

negligible cross-flow near the well bore, and the pressure transient in the pump well is sufficiently approximated by the Cooper -Jacob equation. The flow into the well from each layer is then proportional to the transmissivity of the layer (Witherspoon and Javandel, 1969):

$$Q_i = \alpha T_i = \alpha K_i b_i \tag{9.2}$$

where α is a constant of proportionality, K is the average horizontal hydraulic conductivity over the interval b, and the subscript i denotes a particular depth interval. Since

$$Q = \sum_{i=1}^{n} Q_i = \alpha \sum_{i=1}^{n} K_i b_i = \alpha T \tag{9.3}$$

it follows from (9.2) and (9.3) that

$$K_i = \frac{TQ_i}{b_i Q} \tag{9.4}$$

or

$$T_i = \frac{TQ_i}{Q} \tag{9.5}$$

Equation (9.5) can be solved if the transmissivity of the formation and percentage of total pumped water is known. The formation transmissivity can be determined from analysis of the pressure transient during pumping. By simple rearrangement of (9.1), it is straightforward to show that

$$T = \frac{2.3Q}{4\pi(\Delta s / \log \text{ cycle})} \tag{9.6}$$

The transmissivity can therefore be found from (9.6) by plotting the drawdown vs. the logarithm of time and noting the slope of the first straight line portion of the curve.

An alternative approach is to consider each interval as a distinct layer for which the Cooper-Jacob equation applies. The drawdown in each layer is expressed in a fashion identical to (9.1), except that the bulk parameters are replaced by the parameters of each layer, s_i, Q_i, T_i, S_i, where i represents a particular layer. The transmissivity of each layer is then solved iteratively (Rehfeldt et al., 1989). However, this method requires that the radius of the well and the storativity of each layer be known, and these are essentially

impossible to define. Furthermore, the differences between the real flow geometry and that assumed in the analytic model are already too great to warrant such an approach.

The application of the analysis method above can yield useful estimates of the transmissivities of different conductive fractures or fracture zones. As with any aquifer analysis, however, one must understand how deviations from the idealized case from which the equations are derived influence the accuracy and relevance of the calculated values.

9.1.4 Validity of Analysis and Extraneous Effects

The above analysis assumes horizontal and radial laminar flow towards a fully penetrating well in a layered and confined aquifer. This may be a reasonable approximation for systems where continuous bedding plane fractures intersect the well, for example. In most fractured systems, however, the flow geometry is very complex and unknown. Very importantly is that late-time pressure transients can plot as a straight line on semilog plots regardless of the type of fracture system and boundary conditions, and this transient can be unrelated to the flow properties near the well. This and other potential effects such as well bore storage is addressed in Chapter 6 (Pumping Tests). Further, there are potential head losses associated with the presence of the pump, because of turbulence, and from other factors. Rehfeldt et al. (1989) describe many factors affecting flowmeter measurements. The condition of a confined aquifer is probably satisfied if the flowing fractures are beneath the water level in the well.

In light of the fact that the actual flow geometry is unknown, and since numerous factors influence the pressure transient, the T_i estimate obtained by applying equation 8.5 and 8.6 should be considered an order of magnitude estimate. One alternative is to use the ratio Qi/Q as a descriptor of the relative conductivity of a particular interval. A practical problem with these tests is that a particular well may be very low yielding, thereby making it impossible to sustain water levels above fractured intervals and/or the pump. For this reason, it is very helpful to know which wells are high yielding. Results from drilling logs may indicate such conditions (see Chapter 5; Well Drilling). The instrument may need to be calibrated often because of bearing degradation. The fact that impeller stall velocities are relatively high can result in a situation whereby no flow is detected beneath a particular depth although upward vertical flow is present. This occurred at Raymond, for example.

9.1.5 Measurements and Analysis of Results at Raymond

For the sake of brevity only the results from well SW-1 are discussed here. Figure 9.4 shows the semilog drawdown plot for the flowmeter test conducted in well SW-1. The fluctuations in water levels at later times correspond to the inflating and deflating of the packer. The inflating and deflating of the packer did not change the overall drawdown slope, and therefore they do not significantly alter the transient behavior in the well bore. Pressure transducer data was recorded every 30 seconds. To insure that the packer sealed the borehole, it was inflated at depths where only minor fractures and no blowouts are present. In addition, it was inflated to slightly higher pressures at greater depths to compensate the compression caused by the additional height of water above it. The transmissivity over the entire uncased wellbore is determined using equation 9.6. However, the test in well SW-1 followed shortly after the test in well SE-1. Therefore, the transmissivity determined from a previous pumping test in well SW-1 was used . The drawdown that would have occurred in well SW-1 if the test in well SE-1 had not been conducted earlier was determined by subtracting the superimposed effects of the aquifer recovery from the drawdown observed in well SW-1. The transmissivity calculated from this drawdown was the same as that calculated from the earlier test in well SW-1. This is additional evidence that the mechanics of the flowmeter test did not significantly alter the drawdown response in the pump well.

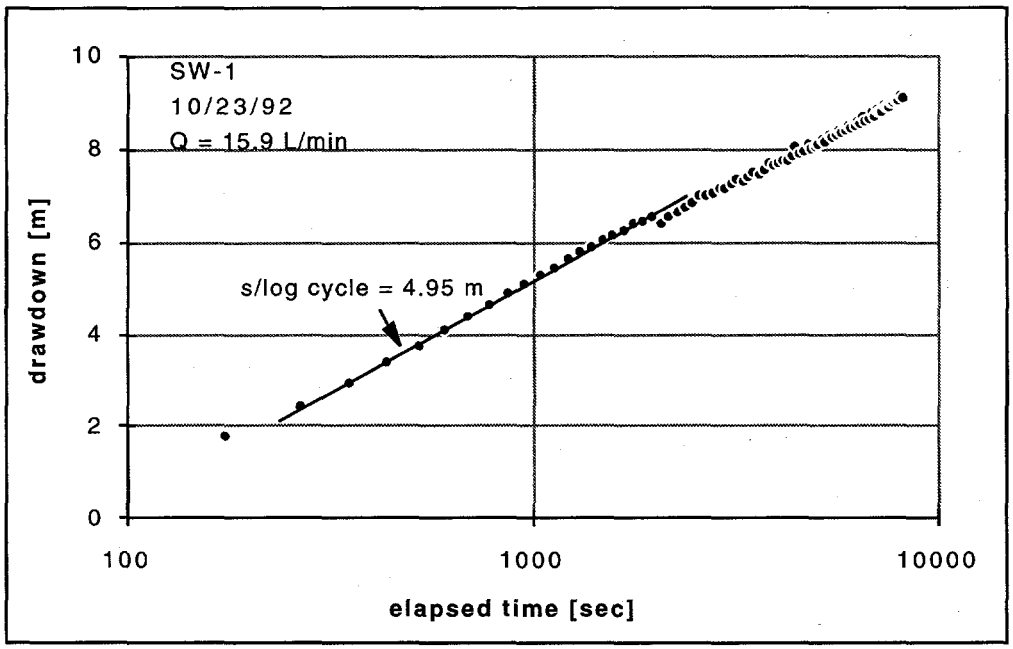

Figure 9.4. Semilog plot of drawdown vs. time in well SW-1 during impeller flowmeter test.

Figure 9.5 shows the vertical flow profile in well SW-1 and the calculated flows between measurements. The flow rate below the pump is assumed to equal the pumping rate. The calibration of the downhole flowmeter prior to the test in SW-1 revealed that the impeller had a stall velocity below 21 rpm (1.2 gpm). Therefore, a measurement of zero rpm does not necessarily indicate that no flow entered the wellbore beneath the depth of measurement. A measurement beneath 64.5 m yielded a zero value, so the flow entering the well in the interval between the bottom of the well and 64.5 m was taken as the discharge recorded at 64.5 meters. Additionally, where measured downhole flow did not vary significantly between different depths, the interval between those measurements was considered a no-flow zone. This was the case for the interval between 27.6 and 64.5 meters. The calculated flows and the total transmissivity calculated above were used in (9.5) to calculate the transmissivity of each flow interval.

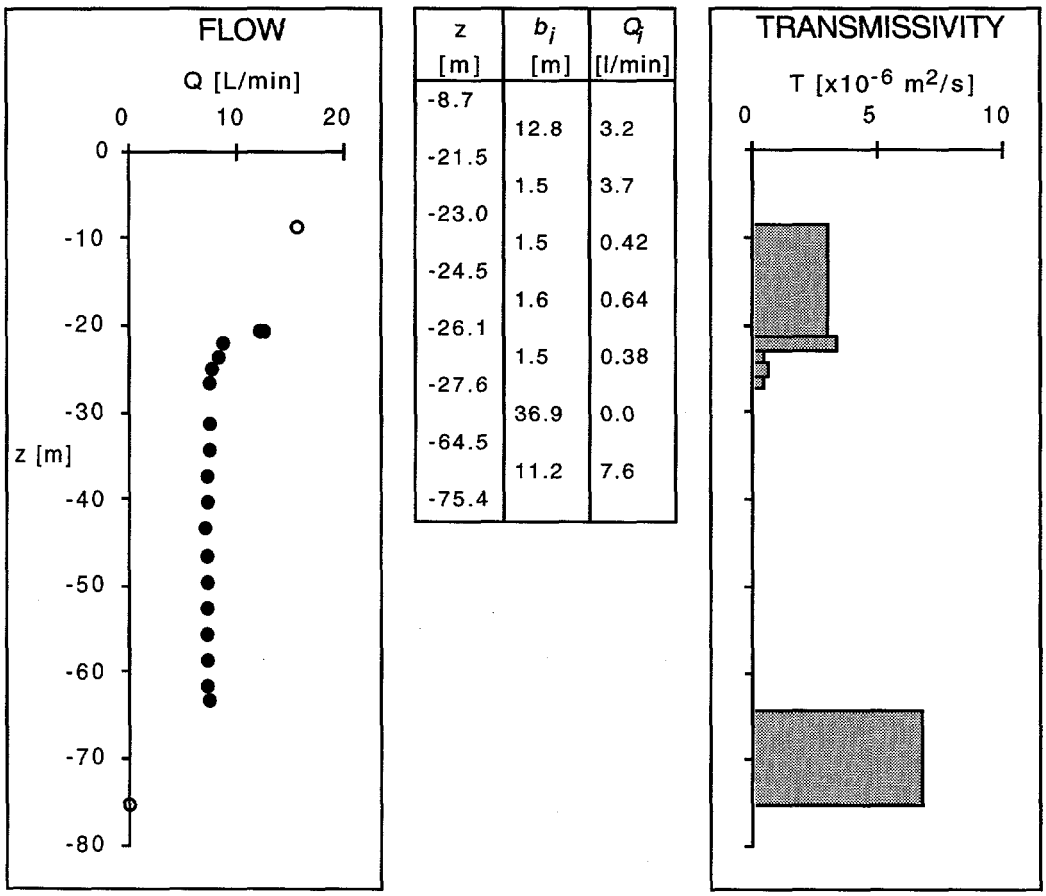

z [m]	b_i [m]	Q_f [l/min]
-8.7		
	12.8	3.2
-21.5		
	1.5	3.7
-23.0		
	1.5	0.42
-24.5		
	1.6	0.64
-26.1		
	1.5	0.38
-27.6		
	36.9	0.0
-64.5		
	11.2	7.6
-75.4		

Figure 9.5. Vertical flow profile in well SW-1 measured with impeller flowmeter and calculated transmissivity distribution.

9.2 Thermal-Pulse Flowmeter

Thermal-pulse flowmeter surveys were conducted by the Borehole Geophysics group at the U. S. Geological Survey, Denver between August 14 and 20, 1992. These surveys consisted of profiling the vertical flow in several observation wells while one well was being pumped. In addition, one well was profiled during aquifer recovery after pumping, and another during the injection of water into an adjacent well. The locations of conducting fracture zones were identified by noting changes in vertical flow with depth, an indication that flow either enters or exits the borehole. Interpretation was aided by comparing the results with various geophysical logs, and is described in Chapter 10. No quantitative description of the conductivity of fractures could be determined because observation wells were profiled during the pumping of a central well.

9.2.1 Tool description

The thermal or heat-pulse flowmeter used by the U. S. Geological Survey is described by Hess (1986). Other works describing its application to hydrogeological characterization of fractured formations include Paillet et al. (1987) and Williams and Conger (1990). A schematic of the tool is shown in Figure 9.6. The instrument measures vertical flow in a borehole. Flow direction and velocity are determined by observing the direction and time of travel of a heated parcel of water. A grid of resistance wire situated in the center of the sensor tube is pulsed with an electric current, thereby heating a small parcel of the flowing water. Temperature sensors (thermisters) are located above and below the heater grid along the flow axis. The thermisters form two arms of an electric bridge, which becomes unbalanced when the heated water passes one of them. An electric signal proportional to the bridge imbalance is transmitted through a logging cable to the surface unit, where it is amplified and recorded on a clock driven strip-chart recorder. The direction of water movement is determined by noting the direction of bridge unbalance, which is indicated by the direction of the signal. A positive and negative pulse trace indicate upward and downward flowing water, respectively. The time of parcel travel from the heating grid to the thermister is proportional to the distance between the heat pulse trigger and response peak. This response time ranges from less than 1 second for fast flow to more than 1 minute for very slow flow (Hess, 1986). An inflatable packer may be used to fill the annulus between the measurement section and the borehole wall, thereby forcing all the water to flow through the flow section. Calibration of the tool in the laboratory allows for the calculation of flow rate from the

observed heat pulse response time. The USGS heat-pulse flowmeter can measure flow between 0.04 to over 75 L/min (0.01 to 20 gpm) in boreholes. When a packer is used it can measure flow ranging between 0.05 to 10 L/min (Paillet, 1991). It can operate in boreholes with diameters ranging from 5 to 38 cm (2 to 15 inches) (Hess and Paillet, 1990). Commercial versions of the heat-pulse flowmeter have been developed. These versions have similar lower detection limits, but narrower flow ranges than the USGS version. Some are utilizing inflatable packers to concentrate flow, and one version is capable of detecting horizontal flow (Crowder, et al., 1994; Kerfoot, 1988).

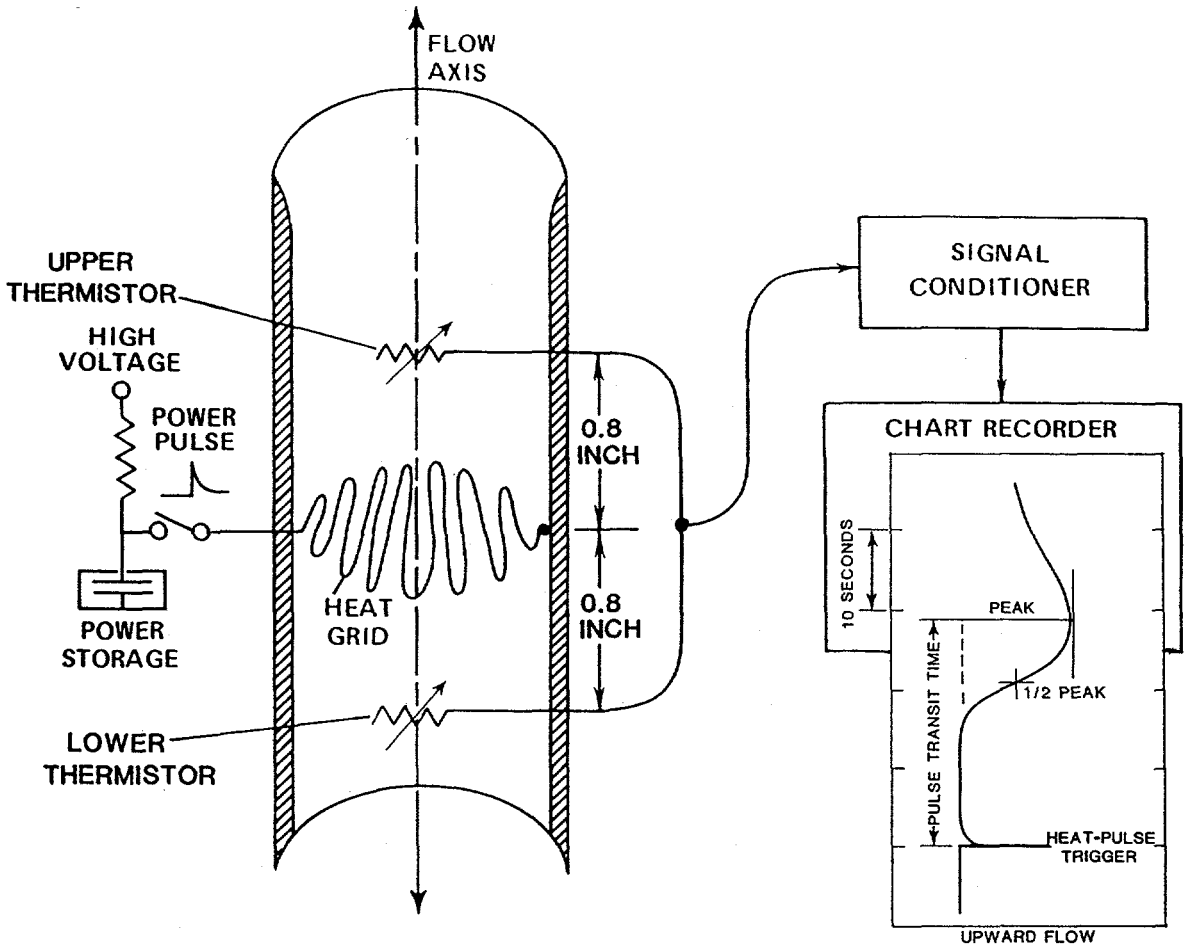

Figure 9.6. Schematic of heat-pulse flowmeter (modified from Hess, 1990).

9.2.2 Flow measurements

Flowmeter measurements can be made during natural conditions, while an adjacent borehole is pumped or injected, or during the recovery of the system after pumping. Measurement made in boreholes under natural conditions have indicated the locations of conducting intervals (Paillet, et al., 1994), although no flow was detected in the Raymond boreholes without pumping.

Pumping or injection establishes a flow field within the formation, and hence flow within and between boreholes which may otherwise not be observable during natural conditions. For the case when a central well is pumped and observations are made in adjacent boreholes, the flowmeter is positioned near the upper portion of an adjacent well at the beginning of the test and vertical flow is monitored. After large flow fluctuations at that depth subside, profiling is initiated. After the probe has been moved to another depth several minutes are allowed to pass before measurements are taken in order to let the turbulence created by moving the instrument subside. Several heat pulses are transmitted, and the measurement is taken after successive readings yield the same response time (Hess, 1987). This procedure is then repeated at different depths. Ideally, different vertical flows at different depths indicate fluid either entered or exited the borehole within that depth interval. Figure 9.7 shows a hypothetical flow profile in a well adjacent to the pumping well. Negative flow is downward and positive flow is upward. The example measurements indicate that flow is entering the borehole at two lower depths, moving upward, and then exiting the well bore near 25m. Flow above 25 m moves downward and exits at 25 m.

It may be possible to make flow measurements in a well while it is pumped near its upper portion, and the results could be analyzed to obtain estimates of the transmissivity of particular depth intervals. The analysis of test results obtained would be identical to the one described in the impeller flowmeter section. The thermal-pulse flowmeter was not used in this way at Raymond.

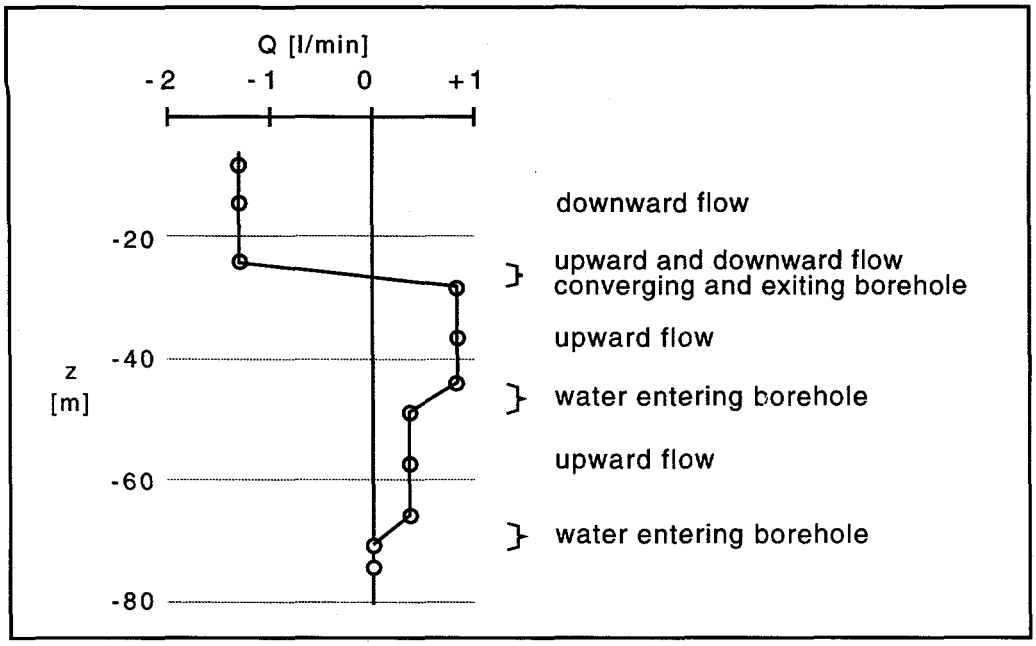

Figure 9.7. Hypothetical flow profile in a well during pumping in an adjacent well.

9.2.3 Extraneous Effects

A report by Paillet and others (1994) describes the numerous factors affecting the accuracy of the measurements and hence the interpretation of the results. Problems generally arise because the flow field is transient during the pumping of a well, because of turbulent flow created by the presence of the instrument, because of well bore radius variations, and because of natural flow along the wellbore. For the tests conducted at Raymond, the interpretation of results were affected most by transient effects.

When the test is conducted during the pumping or injection of an adjacent well, the flow field is in a transient state. Therefore, differences in flow measured at different depths not only result form borehole inflow or outflow, but also because the flow field is evolving with time. Depending on the aquifer properties and the time since pumping was initiated, observations can be skewed because of this transient. Therefore, the time between measurements needs to be considered when interpreting test results.

When the instrument is used without a packer to concentrate flow, fluid flowing around the tool can generate eddies which disturb the flow field and possibly create secondary flow through the measurement section. Misidentification of flow rate and/or direction can result (Paillet, 1994). Also, because flow rates are determined by

comparing the results to a calibration curve obtained for a particular borehole diameter, regions of enlarged diameter, such as solution cavities or break-out zones, may yield values lower than the true flow rate, as well as create highly non vertical flow. The tests conducted at Raymond utilized an inflatable packer to concentrate flow, so these problems were generally avoided, although improper sealing of the packer in fractured zones may have allowed fluid to bypass the measurement section.

The practical appeal in using the flowmeter during the pumping of a well is that larger, measurable flows are created in boreholes, and the identified fractures indicate a connection to the flow field established. A practical problem with these tests is that a particular well may be very low yielding, thereby making it impossible to sustain water levels above fractured intervals and/or the pump. This occurred in a well at Raymond, and has occurred at other sites (e.g. Paillet et al., 1987).

Several of these effects influenced the tests conducted at Raymond, and are described in the next section.

9.2.4 Measurements and Analysis of Results at Raymond

Several different thermal-pulse flowmeter tests were conducted at the Raymond Field Site. The first consisted of pumping well 0-0 and profiling wells SW-1, SE-1, SE-2, and SW-2. The flow resolution in this study was approximately 0.1 L/min. Zero flow was assigned to a particular depth if the response time was greater than 60 seconds, an indication that flow must be less than 0.04 L/min. The measurements are displayed in Figure 9.8, and the inferred profiles are shown superimposed over the data.

The results from well SW-1 are quite straightforward: they clearly show that there are no changes in flow rate or direction between 20 and 60 m, but that water exits the borehole between 62 and 64 meters. Therefore, there is at least one flowing fracture or fracture zone within this lower depth interval.

The profiling results from the other boreholes are not as straightforward. The results from well SE-1, for example, show that there is a flow zone between 57 and 64 meters, and that flow moves both up and down the borehole toward a central exit near 34 m. In addition, there appears to be several flow zones above 30 m. Because the flow measurement at 27 m was made 40 minutes after the measurement at 23 m, there is some ambiguity as to whether this difference is the result of changes due to the evolving transient flow field, or because there is indeed flow out of the wellbore within this depth

interval. There is also the possibility that measurements are different because the packer used to concentrate flow into the measurement section did not seal completely, thereby allowing flow around it to occur (Paillet et al., 1987). For these reasons, all intervals within which a flow change is measured are considered possible flow zones, which are then correlated with the other geophysical logs to infer which may indeed be flowing.

The results from SE-2 include similar ambiguities. The strange discrepancy near 30 m suggests flow, although it is not clear what is happening. Flow between 37 and 40 m and between 58 and 60 meters is quite apparent, as well as a slight convergence of flow out of the borehole to a region somewhere between 40 and 58 m.

The results from SW-2 exemplify the potentially large effects of transient fluid flow and/or incorrect measurements on the interpretation. Note that the two measurements at 21 m are different by nearly 0.5 L/min. Perhaps this is due to the fact that the measurements were taken 37 minutes apart, because improper packer seating, mismeasurement, or a combination of each. Nevertheless, the latter measurement adds some uncertainty to our interpretation. Because there is a systematic change in measured flow from 40 to 53 m, flow between each measurement within this interval is considered a possibility. Flow is exiting the borehole between 40 and 53 meters.

The second test was conducted the next day. Wells SW-1, SW-3, SE-3, SE-4 were profiled during a new pumping of well 0-0. The measurements and inferred profiles are shown in Figure 9.9. The numerous different measurements at 23 meters in SW-1 result from the large transient behavior at early times after pumping. The profile from well SE-4 is not included because no flow was detected in it during this test.

Well 0-0 was profiled during the second test after the pump was turned off. The results and inferred distribution are shown in Figure 9.10. Well 0-0 was again profiled the next day during the pumping of well SE-3, but because SE-3 is a low yielding well, the water level dropped below the pumping interval and the pumping was stopped. The measurements that were taken during and after pumping indicate some of the same flow zones as in Figure 9.9, but also include several ambiguities, most likely due to the abruptly altered flow field.

No flow in well SE-4 was detected during the pumping of SE-3. Later, water was injected into well SE-3, and some flow was observed in SE-4, as indicated in Figure 9.10.

The integration of the flowmeter measurements with other geophysical logs to identify the conductive fractures in each well is presented in Chapter 10. As it is shown, the thermal-pulse flowmeter logs are extremely useful when used in conjunction with other geophysical logs. The above discussion exemplified typical well responses including extraneous effects.

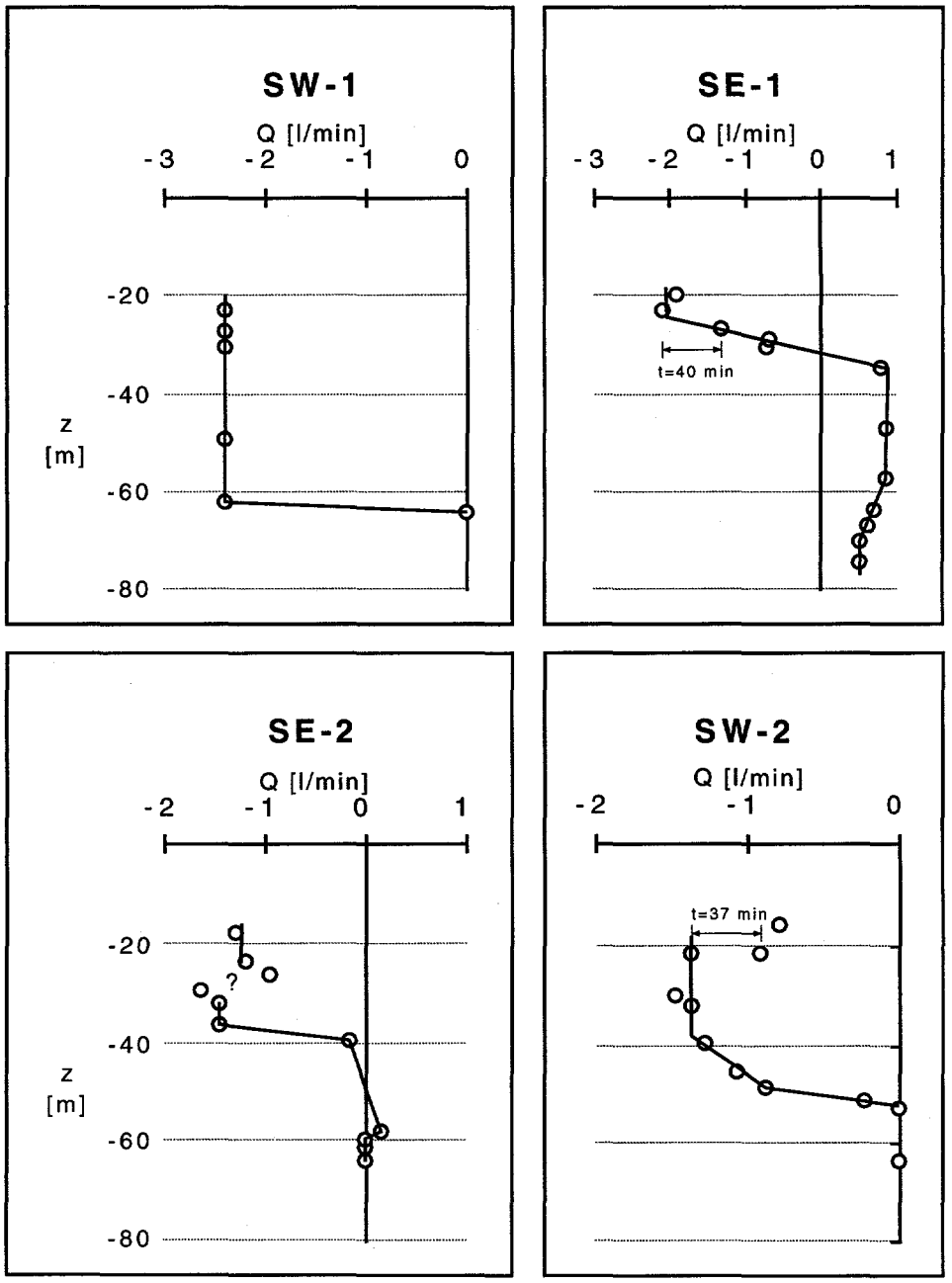

Figure 9.8. Heat-pulse flowmeter results in wells SW-1, SE-1, SE-2, and SW-2 during pumping of well 0-0.

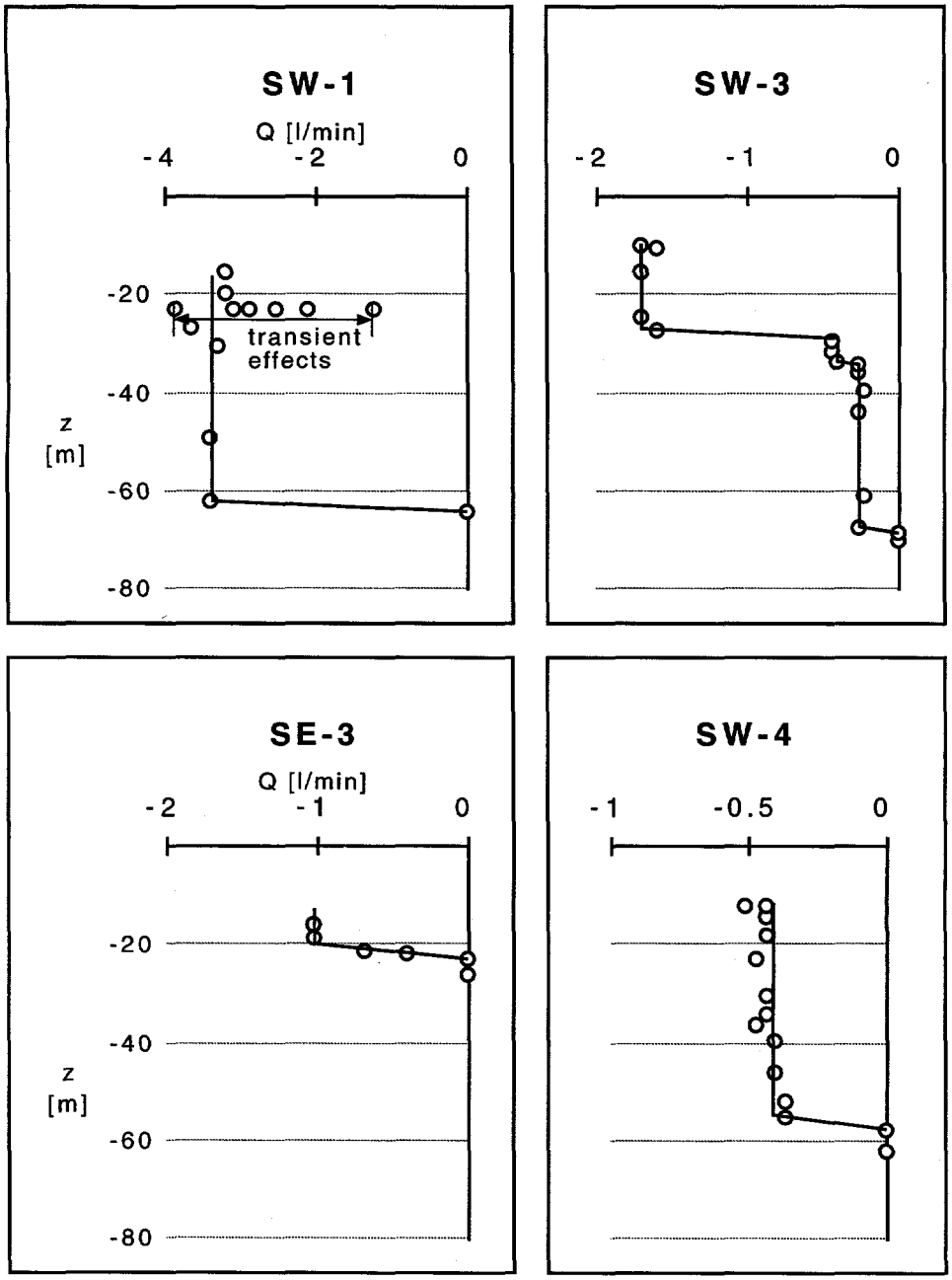

Figure 9.9. Heat-pulse flowmeter results in wells SW-1, SW-3, SE-3, SE-4 during second pumping of well 0-0.

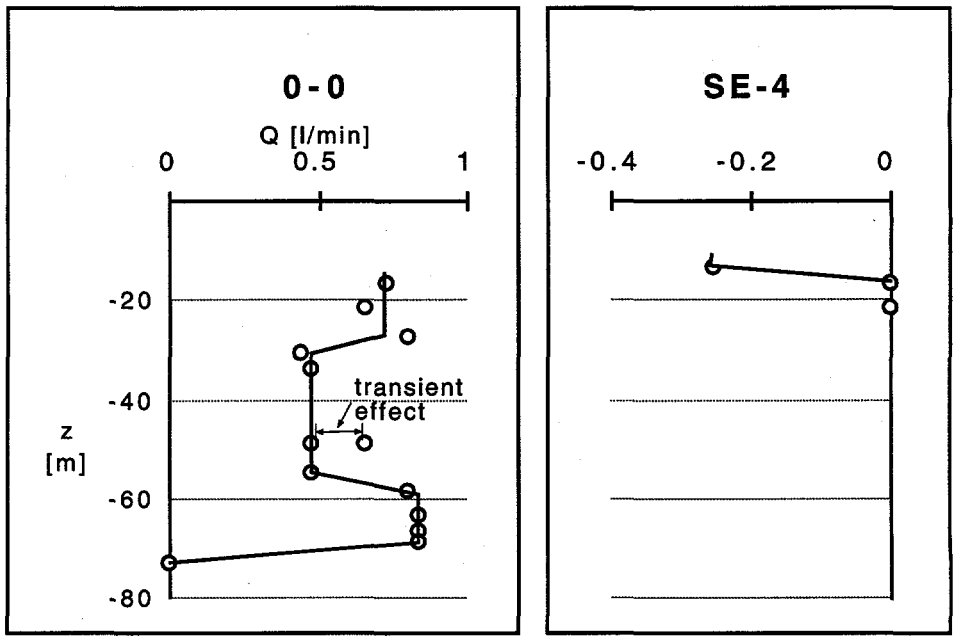

Figure 9.10. Heat-pulse flowmeter results from well 0-0 after pump was turned off, and results from well SE-4 during injection into well SE-3.

9.3 Fluid Conductivity Logging

Fluid conductivity logs were obtained for seven of the nine wells between April 11 and 14, 1994. These logs show the fluid electrical conductivity with depth at different times in a well during pumping. Formation water flows into the well through conductive fractures, and this water is of a higher electrical conductivity than the deionized water that is initially placed into the wellbore. Peaks on the profiles therefore indicate the locations of conductive fractures. The logs are suited to quantitative analysis whereby the transmissivity of fractures can be calculated. This was not done for the logs collected here. Rather, they were used qualitatively to identify the locations of conductive fractures.

9.3.1 Tool Description

Tsang et al. (1990) describe the instrument, data analysis method, and its application and validation in fractured crystalline bedrock. The technique is referred to as fluid conductivity logging, ion logging, and by the trade name Hydrophysical logging. Pedler et al. (1990) describe its application to environmental investigations in shallow, fractured crystalline bedrock near two landfills in New England.

The tool itself is rather simple, consisting mainly of a downhole logger equipped with an electrical conductivity, pH, and temperature probe. The utility of the instrument derives mainly from the overall test methodology. The method consists of replacing the fluid in the well bore with deionized water, which has a much lower electrical conductivity than the formation water. Replacement is achieved by simultaneously pumping formation water near the upper portion of the well and replacing deionized water to the bottom through downhole tubing. The deionized water is either formation water or potable water with their dissolved ionic species removed. After replacement is complete, the well is then pumped at a low and constant rate and a time sequence of upward and downward logs are collected. This procedure is repeated for each well. Packers are not needed. As natural formation water is drawn into the well through conductive fractures, the electrical conductivity of well water near those fractures increases. The time sequence of fluid conductivity logs is used to determine the locations of conductive fractures, or can be used in conjunction with the temperature logs and a computer algorithm to determine fracture specific parameters such as transmissivity. Hydrochemical properties of the fracture-specific formation water can also be determined, such as oxidation-reduction potential and pH.

The conductivity log of well 0-0 at Raymond is shown in Figure 9.11 for example. The sharp peaks at early times are characteristic of fracture inflows, and the relative magnitude of the peaks are roughly proportional to the relative conductivities of the fractures. If the inflows were from a porous medium layer, the early-time peaks would be flat topped (Tsang et al., 1990). The down scans are used to identify conductive fractures for reasons described below. The conductivities increase with time as more formation water enters through the fractures. In order to quantify the conductivity of flowing fractures, the ion concentration of the inflowing fluid is needed. A linear or quadratic equation relating conductivity to salinity can be used for most cases. Also, the fluid electrical conductivity depends on temperature, so the temperature log is used to normalize the measurements. The early time peaks may be analyzed by simple means to roughly yield fracture conductivity. At later times, however, inflows from different fractures become superimposed because the well water is moving toward the pump near the upper portion of the well. A computer algorithm is needed to account for this mixing and dispersion if transmissivity values are sought (Hale and Tsang, 1988).

The extremely high resolution of this method enabled us to clearly identify the particular fractures contributing to flow in the wells at Raymond. Tsang et al. (1990) were able to determine fracture transmissivities that varied over 3 orders of magnitude.

9.3.2 Extraneous Effects and Detection Limits

Tsang et al. (1990) describe some practical aspects and limitations of the technique. Easily correctable effects are those resulting from the direction of logging and induced disturbances in the well bore. During upward logging the cable and tool act to displace and disturb the fluid, thereby resulting in an apparently shallower and/or smeared conductivity peak. The conductivity profiles obtained during downward logging can be used for analysis, so this effect generally poses no problems.

An obvious necessity is that a significant contrast in electric conductivity exist between the formation and borehole fluid. In formations containing low conductivity water, the borehole fluid can be replaced with high conductivity water rather than lower conductivity, as described above. However, this might not be suitable for drinking or irrigation wells.

Solute dispersion and dilution of the inflowing formation water place lower detection limits on the method. Dispersion results because fluid is migrating upwards

through the borehole towards the pump (Taylor dispersion). Therefore, conductivity peaks become more dispersed with decreasing depth. Similarly, low conductivity peaks can be diluted by the upflowing, higher concentration fluid from below. Also, plateaus form as conductivity saturations are reached. These effects occurred at Raymond, and are described and shown graphically in the following section. They may be reduced somewhat with the use of a packer (Tsang et al., 1990).

When inflow from fractures is very rapid, the conductivity in the well above a highly conductive fracture may reach formation concentration even before the first logging profile is taken. This condition creates an upper detection limit, since none of the conductive fractures within the upper interval can be detected. Tsang et al. suggest that other flow detection techniques such as impeller flowmeters may be more appropriate in these circumstances.

The log for well 0-0 (Figure 9.11) exemplifies the effects of dispersion on fracture detection. The early-time profile exhibits two distinct peaks at approximately 30 meters, therefore indicating the presence of two closely spaced, conductive fractures. Because water is being drawn up the borehole towards the pump, the inflows from each fracture overlap. Therefore, at late times the upper fracture is not detectable. Well 0-0 was not grouted around the casing, and the conductivity peak at around 12.5 meters is caused by water seeping into the well from the bottom of casing.

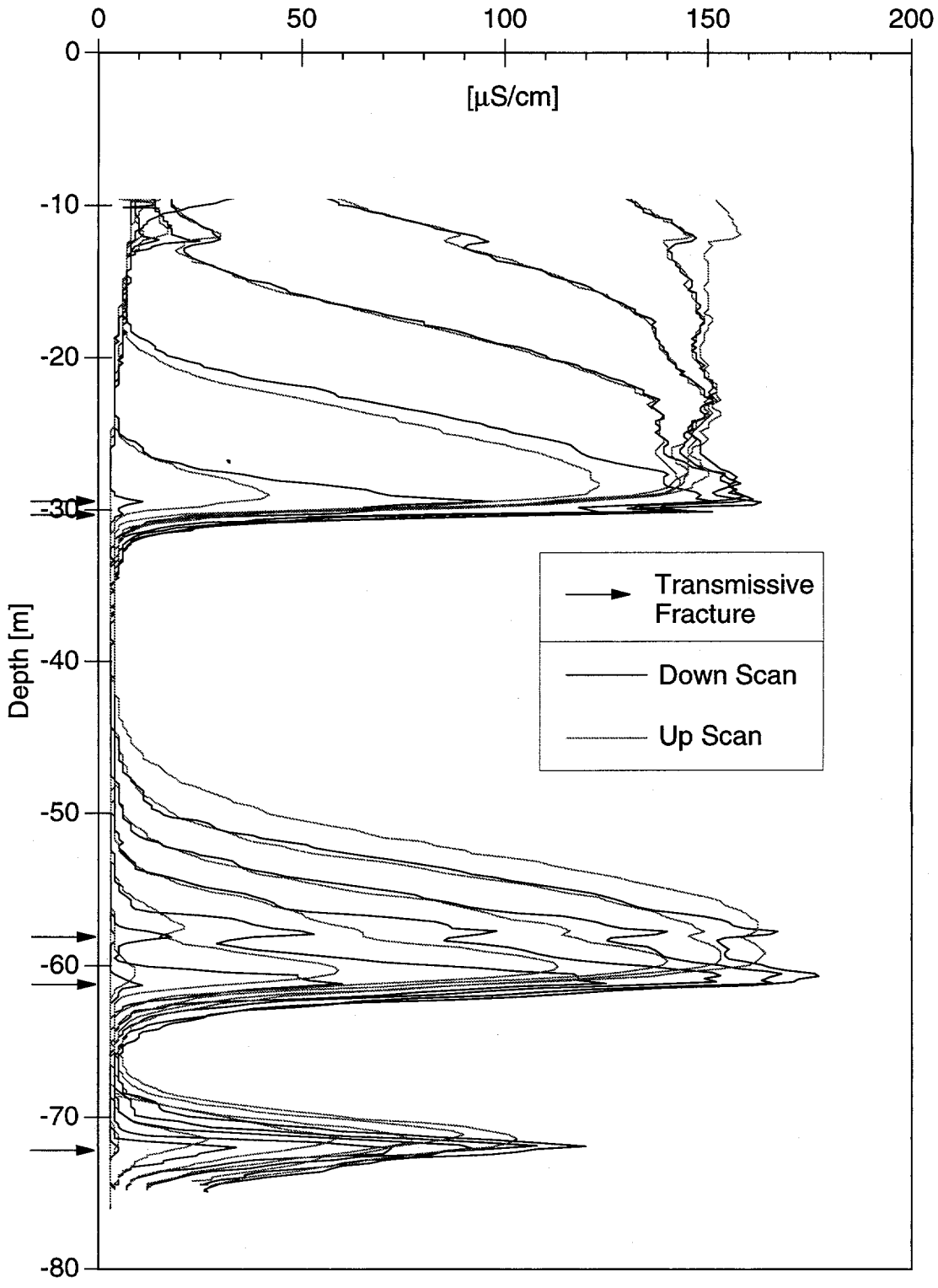

Figure 9.11. Fluid conductivity log of well 0-0 at Raymond, for example.

9.3.3 Measurements and Results at Raymond

All wells except SE-3 and SW-3 were logged. Well water was replaced with deionized water as described above. The constant pumping method was used for all wells except SE-4 and SW-4. These wells are very low yield wells, so a slug removal and recovery method was used instead. Profiling during well recovery was conducted after a fixed volume of water was quickly removed. The other wells were pumped at rates between 7 and 20 L/min. Six conductivity profiles were collected in each well at a rate of approximately 7.5 m/min. Each well therefore took about 1 hour to log.

The logs are shown in Figure 9.12 and 9.13. The downward profiles were used as the representative profiles since the upward profiles were less precise for reasons described above. All of the logs exhibit noticeable peaks at conductive fracture locations, so determination of the particular fracture contributing to flow was straightforward, requiring only a brief inspection of the acoustic televiewer and/or television logs. Many more conductive fractures were identified by this method than by the impeller of thermal-pulse flowmeter. Equally significant is that the measurements were more precise and enabled quick and confident assessments of the locations of the particular conductive fractures. Section 9.5 compares the results from each method, and the integration of the flowmeter measurements with other geophysical logs to identify the conductive fractures in each well is presented in Chapter 10

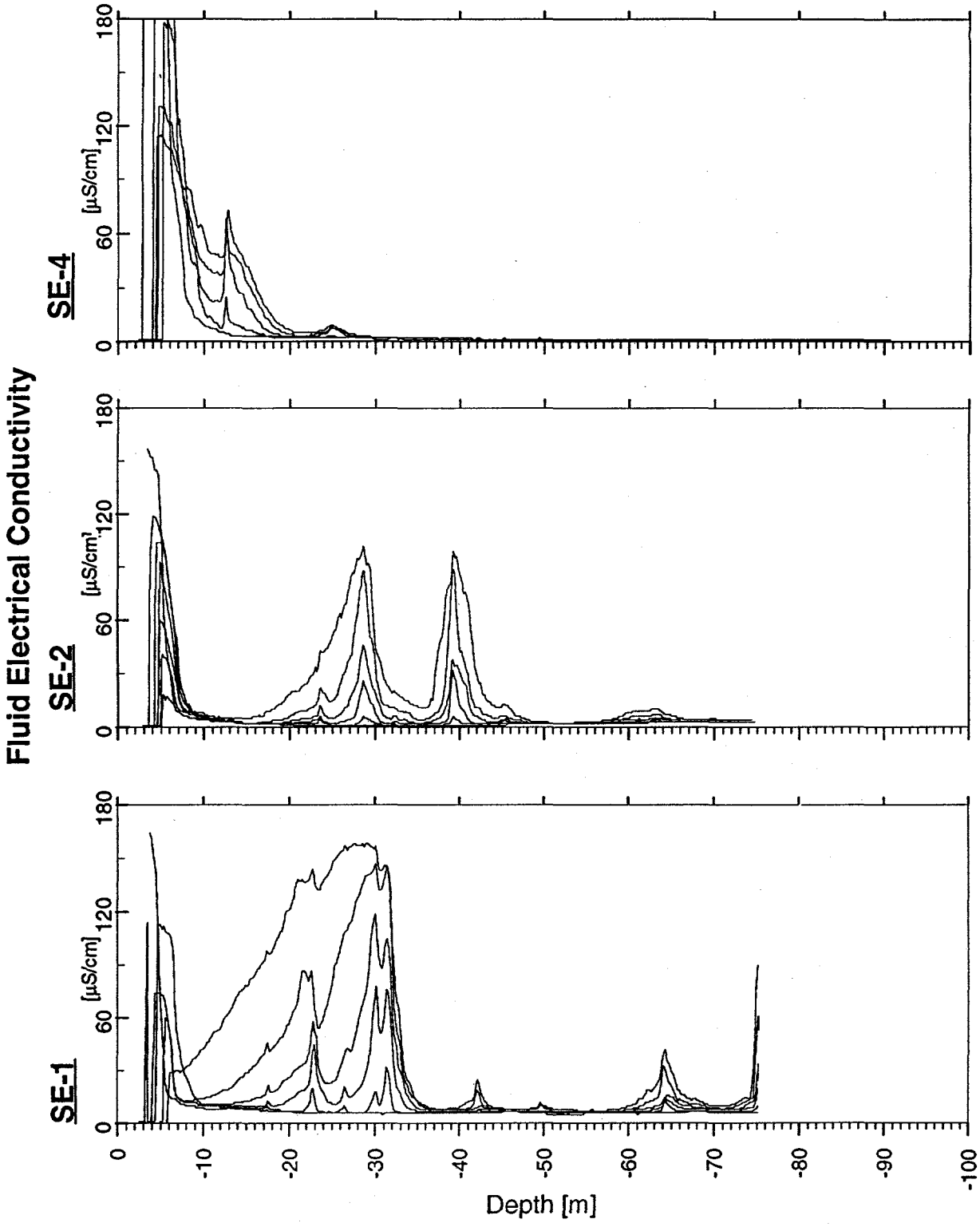

Figure 9.12. Fluid conductivity logs of wells SE-1, SE-2, and SE-4.

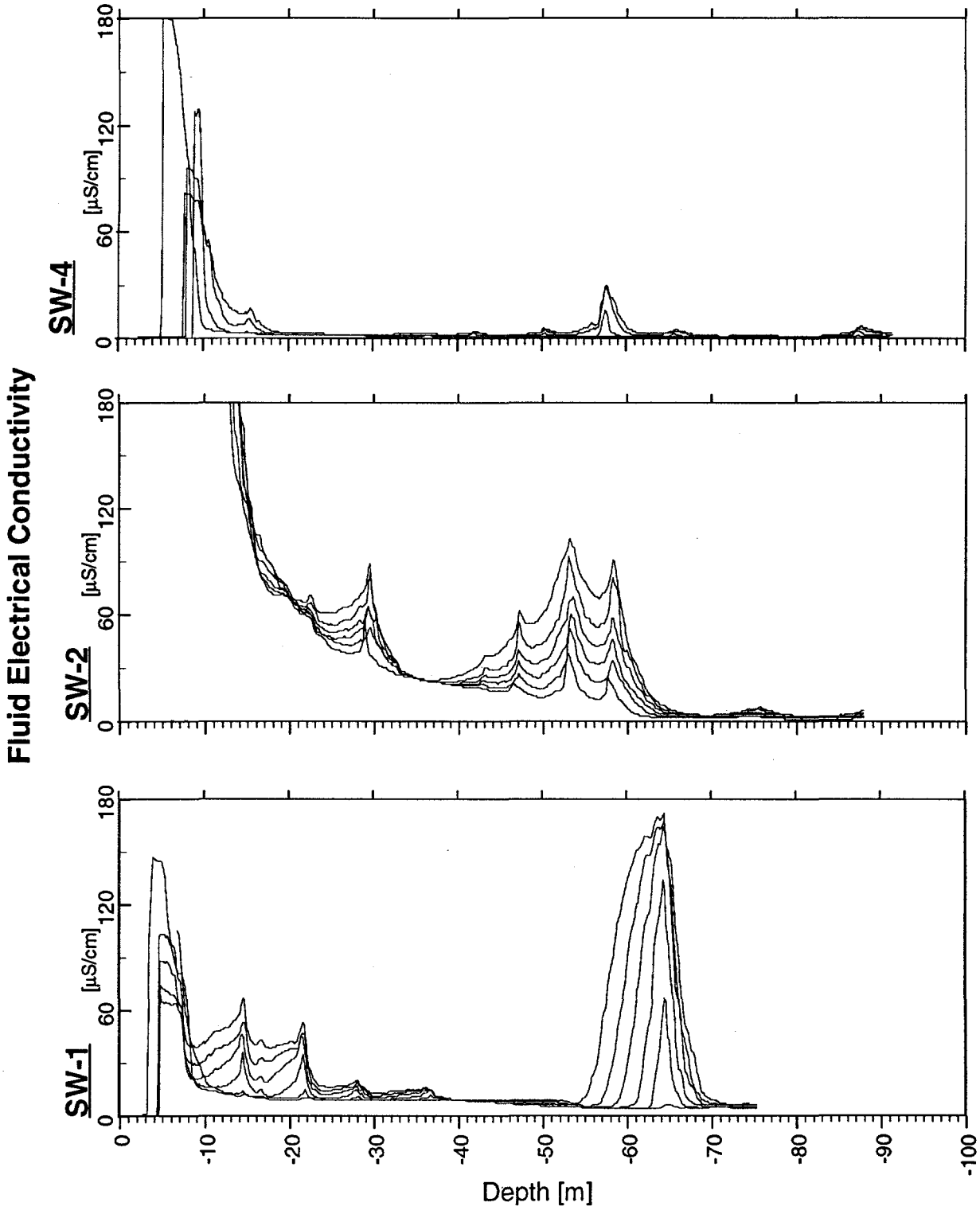

Figure 9.13. Fluid conductivity logs of wells SW-1, SW-2, and SW-4.

9.4 Straddle Packer Injection Tests

Straddle packer injection tests were performed in all nine wells. These tests consisted of injecting water at constant pressure into packer-isolated sections of the borehole. An approximate transmissivity value for the test interval was calculated based on the observed flow rate and injection pressure. Successive depth intervals were tested in each well, resulting in a profile of transmissivity with depth.

9.4.1 Test Configuration and Methodology

A schematic of the test design is shown in Figure 9.14. The main features are the dual-packer assembly, pressurized fluid tank, in-line flowmeter, and pressure transducers. The packers are mounted on a section of downhole piping. Care must be taken to insure the packers will seal the test section, so standard geophysical and acoustic televiewer logs are used to determine where the borehole wall is relatively unaltered and unfractured. Pressure transducers are positioned above and below the test section in order to monitor possible flow leakage around the packers and/or flow 'short circuiting'. Short circuiting occurs when conductive fractures intersecting the test section are connected to others that intersect other portions of the borehole.

An ideal test response is shown schematically in Figure 9.15. The inflation of the packers causes a slight increase in fluid pressure in and around the test interval. Testing is initiated after this effect dissipates. Injection pressure is regulated by the air tank pressure. Injection begins when the pneumatic injection valve is opened via a surface switch. The flow rate entering the section is measured with an in-line impeller flowmeter. An automated data acquisition system records and displays the flow rate and downhole pressures. Ideally, fluid only flows into conductive fractures intersecting the test interval under the induced steady pressure head. The flow rate declines asymptotically towards a steady value, and injection is continued until a pseudo-steady flow is attained. This is on the order of minutes to tens of minutes. The valve is then closed, and the pressure in the interval subsides. This procedure is repeated at different depth intervals, and the transmissivity of each interval is calculated using the equations described below and the observed flow rates and injection pressures.

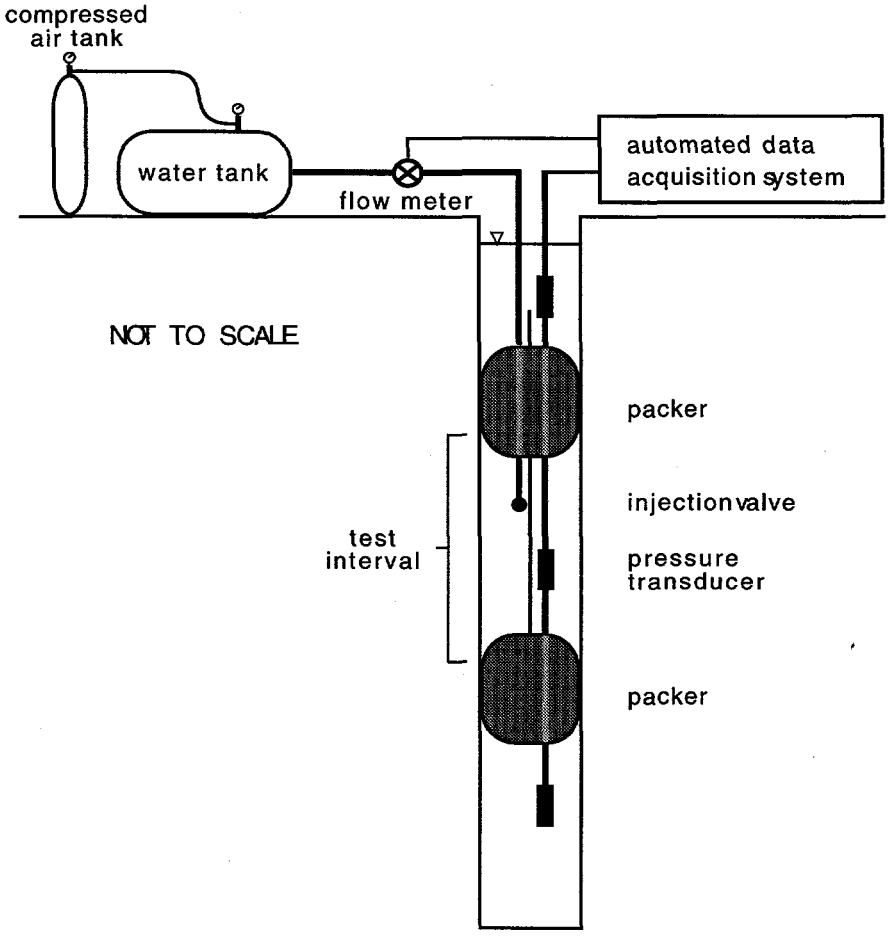

Figure 9.14. Schematic of straddle-packer injection test.

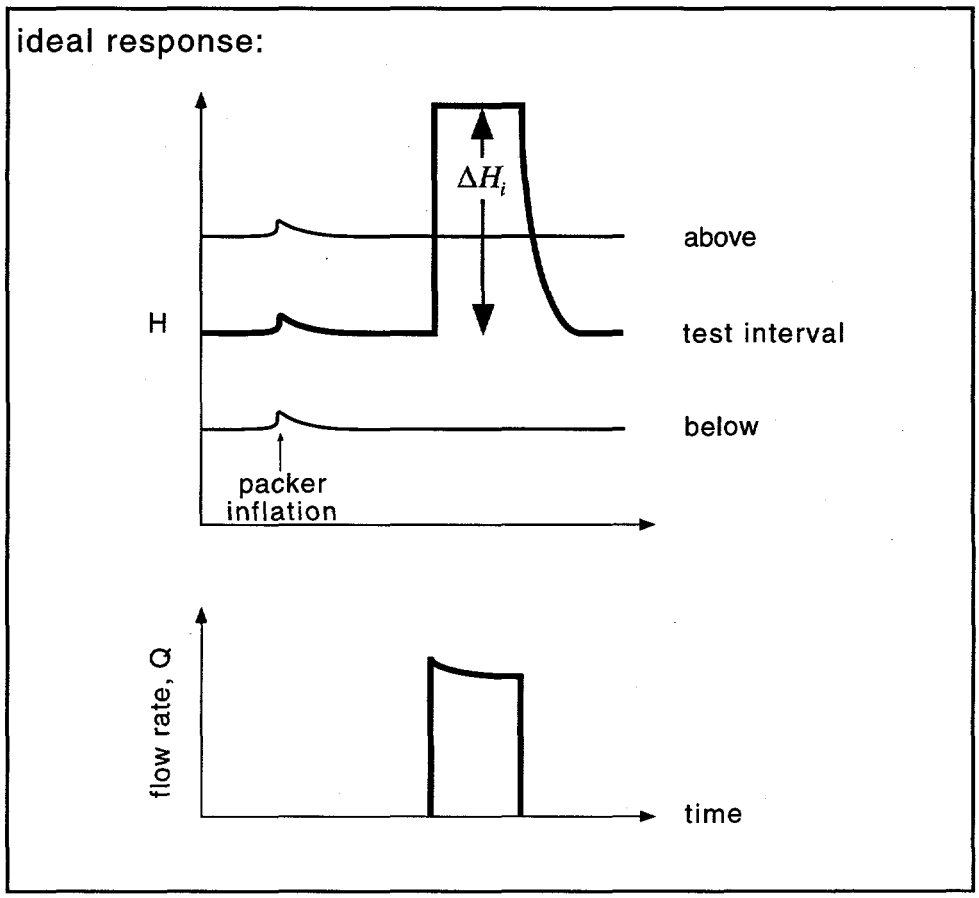

Figure 9.15. Ideal test response of straddle-packer injection test.

Determination of cross-well hydraulic connections can be determined by equipping observation wells with pressure transducers and packers, thereby allowing measurement of pressure responses induced by injection in particular wells or well intervals. A sophisticated version of this method was implemented at Raymond, and is described by Cook (1995).

9.4.2 Data Analysis

The simplest way to obtain a transmissivity value for the test interval is to use the Theim equation, which is the solution for steady-state laminar radial flow in a homogeneous, constant thickness medium. The equation for transmissivity is

$$T = \frac{Q}{2\pi\Delta H_i} \ln\left(\frac{R}{r_w}\right) \tag{9.7}$$

where Q is the steady flow rate, ΔH_i is the induced hydraulic head, R is the radius of influence, and r_w is the radius of the well. The calculated transmissivity value, however,

should be viewed as an order of magnitude approximation, since the assumptions inherent in the equation are rarely satisfied. Even under ideal conditions when the injection pressure is constant and the flow rate becomes steady, the flow geometry, radius of influence, and even the effective well radius are impossible to define. The flow geometry may be linear, radial, spherical, or somewhere in between. In additional, the systematic injection tests within a borehole result in the superposition of numerous pressure transients. In theory, R is the distance to a constant head boundary, which in general does not exist. Instead, the fictitious radius of influence is used. It is roughly defined as the distance at which the induced injection pressure is not observed. The effective radius of the well is often different than the measured radius because of drilling effects and/or because the properties around the well are naturally different from those further away. For example, a region of relatively very high transmissivity around the well (referred to as a negative skin), caused either by drilling disturbances or by the natural heterogeneity of the rock, has almost negligible hydraulic resistance. Therefore, the well has a larger effective hydraulic radius. In practice, the actual well radius and an estimate of the radius of influence are used in (9.7). Because the logarithm of the ratio of these radii are used, differences in the chosen values do not alter the transmissivity estimate significantly.

The greatest uncertainty associated with calculated transmissivity value arises when the test response is non-ideal, as described below.

9.4.3 Problematic Effects

Non-ideal test responses include packer leakage and short circuiting, and transient flow and injection pressures. Truly steady flow generally does not occur because the duration of injection is too short for the system boundaries to be felt. Instead, the test is conducted until flow becomes pseudo-steady. In practice, the on-set of this condition is arbitrarily defined and is decided upon by visually observing the flow rate with time. This approximation does not produce significant errors in the calculations. However, termination of the test prior to establishment of a pseudo-steady flow is problematic. Figure 9.16a represents a case where the test was not conducted long enough and the final flow rate is probably higher than what might be called pseudo-steady.

Flow around the packers into the section above or below the test interval can result if the packers are positioned at rough or fractured borehole sections. Figure 9.16b shows an example of simple leakage. Here, the pressure in the upper interval is

increasing nearly linearly because of a fraction of the injected flow is leaking past the packer under the nearly steady head differential. Packers should be positioned elsewhere when this is detected.

Leakage and short circuiting can create both non-steady flow and transient injection pressures. Injection into a section with very high conductivity fractures is difficult. Because of the high conductivity, the flow rate into the section becomes limited by the flow resistance in the tube. Pressure losses over the distance of the injection line become significant, and the pressure in the injection interval is much lower than the pressure in the injection tank. Hence, the pressure slowly builds up, but doesn't reach the injection pressure. This behavior is coupled with a non-steady flow rate, too, so the system is rather dynamic. These effects may be minimized by using a large injection tubing to reduce resistance. Hsieh and others (1993) describe the use of packer injection with two injection lines: one for low flow and one for high flow.

Analytical solutions that account for the transient behavior are available, but their use is generally not warranted given the other uncertainties associated with flow geometry, short circuiting, and leakage. In light of the fact that the model assumptions are not meet, it may be more meaningful to evaluate the conductivity of intervals using the ratio $Q/\Delta H$. This yields relative magnitude estimates among injection intervals.

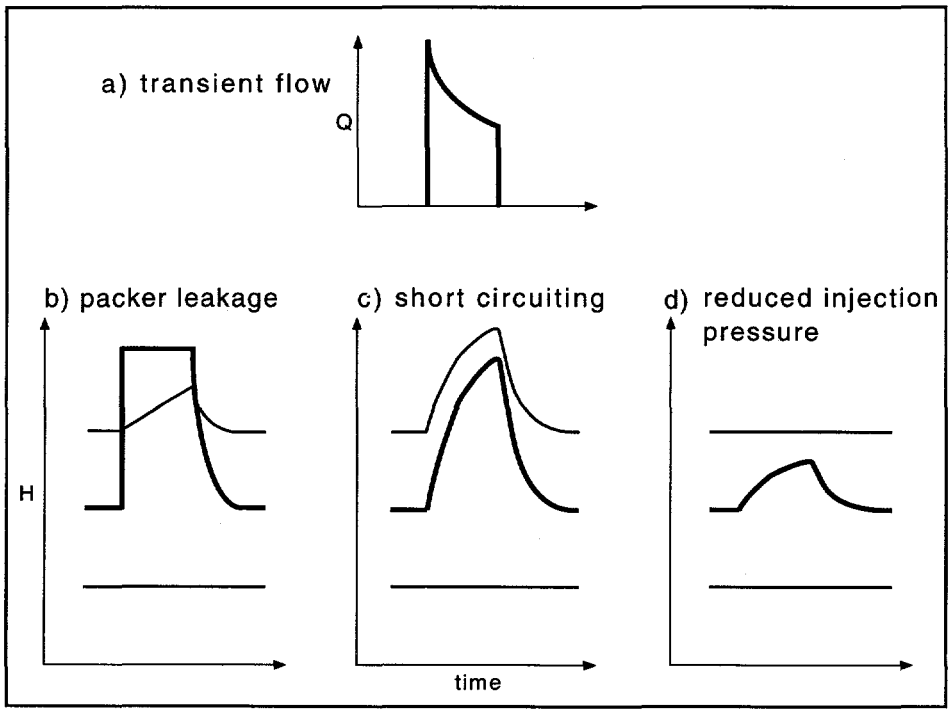

Figure 9.16. Potential problematic effects during straddle-packer injection tests.

9.4.4 Measurements and Analysis of Results at Raymond

Tests were conducted in the manner described above. The injection interval was 6.1 meters. Injection pressures ranged between 20 and 30 psi, corresponding to hydraulic heads between 15 and 20 meters. Test durations ranged between 5 and 20 minutes. Low conductivity zones attained quasi-steady flow within several minutes. The flow rates were observed on the automated data acquisition system display, and the decision that flow was sufficiently steady was made visually. The lowest measured flow rate during testing was 0.07 L/min.

Flow into very high conductivity zones usually remained transient throughout the entire test duration because of flow-line resistance effects. The final ΔH and flow rate observed during a test was used to calculate the ratio $Q/\Delta H$ for each interval. Obvious leakage around a packer occurred once, and this was corrected for by subtracting the leakage rate from the flow rate. Otherwise, for the many cases in which the upper or lower isolated zones also responded, no correction was made simply because its difficult to know what to correct for. For the purpose of illustrating the locations of relatively high and low conductivity zones, Figure 9.17 shows the profiles of $Q/\Delta H$ for all the wells. The results are generally consistent with the other tests in that they reveal the same dual-zone structure. The upper fracture zone on the east side is clearly more conductive.

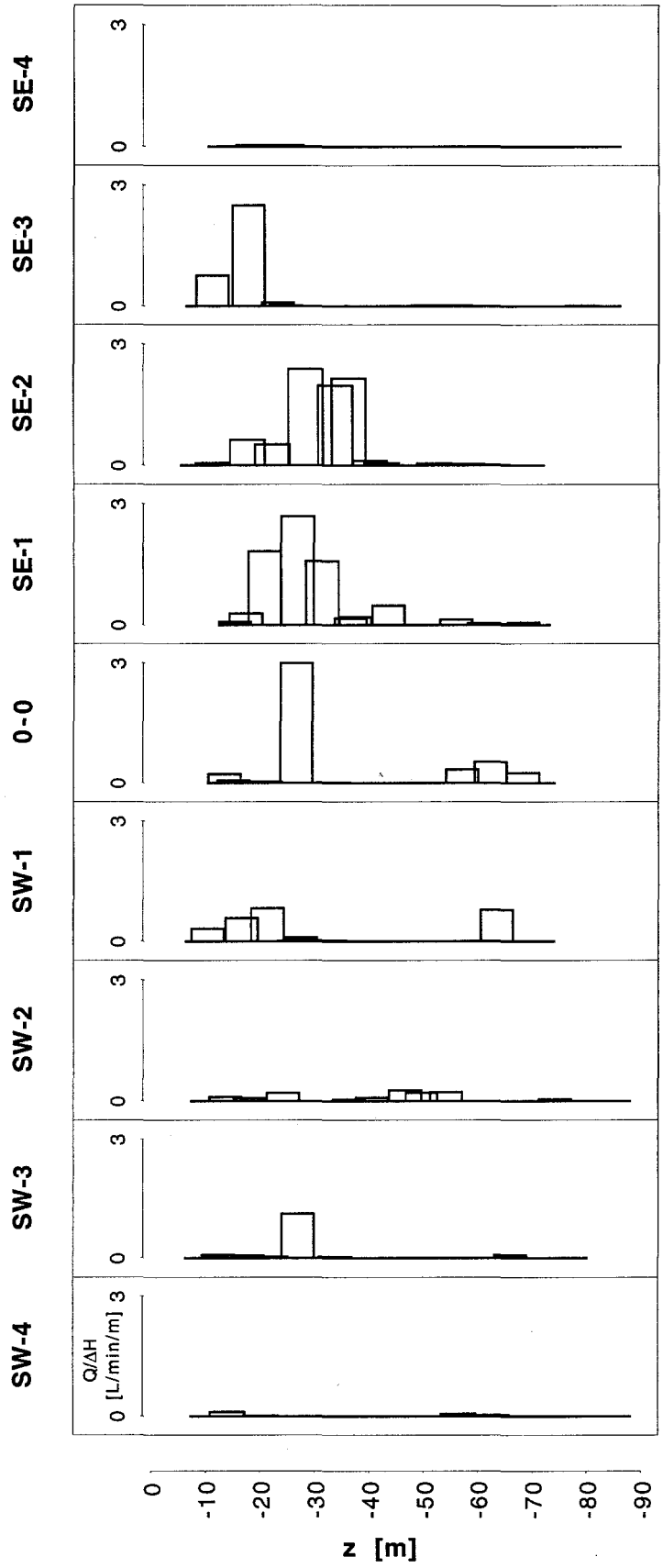

Figure 9.17. Profiles of Q/ΔH in all nine wells obtained from straddle-packer injection tests.

9.5 Comparison of Techniques

All of the techniques enable detection and measurement of flowing intervals/fractures to varying degrees. The advantages and disadvantages of each technique are outlined below.

IMPELLER FLOWMETER:

advantages:	disadvantages:
• least expensive and most available method	• can not detect very low flows
• high upper flow detection limit which makes it appropriate for high yielding wells	• some versions do not detect direction of flow
• can be used to profile vertical flow in boreholes under natural conditions	• if packer is not used, turbulence, well bore radius variations affect the measurement
• can be used to profile multiple wells during the pumping of a single well	• oil filled versions may not be suitable for environmental investigations
• can install transducers in adjacent wells and perform a pumping test simultaneously	• packers/ flow diverters needed to get high resolution results
	• debris can affect impeller performance
	• calibration drift because of bearing degradation

THERMAL-PULSE FLOWMETER:

advantages:	disadvantages:
• low lower flow detection limit allows measurement of minor vertical flow under natural conditions	• has an upper flow limit ~ 20 gpm
• can profile in multiple wells during the pumping of a single well	• debris can inhibit heat pulse generation
• can measure upward and downward flow	• if packer is not used, turbulence, well bore radius variations affect the measurement
• one version is capable of detecting horizontal flow	• transient well bore flow may present problems in the analysis

FLUID CONDUCTIVITY LOGGING:

advantages:	disadvantages:
• very low detection limit	• not all wells can be profiled during the pumping of a single well
• no packers needed	• need to replace borehole fluid
• highest resolution; specific fracture inflow points are easily recognized	• can not use to profile wells under natural conditions
• measurements can be analyzed to determine transmissivities of individual fractures	• extremely high transmissivity zones may not be detected
• not sensitive to borehole radius variations	
• replacement fluid is benign from environmental standpoint	

STRADDLE PACKER INJECTION:

advantages:	disadvantages:
• high resolution	• very time consuming and expensive, and requires sophisticated field equipment
• can be used with other pressure transducers to determine cross-hole connections	• high injection pressure could alter conductive fracture properties
• measurements can be analyzed to determine transmissivities of individual fractures	• introduces a lot of disturbance in the well bore, highest potential to smear contaminant locations
	• short-circuiting effects make it difficult to assess conductivities of individual zones
	• not well suited for identifying fractures, better in assessing their transmissivity after features have been found by other methods.

9.6 Summary

9.6.1 General

Impeller flowmeter, thermal-pulse flowmeter, fluid conductivity, and injection profiling were performed at the Raymond site. The impeller flowmeter was used to profile wells while they were pumped. The surveys revealed dominant flow intervals in the wells, but flow intervals near the lower portions of the well were poorly defined because of the relatively high stall velocity of the impeller. The use of an inflatable packer attached to the instrument increased the flow sensitivity and allowed us to use only one calibration curve determined in the laboratory. Estimates of the transmissivity of flowing intervals were calculated based on the measured flows and the pressure transient in the well.

The thermal-pulse flowmeter was used to profile multiple wells during the pumping of a single, relatively high yielding well. This allowed determination of those fractures contributing to flow during the test, although no quantitative estimate of the conductivity of these intervals could be determined. The thermal-pulse flowmeter method detected more flowing intervals than the impeller method. This is consistent with the fact that it has a lower minimum detection limit. In theory, the thermal-pulse flowmeter could be used in the same manner that the impeller was used in this study, thereby allowing calculation of interval conductivities. Transient flows in some wells were pronounced. Some intervals yielded ambiguous readings which need to be further interpreted by viewing other geophysical logs. In one well, the thermal-pulse flowmeter did not detect a flowing interval identified by the impeller method. This is most probably an artifact of the test methodology, not the instrument. A particular fracture may contribute flow differently when a well other than the one the fracture intersects is being pumped.

Fluid conductivity logging was performed in seven wells. This method enabled detection of the greatest number of flowing intervals and provided the highest resolution. All of the logs exhibit noticeable peaks at conductive fracture locations, so determination of the particular fracture contributing to flow was straightforward, requiring only a brief inspection of the acoustic televiewer and/or television logs. Many more conductive fractures were identified by this method than by the impeller or thermal-pulse flowmeter. Equally significant is that the measurements were more precise and enabled quick and confident assessments of the locations and relative magnitude of the conductivity of

particular conductive fractures. The results of the tests are amenable to analysis whereby the transmissivity of particular fractures is determined, although this was not done in this study.

Straddle packer injection tests were performed in all nine wells. These tests required sophisticated equipment and were the most time consuming. In relatively low conductivity test intervals, a constant injection and flow rate was quickly attained and usually without extraneous effects. In high conductivity intervals, cross-circuiting often occurred and transient injection pressure and flow rates persisted because of flow-line resistance effects. Therefore, the conductivities of the highest conductivity intervals were underestimated. This problem can be avoided if a separate, larger flow line is used in these intervals. The results are consistent with the other techniques but in some cases indicate very low flow where others do not.

9.6.2 Recommendations

Flow logging is a critical necessity in the characterization study. It provides a means to identify and quantify the transmissivities of only the relatively few fractures or fracture zones which are in fact conductive. This information provides knowledge of the general structure of the aquifer, from which all future remedial planning emanates. Results from flow logging are best when integrated with other geophysical logs. Examples are given in the following chapter.

A downfall of all flowmeters is that pumping or injection of the well bore is required. Therefore, a flow field may be established in the contaminated field, and contaminants can migrate to previously uncontaminated areas. In order to minimize these effects, profiling should first be conducted in wells under natural conditions. In theory, either the impeller or thermal-pulse flowmeter could be used at this stage, although the lower sensitivity of the latter is probably the better choice since flows are likely to be very low. Vertical borehole flow will probably be greatest soon after drilling when fractures are being connected by the installation of the well and the system is in a highly transient state. After this initial profiling, the method of profiling multiple wells during the pumping of a single well should be implemented. The highest yielding well should be used as the pumping well, and driller's logs can provide this information. Profiling in the pump well with the impeller flowmeter allows determination of transmissivities of intervals adjacent to the well, and by installing pressure transducers in neighboring wells, a multi-well pumping test is effectively conducted. This eliminates the need to perform a

separate pumping test. Alternatively, one well can be used for pumping and other wells profiled with a heat-pulse flowmeter, for example. The information gained is somewhat different, but perhaps more informative since you can determine which fractures are transmissive in other wells, although not quantitatively. If the impeller or thermal-pulse is used, we recommend using a downhole inflatable packer around the flow casing to increase the sensitivity and avoid borehole variation and turbulence effects and to reduce the number of calibrations needed.

We do not recommend the use of packer injection tests under most situations. The method is expensive and time consuming and creates the greatest non-equilibrium condition in the aquifer. A method like the fluid conductivity logging yields precise locations of transmissive fractures and can be analyzed to determine the transmissivities of these fractures. The method is probably not appropriate as a means to detect flowing fractures but perhaps as a later investigative phase once flowing fractures are found and some quantitative assessment is sought.

All of the different logs are most beneficial when used together with the ATV and other geophysical logs. This aids in the determination of the particular fracture(s) contributing to flow, and provides a means to determine the kinds of fractures that are conductive. Measurement of the fracture orientation from the ATV logs may also enable one to extrapolate and determine where a particular conducting fracture intersects another well, for example.

10 INTEGRATION OF GEOPHYSICAL LOGS

Conventional geophysical logs were used in conjunction with flowmeter logs in order to identify the particular hydraulically conductive fractures and/or fractured zones intersecting the boreholes. We found that by integrating the flowmeter results with the acoustic televiewer, television, 16-inch normal resistivity, caliper, and gamma logs, the particular conductive fracture or fractured zone could be determined. After the conductive fractures were identified, interpolation of properties between wells was made based on similarities in various fracture geophysical properties, and the general hydrologic structure of the aquifer was deduced. The integration of various geophysical logs, an essential component to the characterization effort, is thus illustrated. Keys (1990) refers to this integration as a synergistic log analysis.

In addition to the ATV and heat-pulse flowmeter logs, three-arm caliper, fluid conductivity, 16- and 64-inch normal resistivity, natural gamma, temperature, single-point resistance, spontaneous potential, and lateral logs were collected in each well by the U. S. Geological Survey. Resistivity logs may indicate where hydraulically conductive fractures are located, for example, because clays and ferric oxides associated with hydraulically altered fractures high electrical conductivities compared to the parent rock. Caliper logs show the locations of increased borehole diameter. Zones of intense fracturing such as in areas where there are many closely spaced, subhorizontal fractures can easily be detected. Individual open fractures can be detected if their aperture is large enough. Natural gamma logs measure the gamma radiation in a borehole. Pegmatitic dikes contain potassium 40, a significant gamma-emitting radioisotope. Local peaks on the gamma log can indicate the location of a pegmatitic dike, for example (Keys, 1990).

10.1 Identification of Transmissive Fractures

10.1.1 Heat-Pulse Flowmeter and Standard Geophysical Logs

The integration process is described for only three of the Raymond wells for brevity. The method would apply to other types of flowmeter logs in a similar manner. Figure 10.1 shows the geophysical and heat-pulse flowmeter logs for well SW-1. The flow interval occurs near a southwardly dipping and subvertical fracture at approximately 63 meters. The caliper log indicates an increase in borehole diameter at the fracture

depth, and viewing of the television log clearly shows that this is an open fracture not surrounded by other open fractures. We conclude that this fracture is the transmissive fracture responsible for flow.

Figure 10.2 shows the geophysical and heat-pulse flowmeter logs for well SE-1. The individual conductive fractures are more difficult to infer. There does not appear to be an obvious feature associated with the convergence of flow between 29 and 35 m, although there is a zone near 31 m that exhibits borehole enlargement, relatively low resistivity, and relatively high gamma activity. The fracture at 31 m may be the one, or one of the several producing fractures within this interval. Flow between 23 and 29 meters is believed to emanate from the highly altered and broken out zone between 25.5 and 27.5 m, and from the single, discrete fracture at about 22.5 m. Although this fracture lies slightly above flowmeter measurements, the fact that it is visibly open and not surrounded by other fractures as seen on the TV log, and has low resistivity and high gamma suggests it may be an open, conductive, pegmatite dike. Inspection of the TV log indicated that the gamma peaks at 26 and 28 m result from pegmatite dikes, although it could not be said conclusively that they were the flow sources, but pegmatite dikes were found to be major contributors to flow in other wells.

Figure 10.3 shows the geophysical and heat-pulse flowmeter logs for well SE-2. Inspection of the TV log revealed that the high caliper anomaly at 59 m is associated with a large fracture with orange-red staining. This altered fracture is located within a zone of closely spaced, subhorizontal and altered fractures which are associated with flow in many of the wells. Although fracture at 59 m has the same orientation as the other fractures in this zone, the TV allowed us to identify the particular fracture responsible for flow. The convergence of flow between 40 and 58 m is possibly due to a conductive fracture within the altered zone up to 52 m, or near the small blowout at 43 m. Inspection of the TV log could not provide a conclusive answer one way or the other, such as if the fracture at 43 m was obviously sealed or not. Digital borehole scanner results may provide additional information. The flow between 36 and 40 m is quite obviously coming from the fractured pegmatite at 38 m. The TV log showed its large reflective crystals, and that it is open with no open fractures around it. The anomalous gamma, resistivity, and caliper signatures between 20 and 30 m are associated with altered subhorizontal and pegmatitic dikes which are likely to be conductive features, although the ambiguous flowmeter measurements make it difficult to identify the particular features.

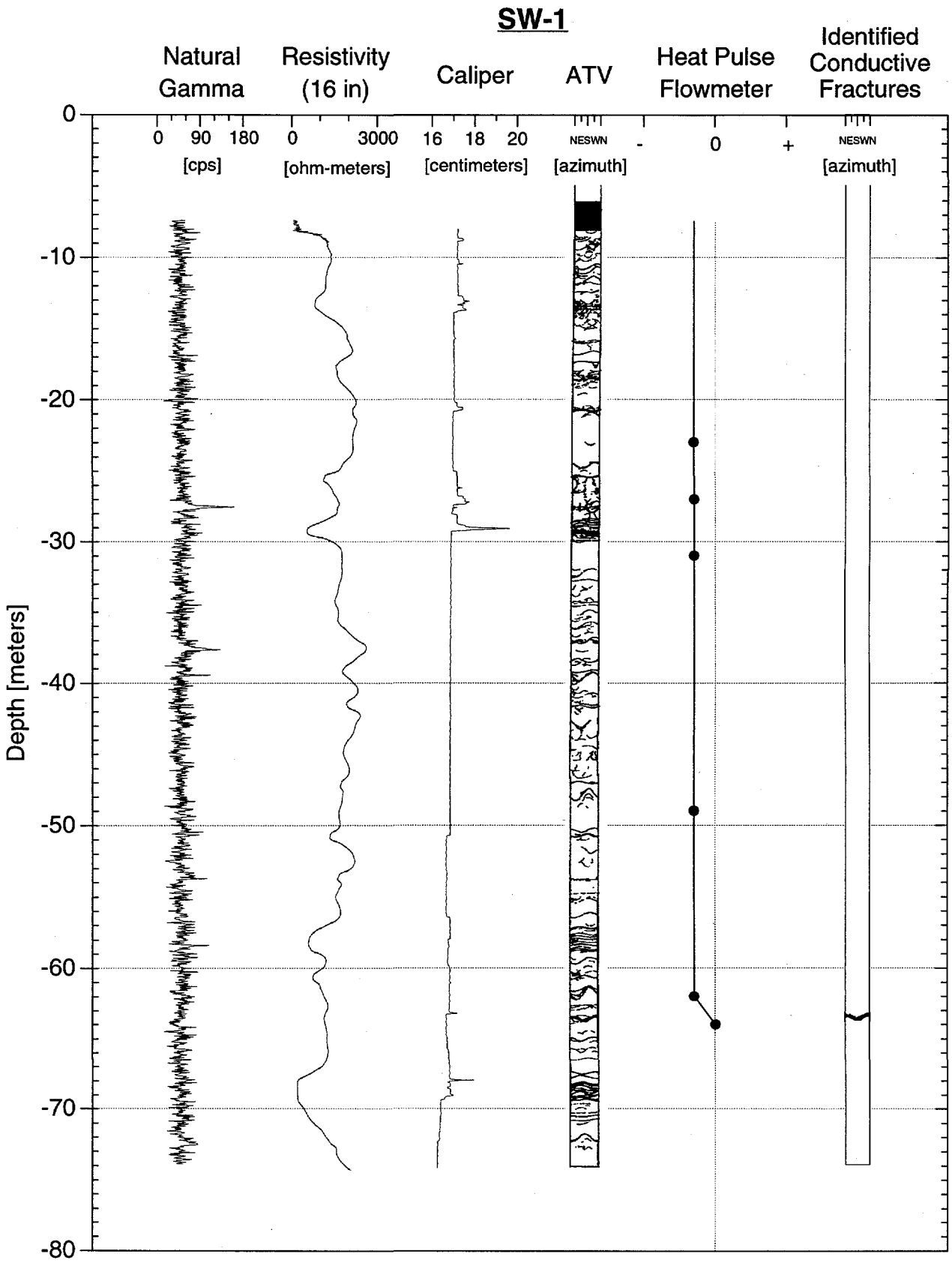

Figure 10.1. Conventional geophysical and heat-pulse flowmeter logs for well SW-1.

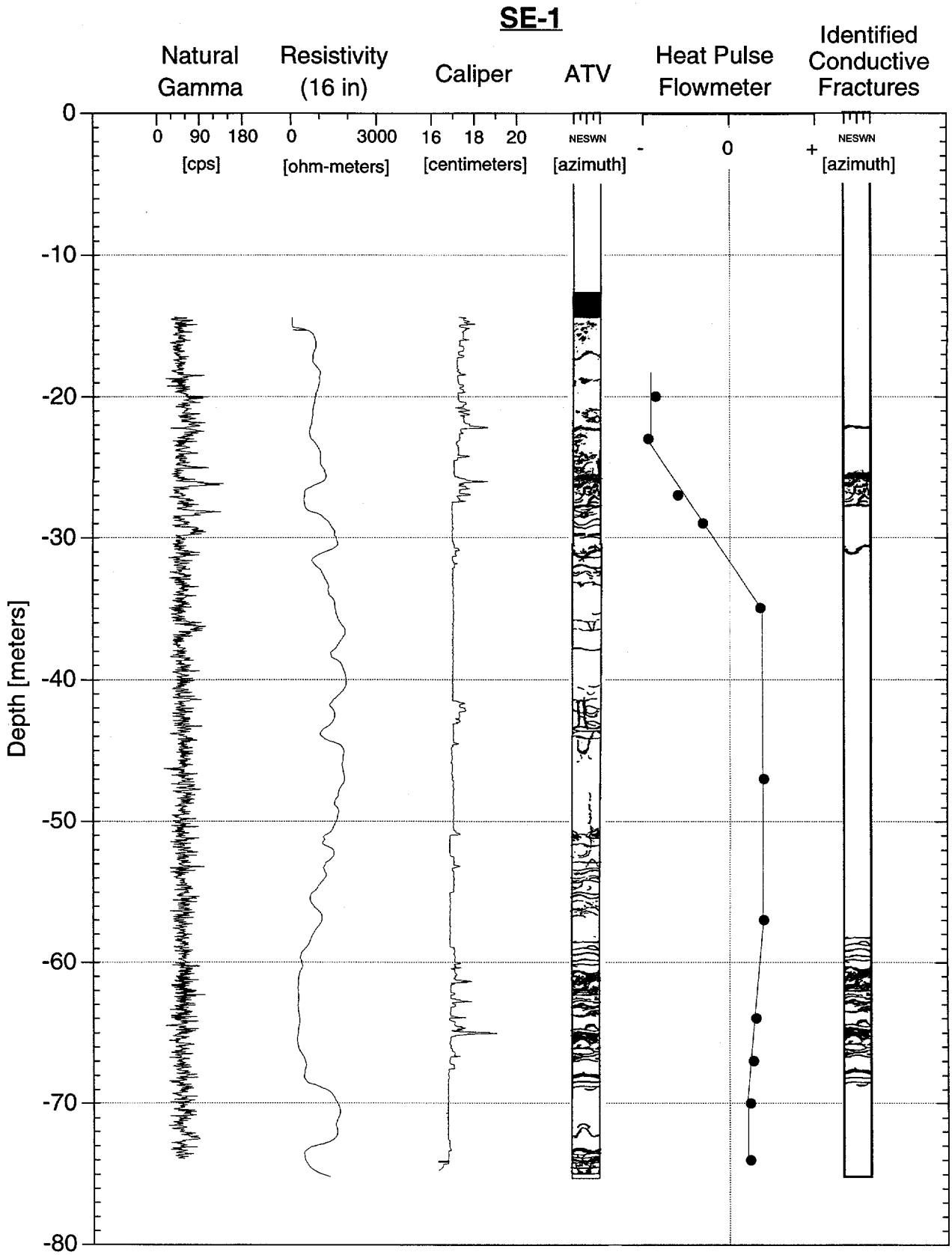

Figure 10.2. Conventional geophysical and heat-pulse flowmeter logs for well SE-1.

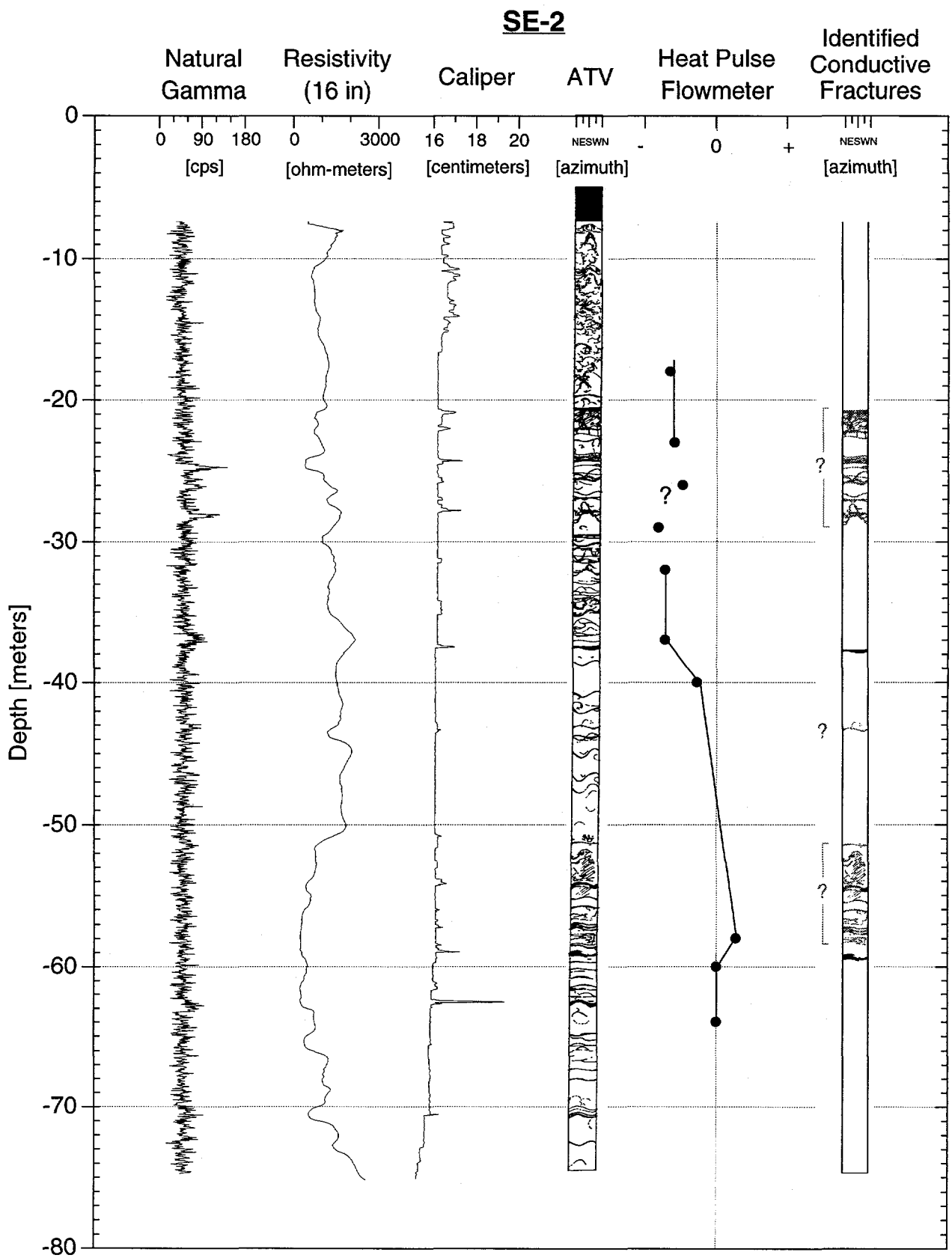

Figure 10.3. Conventional geophysical and heat-pulse flowmeter logs for well SE-2.

10.1.2 Fluid Electrical Conductivity and Standard Geophysical Logs

Figures 10.4, 10.5, and 10.6 show the same wells and geophysical logs as outlined above with the results of fluid electrical conductivity logging described in section 9.3. The combination of these logs make it very clear which of the fractures are transmissive. The sharp peaks of the conductivity logs very obviously show which fracture shown on the ATV log is conductive. Most are accompanied by caliper anomalies, and some with gamma peaks associated with fractured transmissive pegmatites. In several cases it was unclear exactly what fracture produced flow because they occurred in clustered fracture areas. However, a quick look at television logs showed which were more likely to be the conductive fracture. The vertical position of the geophysical and flow logs for SE-2 is slightly distorted, but the identified fractures are indeed correct.

10.1.3 Comparison of Results

Figure 10.7 shows a comparison of the conductive fractures identified from heat-pulse flowmeter logs and fluid electrical conductivity logs. The fluid electrical conductivity logs reveal more conductive fractures and with less ambiguity than the thermal-pulse flowmeter logs do. Although the electrical conductivity logs have higher resolution in general, some of the observed differences result from differences in test methodologies, not because of instrument sensitivity. The heat-pulse logs were obtained in wells adjacent to a pumping well, while the fluid conductivity logs were obtained in a well being pumped. Not all conductive fractures intersecting a well may contribute to flow during a particular pumping test, and the vertical flow transient in an observation well associated with flow into a conductive fracture could diminish to unobservable levels or to zero by the time the well is profiled. In addition, the measurement intervals for the heat-pulse logs are larger than the fluid conductivity logs. Finer measurement intervals would help reduce the ambiguity of some measurements.

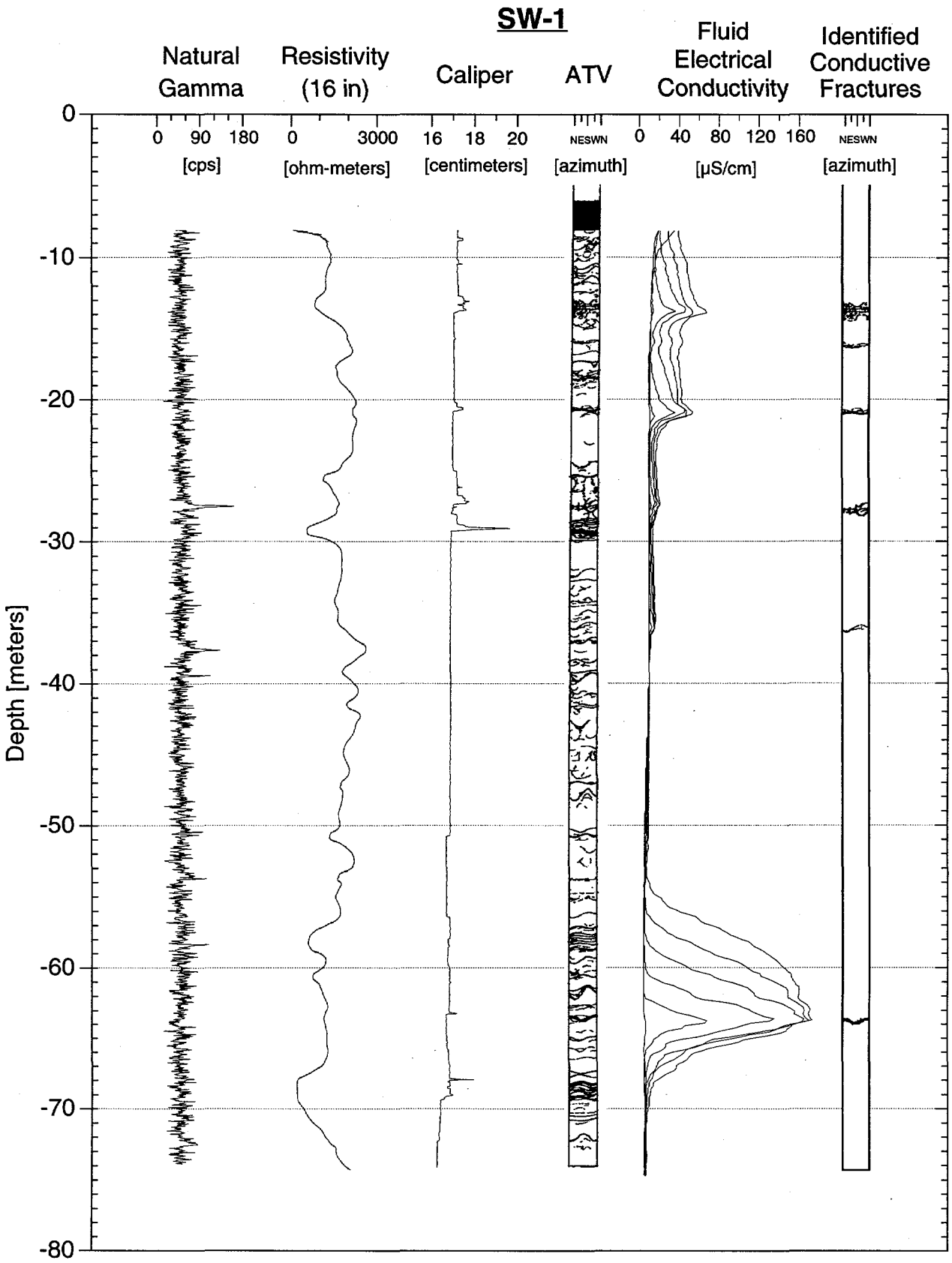

Figure 10.4. Conventional geophysical and fluid electric conductivity logs for well SW-1.

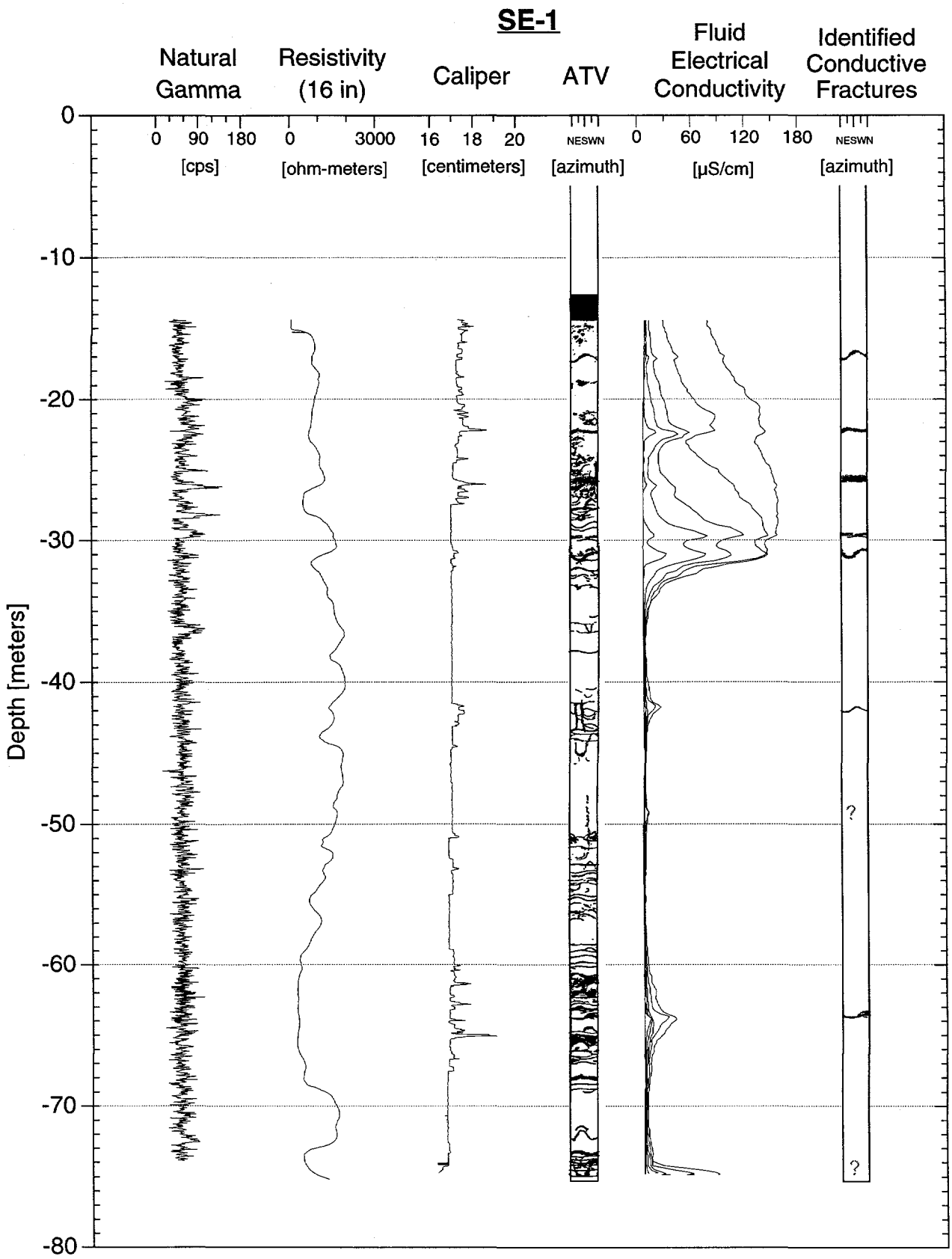

Figure 10.5. Conventional geophysical and fluid electric conductivity logs for well SE-1.

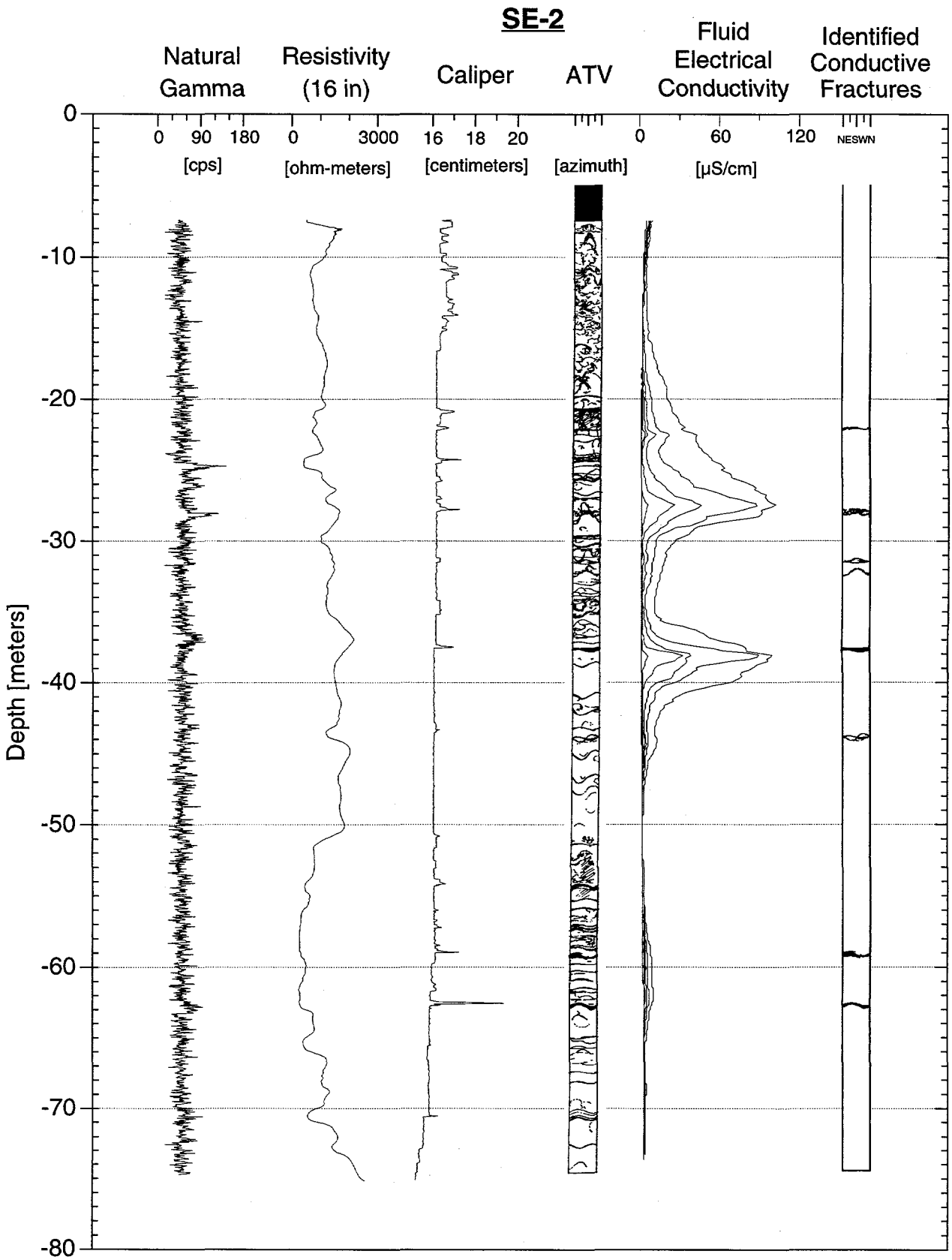

Figure 10.6. Conventional geophysical and fluid electric conductivity logs for well SE-2.

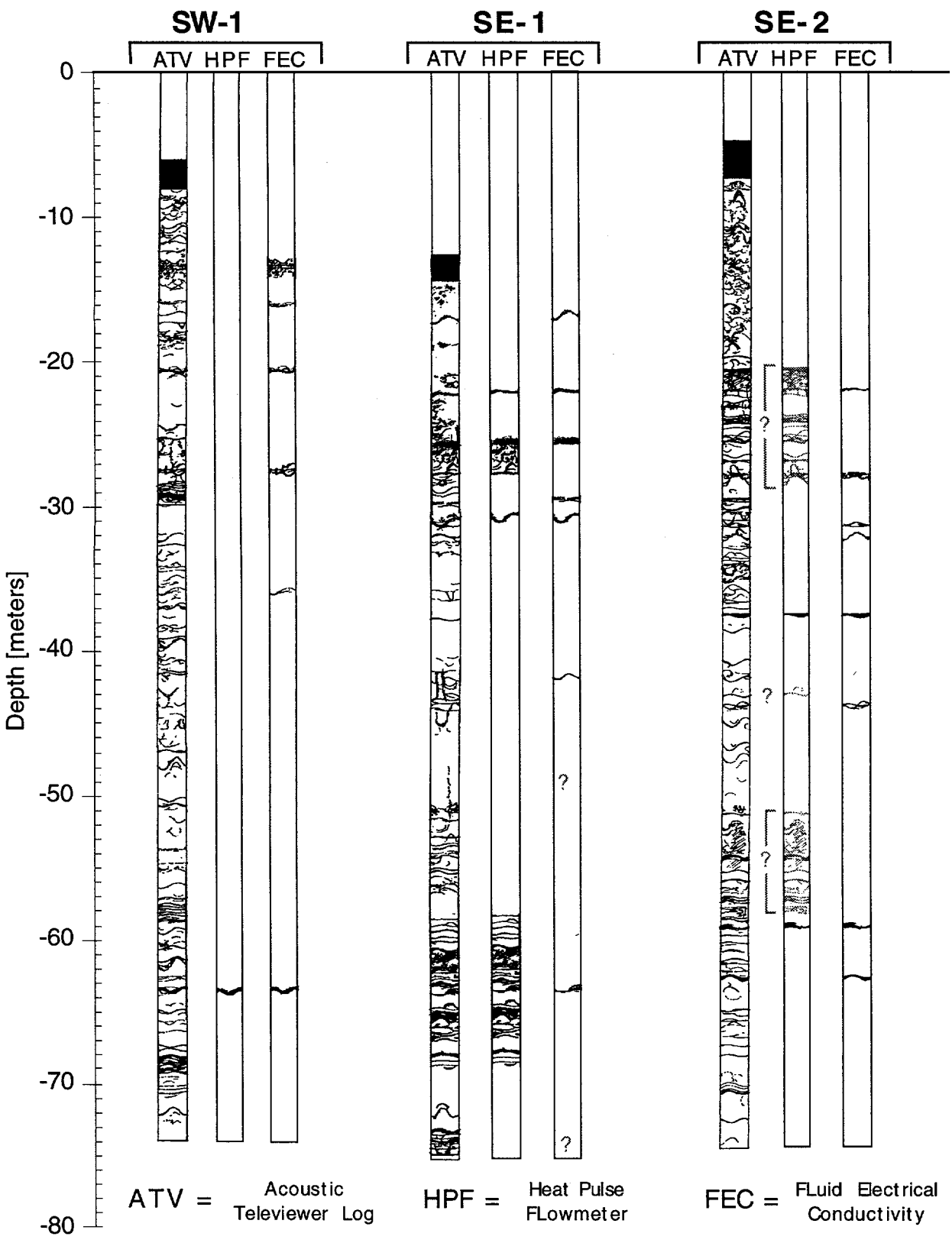

Figure 10.7. Comparison of transmissive fractures identified from heat-pulse flowmeter logs and from fluid electric conductivity logs.

10.2 Determination of General Hydrogeologic Structure

A model of interwell fracture connectivity can be constructed based on similarities of various geophysical properties of the identified conductive fractures in adjacent wells. For example, conductive fractures in different wells may exhibit similar orientations and belong to the same fracture set, and the interpolated fracture plane connecting these fractures may correspond to their respective orientations. This process is analogous to inferring the structure of a stratified aquifer based on the lithology found from borehole logs. Obviously, the complexity of a fractured formation makes the process much more difficult, but in general some general fracture structures can be defined. Conductive fractures from different fracture sets and of completely different orientations may intersect each other between wells in unknown ways, and the three dimensional nature of the fractures and the well field make it difficult to extrapolate features and assess where they may intersect other wells or where they may intersect each other between wells. Computer visualization is very helpful for this purpose, and is described in Chapter 12.

The conductive fractures and fractured zones intersecting each well at Raymond were identified using the geophysical and flowmeter logs in the manner described above. In general, several different types of fractures are transmissive: fractured pegmatite dikes, fractures within zones of closely spaced and westwardly dipping subhorizontal fractures, subvertical tectonic fractures, and to a minor degree partially infilled aplite veins which are very weakly transmissive. The fractured pegmatite dikes are often found within or near the zones of subhorizontal and closely spaced fractures.

Visual inspection of all the normal resistivity, acoustic televiewer, caliper, and flow logs suggest that in general there are two subhorizontal fracture zones beneath the site. These are characterized by the closely spaced, westwardly dipping fractures which exhibit a high degree of alteration indicated by low resistivities, caliper anomalies, and confirmed by inspection of television logs. Subhorizontal pegmatite dikes also accompany these fractures in the upper zone.

Figure 10.8 shows the three-arm caliper and 16-inch normal resistivity logs of wells which show the general characteristics described above. The borehole diameter indicated by the caliper log is based on an average extension of the three arms. Comparison of the caliper logs with downhole television camera logs revealed that zones where the borehole diameter is greater than 18.5 cm are intensely altered and broken into

angular blocks. These are the zones in which the individual constituent fractures could not be measured on the ATV logs, and which have very large apparent apertures. Given that these fracture zones are present at nearly the same depth in each borehole, and since the regions of closely spaced subhorizontal fractures are commonly enlarged during the drilling process (Chapter 8.1.3), it appears that there are two continuous and subhorizontal fracture zones intersecting the boreholes: an upper zone at about -30 meters, and a lower zone between -55 and -70 meters. The smaller caliper anomalies occur in chipped-out portions of near vertical fractures, zones of closely-spaced subhorizontal fractures, and in the zone near the uppermost portion of the uncased borehole in which few or no fractures could be identified. This zone appears to be a transitional region between the shallow regolith and the granitic bedrock.

Visual inspection of the resistivity logs and ATV logs revealed that zones of low apparent resistivity zones are associated with the occurrence of westwardly dipping and closely spaced fractures. The measurements of fractures obtained from ATV logs was used in combination with the 16-inch resistivity logs to confirm that zones with apparent resistivities less than 700 ohm-m are mainly associated with these fractures (Cohen, 1993). The 16-inch normal resistivity log was used rather than the 64-inch log because the volume of investigation of the resistivity probe is considered to a sphere with a diameter approximately twice the spacing of the electrodes (Keys, 1989), and it is more appropriate to correlate measured fractures to properties close to the borehole. It is known that the accuracy of normal resistivity measurements greater than several thousand ohm-meters is questionable and that they should generally only be used in a qualitative way (Keys, 1989), but measurements less than about 1500 ohm-m can generally be used quantitatively (Paillet, oral comm., 1993). Using the apparent resistivity as a descriptive measurement was possible here since aberrations in borehole diameter were small, and the fluid conductivity and temperature were constant with depth and essentially the same in each well. These are factors that need to be corrected for if the true formation resistivity is sought.

Figure 3.2 shows the locations of zones where the apparent resistivity is less than 700 ohm-m and closely spaced subhorizontal fractures are present. Also shown are the locations of identified transmissive westwardly dipping, altered fractures and subhorizontal fractured pegmatites. An upper fracture zone is defined based on the occurrence of similar fractures and geophysical properties in adjacent wells, and is delineated by the dashed lines. The zone dip direction is approximately N70W, which is consistent with the orientation of the individual constituent fractures (section 6.1.4.1).

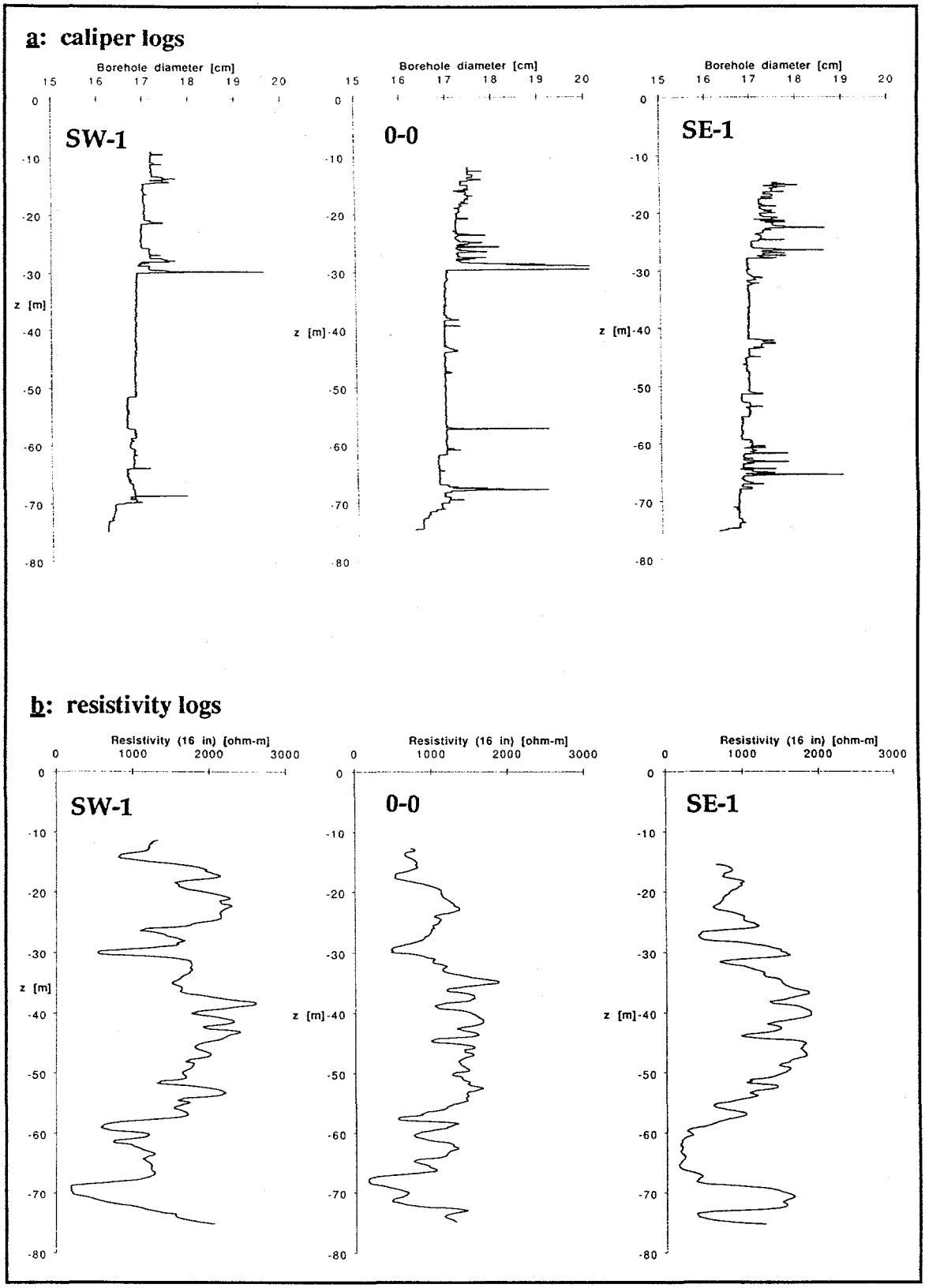

Figure 10.8. Caliper and 16-in normal resistivity logs of wells SW-1, 0-0, and SE-1.

The dip angle is approximately 26°, while the average dip of the fractures is approximately 40°. This suggests that the zone is composed of fractures en-echelon to the zone. Fracture pegmatite dikes comprise many of the transmissive fractures within the zone. The lower fracture zone does not appear to be continuous across the well field, but has the same general orientation. Most of the conductive fractures between the defined fracture zones are fractured pegmatite dikes which may occur along a continuous or semi-continuous pegmatite joint.

Figure 10.9 shows the remaining identified conductive features in the wells. These are separated into two sets: subvertical tectonic fractures and a single group denoted "others" which includes fractured aplite veins and flow from intervals where the particular fracture or type of fracture was not identifiable. The conductive fractures shown are not all significantly transmissive. The tectonic fractures are highly transmissive and the others are generally weekly transmissive. The dual-layer structure agrees with the measured transmissivity in the boreholes (Figure 9.17 and Figure 11.1). How the tectonic fractures may be connected with one another, or how they intersect the subhorizontal zones between boreholes is difficult to determine. The vertical deviation of the boreholes and general 3-D distribution of fractures would make it very tedious to extrapolate a particular fracture to other wells to see where it might intersect. For this reason, computer visualization is preferred (see section 12). It was found that the two subvertical fractures within the lower zone define a planar subvertical fracture, for example.

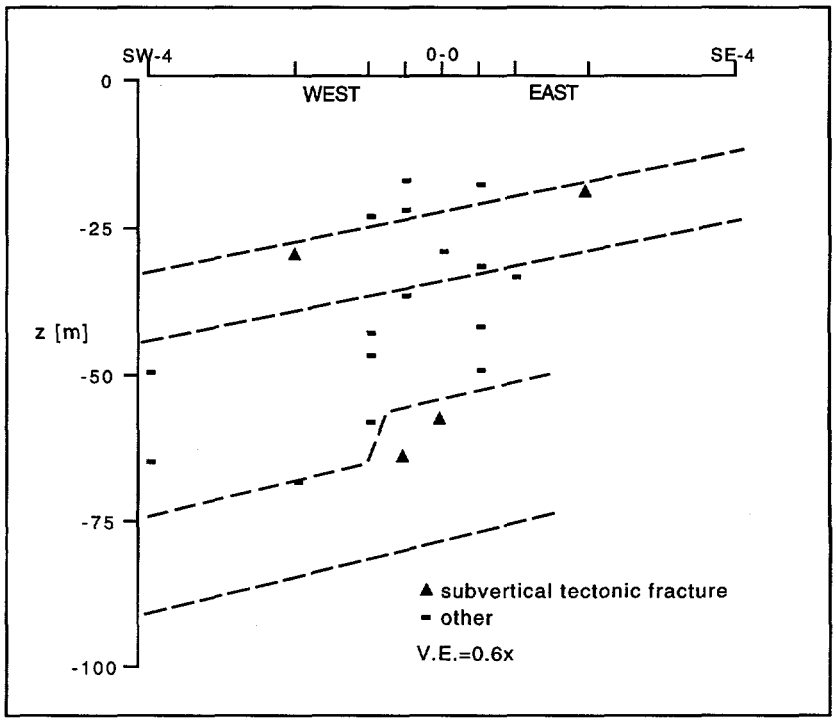

Figure 10.9. Transmissive subvertical tectonic fractures, aplite veins, and other fractures of unknown type.

10.3 Summary

10.3.1 General

Thermal-pulse flowmeter logs and fluid conductivity logs were used in combination with natural gamma, normal resistivity, caliper, acoustic televiewer, and television logs to identify transmissive fractures. Other types of flowmeter measurements could be used in the same manner. The fluid conductivity logs enabled detection of more fractures and with greater precision. In general, several different types of fractures are transmissive: fractured pegmatitic joints, closely spaced subhorizontal fractures, subvertical tectonic fractures, and to a minor degree various partially infilled aplite veins which are very weakly transmissive. The fractured pegmatite joints are often found within or near the zones of subhorizontal and closely spaced fractures. Two subhorizontal fracture zones comprised of the westwardly dipping, subhorizontal altered fractures and pegmatites were delineated based on similarities in fracture geophysical properties in adjacent boreholes. These two zones define general hydrologic structures within the well field. Other important features include subvertical tectonic fractures which may connect these zones.

11 SEISMIC IMAGING TECHNIQUES

Various seismic imaging techniques may provide a means to identify subsurface structures of hydrologic importance. Seismic reflection and refraction surveys have traditionally been used to resolve large geologic structures and stratigraphic sequences using source and receiver arrays at the surface. Since the amount of contaminants that can enter the bedrock is often a function of the depth of overburden, and because common contaminants such as NAPL's will migrate along the sloping surface troughs on the bedrock, this information can be very useful. For example, seismic refraction surveys were used to determine the depth of overburden and hence the slope of the bedrock surface at a contaminated site in New Hampshire. This information was then used to anticipate how the contaminants would migrate (Di Nitto, et al., 1982). Reflection surveys can also be performed using radar signals. Cross-hole seismic surveys are particularly useful for delineating geologic structures between boreholes. This technique can help extend information provided by conventional borehole logging which samples rock properties near a borehole. A sophisticated suite of cross-hole seismic surveys was conducted at Raymond and is described below.

11.1 Cross-Borehole Seismic Tomography at Raymond

11.1.1 Methodology

A series of cross-borehole seismic surveys were conducted at the Raymond Field Site. These were performed in order to deduce the geometry of fractures and fracture zones within the well field. The method of cross-borehole tomography is described in Nolet, 1987, for example. In general, it consists of equipping a borehole with a seismic source such as a piezoelectric source transducer, and an adjacent borehole with a string of hydrophones. A voltage is applied to the transducer, which creates a pressure pulse in the rock that is recorded by the hydrophones. Measurements are recorded as often as several hundred thousand times per second by a computerized data acquisition system at land surface. After the transducer is pulsed at a particular depth and measurements are obtained, it is lowered and pulsed again. This procedure is repeated along the depth of the borehole. Figure # schematically shows the seismic ray paths measured for a typical cross-hole experiment. The seismic data from each receiver during each depth transmission is analyzed to determine the travel time and amplitude of each received

seismic pulse. A matrix that incorporates the positions of each ray path and its respective travel time and/or amplitude is inverted and the velocity and/or seismic attenuation of different elements of a 2-D grid representing the plane between boreholes is determined.

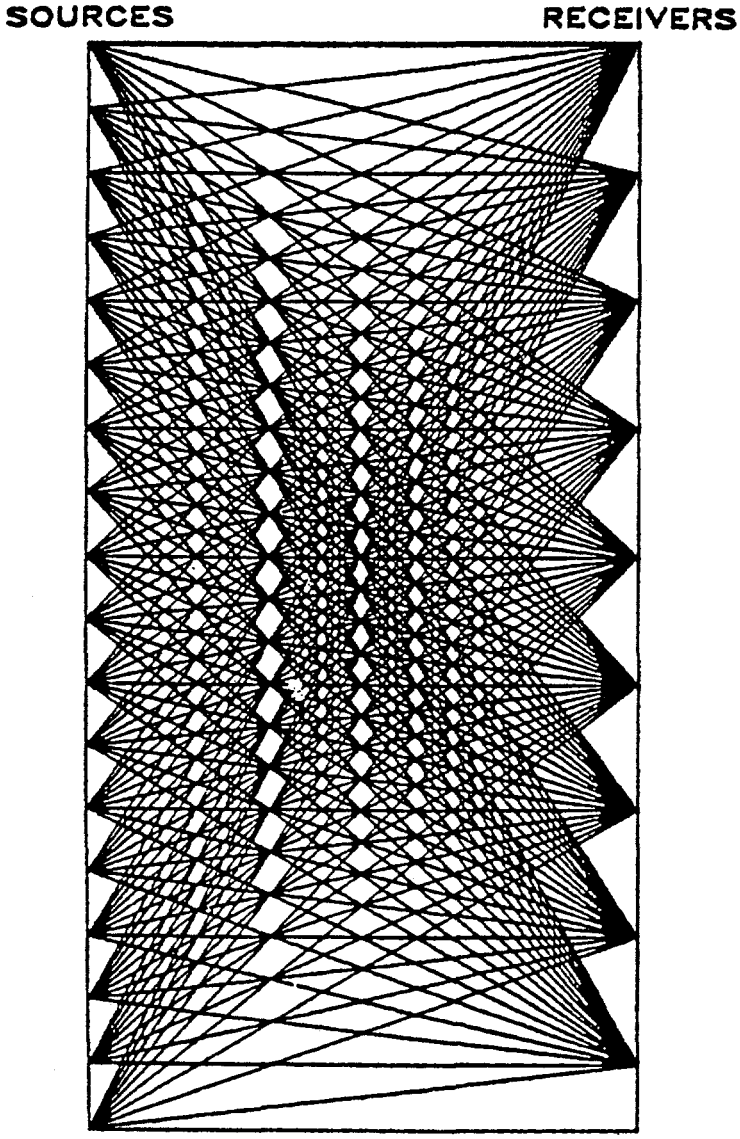

Figure 11.1. Seismic ray paths for a typical cross-borehole experiment (from Peterson, 1986).

For the Raymond experiment the receiver string consisted of 8 hydrophones with spacings of 1 meter. The sources and receivers were spaced at 0.5 meter intervals down their respective wells. This was achieved in the receiver well by moving the receiver string at a 0.5 meter interval to fill in the gap between hydrophones before lowering the string another 8 meters. This geometry produced between 10,000 and 15,000 source

receiver pairs for each cross-hole experiment. Surveys were performed between 9 separate well pairs: SW3-SW2, SW2-00, 00-SE2, SE2-SE3, SW1-SE1, SW2-SE1, SE2-SW1, SW2-SE2, and SW3-SE3. The data analysis and inversion methods used for the Raymond Field Site experiment employed a variety of new techniques. These are described by Vasco et al. (1995) and Peterson (1986). Tomograms of seismic velocity, attenuation, and anisotropy were produced. Only the velocity tomograms are discussed here. Different tomograms are presented by Vasco et al., 1995.

11.1.2 Results and Conclusion

Seismic velocity tomograms were constructed for adjacent well pairs. Figure 11.2 shows the concatenated tomograms of well pairs SW3-SW2, SW2-00, 00-SE2, and SE2-SE3. The results support our other conclusions regarding the general dual-layer, westwardly dipping fracture zones that comprise the general conceptual model of the subsurface. The detection of the low velocity zones is consistent with the fact that they are comprised of hydrologically altered and closely spaced fracture zones as determined from the conventional geophysical logs and television logs.

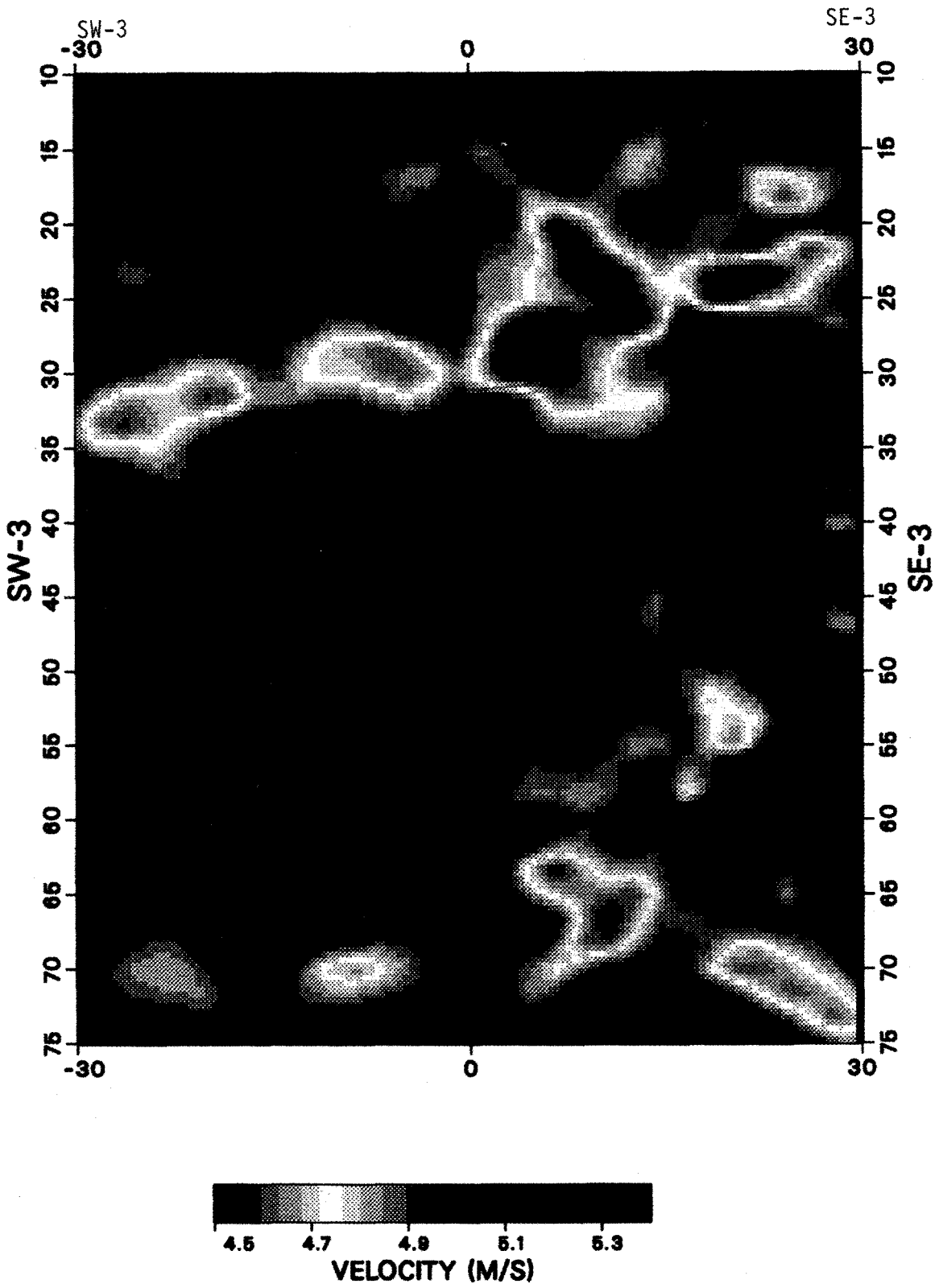

Figure 11.2. Tomogram of seismic velocity between wells SW-3 and SE-3.

12 COMPUTER VISUALIZATION

Computer visualization is a powerful tool that can significantly aid the hydrogeologic characterization process. One very useful feature of some visualization programs is their ability to represent spatially distributed data in a true three-dimensional perspective, and which allow real-time manipulation of the viewing perspective. For example, boreholes and their associated data can be viewed and the entire spatial field can be rotated, exaggerated, etc. This enables detection of 3-dimensional geologic structures which would otherwise not be observable on conventional 2-D plots. Visualization software was used for the Raymond Field Site characterization in an iterative manner to further understanding of the three-dimensional structure of transmissive fractures. Some of the benefits of computer visualization are illustrated below.

12.1 Application to the Raymond Site Characterization

The visualization software Advanced Visualization System (AVS) was used for the Raymond Field Site work. This software possesses the features described above.

Borehole deviation logs were used in conjunction with surface mapping to determine the x,y,z coordinates of the well field. The top of casing of well 0-0 was used as the coordinate 0,0,0, and all other points were referenced to this datum. The coordinates of the tops of the other boreholes were determined from surface mapping, and the coordinates of the points along each borehole with depth were calculated using borehole deviation data relative to the x,y,z coordinate of the top of each well. Secondly, a topographic map of the region around the well field was digitized and transformed into x,y,z coordinates. The coordinates of the well field and topographic surface formed the initial 3-D model upon which to superimpose other features.

One very useful feature of the model was in deducing subsurface fracture connectivity and structure. For example, a transmissive fracture identified by the various geophysical logs and borehole imaging tools in one well was represented as plane and superimposed onto the 3-D well field. The points at which this fracture would hypothetically intersect wells was easily seen. Integrating these images with all geophysical logs allowed us to easily determine if the fracture extended between wells. Figure 12.1 shows the 3-D perspective view of the boreholes. The true 3-D perspective realized when using such software is lost in the 2-D figures shown below. In addition,

the resolution is greatly reduced and color lost. A planar disk representing a known transmissive and subvertical fracture is centered at approximately 210 feet in well SW-1, and is extended outward to intersect other wells. The disk orientation and dip was determined from ATV measurements (Section 8.1). Using this image, the geophysical logs of neighboring wells were checked, and we found that indeed a fracture with the same physical characteristics was present in well 0-0 at the depth observed on the 3-D image (depth markers on the individual wells can not be seen on the image shown). Different orientations were tested to account for fracture measurement error and the possibility that the fracture is not planar. The 3-D structure of the site subsurface was deduced using this iterative method. The complete 3-D image includes the two continuous subhorizontal fracture zones, as well as several discrete fractures that intersect one another and the subhorizontal zones.

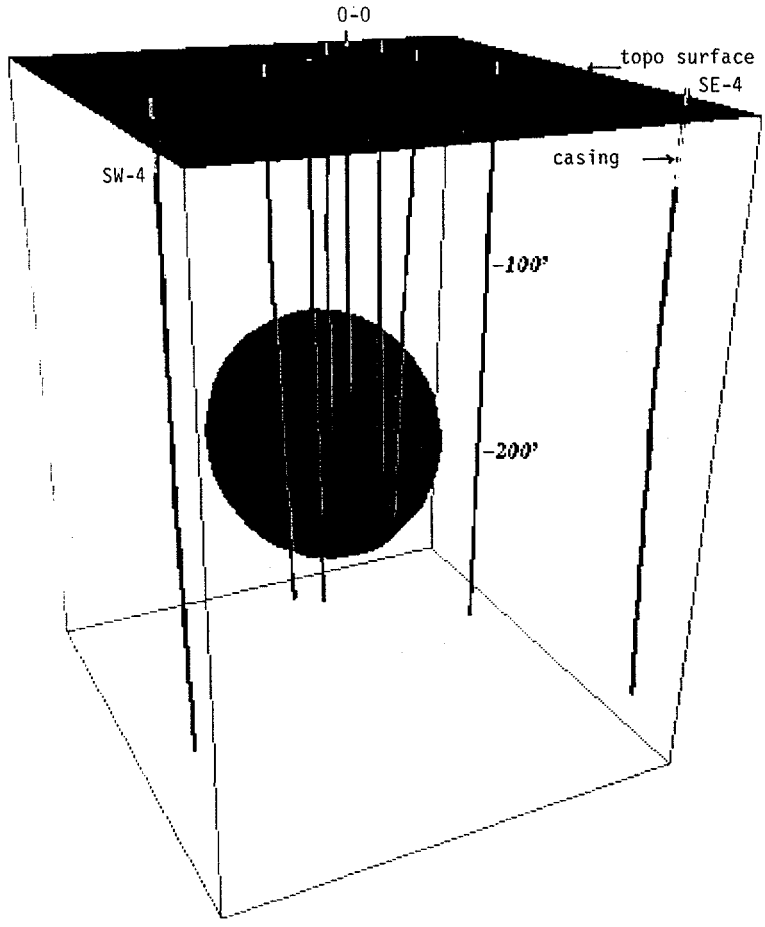

Figure 12.1. Three-dimensional perspective of well field and intersection of southwardly-dipping circular fracture plane through wells.

Figure 12.2 shows a perspective view of the surface topography around the well field (transparent green). The rectangular box beneath the surface at the center of the image is well field shown in the previous figure. The same disk representing the subvertical fracture at 210 feet in well SW-1 has been enlarged in order to see where that fracture might be expressed at the surface. Performing such hypothesis testing and interpolation routines would be exceedingly difficult without the use of visualization software. The possibilities computer visualization can offer certainly extend beyond what has been shown here.

12.2 Conclusions

Computer visualization software is now an affordable reality, and it allows one to deduce complexities not possible from traditional 2-D plots of borehole data. Use of visualization software should be a commonplace tool for subsurface characterization.

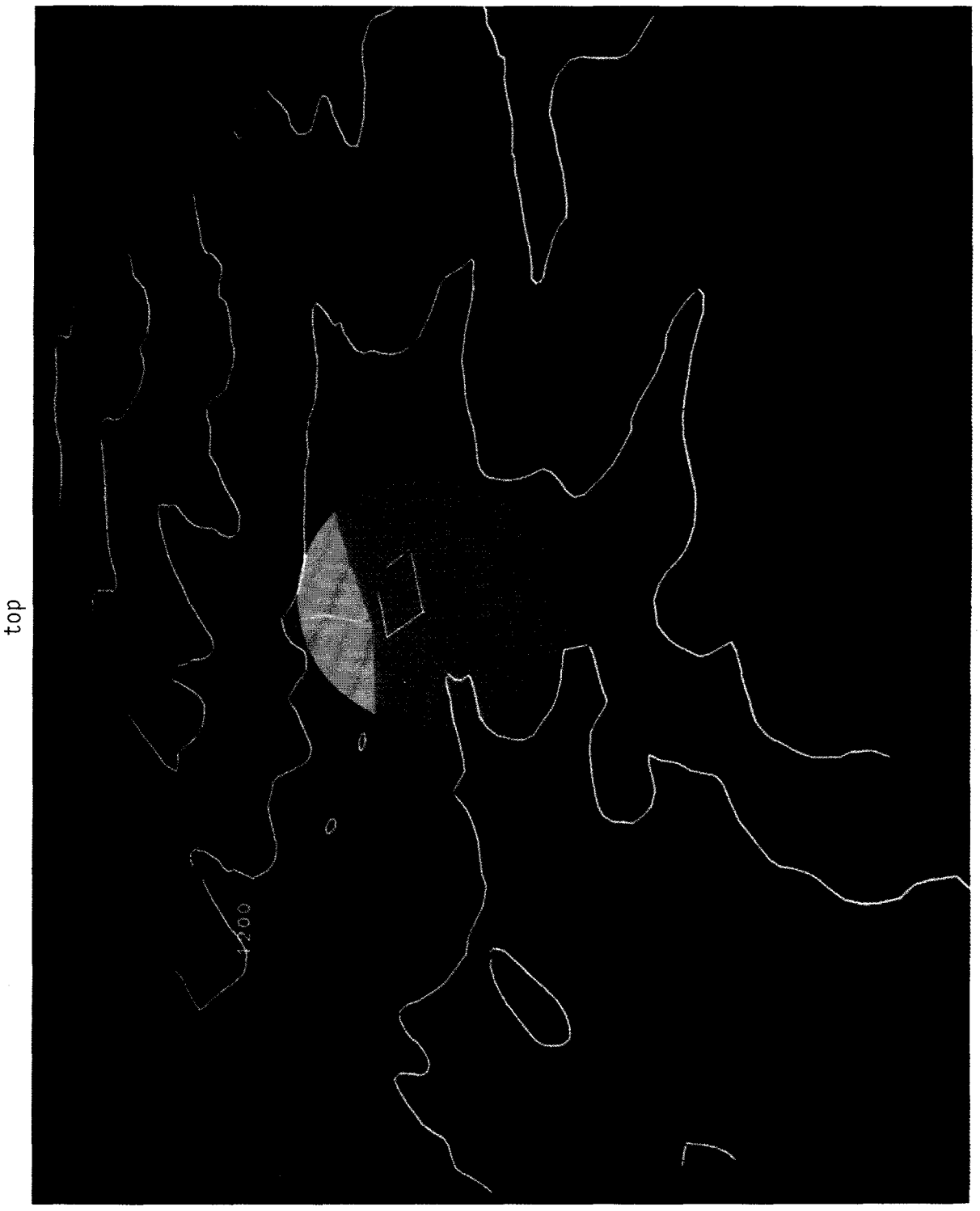

Figure 12.2. Perspective view of surface topography around the Raymond Field Site. Subvertical fracture at 210 feet in well SW-1 is represented as disk and extrapolated through surface .

13 A GENERAL STRATEGY FOR HYDROGEOLOGIC CHARACTERIZATION OF FRACTURED FORMATIONS

Hydrogeologic characterization of every aquifer is difficult, but the extreme heterogeneity of fractured aquifers presents an even greater challenge. Within these formations there are typically many subsurface fractures present on the site scale. However, only a small subset of these fractures dominates the overall flow behavior. Given the degree of complexity, our aim is to discriminate which features largely control subsurface flow, and to develop some quantitative understanding of those features.

Hydrologic and geophysical measurements are influenced by a myriad of subtleties, and determination of flow parameters requires the use of analytical solutions. These solutions describe the behavior of idealized formations. Understanding both the factors that influence measurements and the assumptions inherent in analytic solutions is an absolute necessity. Without this understanding, the formulated site conceptual model and calculated flow parameters may not represent the true characteristics of the system. This is a crucial point which has been highlighted in this report. Failure to recognize this fact translates directly to lost money, effort, and time.

A successful characterization requires that we use a stepwise approach and thoughtfully integrate geologic, geophysical, and hydrologic data. This is no more than recommending that a scientific approach be taken. The tools and methods required for integrated hydrogeologic characterization of saturated, fractured rock formations, along with an illustration of this approach at the Raymond Field Site, have been described in this report.

The flow chart below describes our recommended general procedure for characterization of saturated, fractured crystalline rock formations. The details of each component are described in the chapter or chapter section indicated in brackets. There are certainly other additional techniques or combinations of techniques that can be used in a characterization effort, some of which we have described in this report. Regardless, the goal is to maximize the information and understanding gained at each step and minimize overall cost.

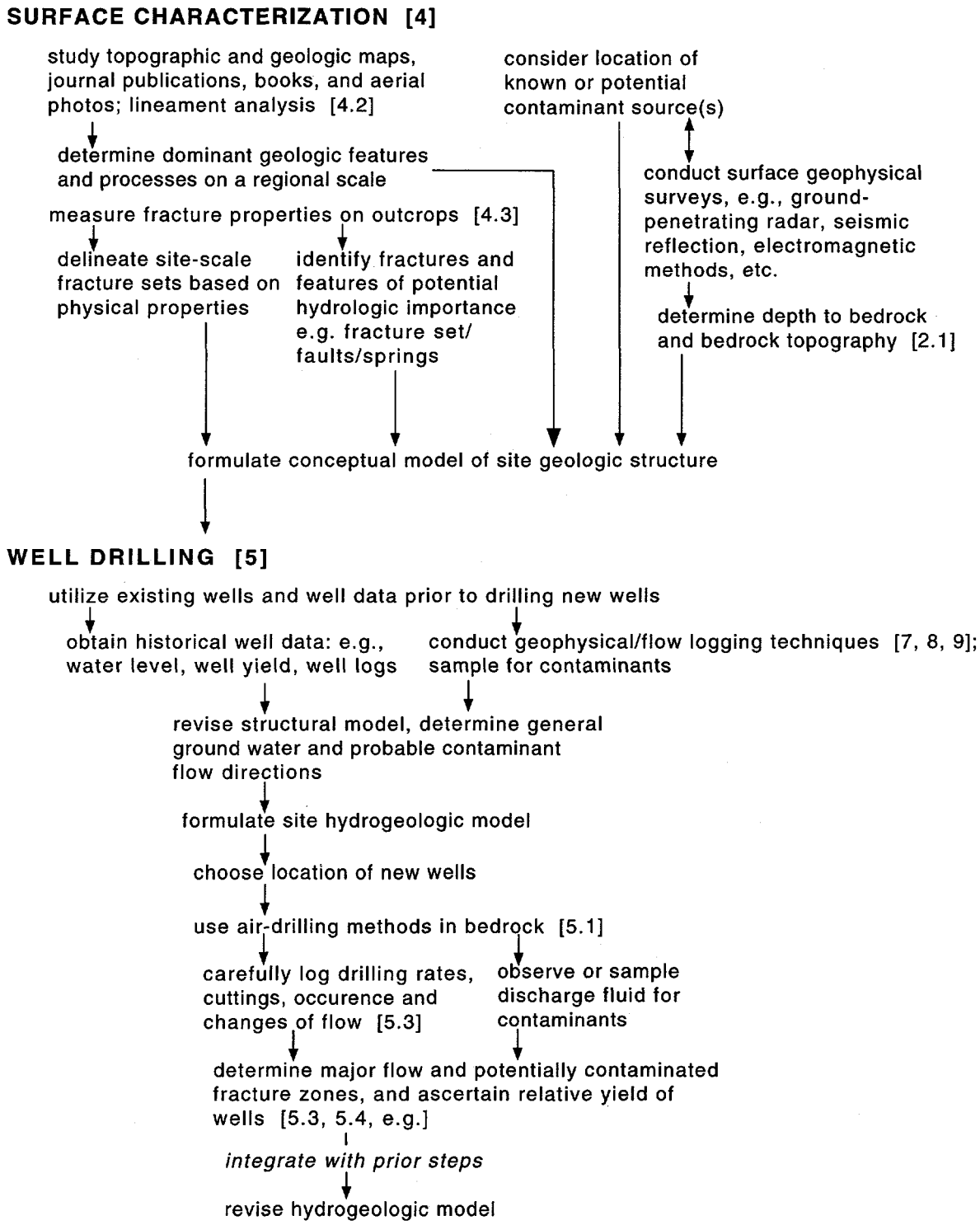

Figure 13.1. Flow chart showing stepwise and integrated characterization procedure.

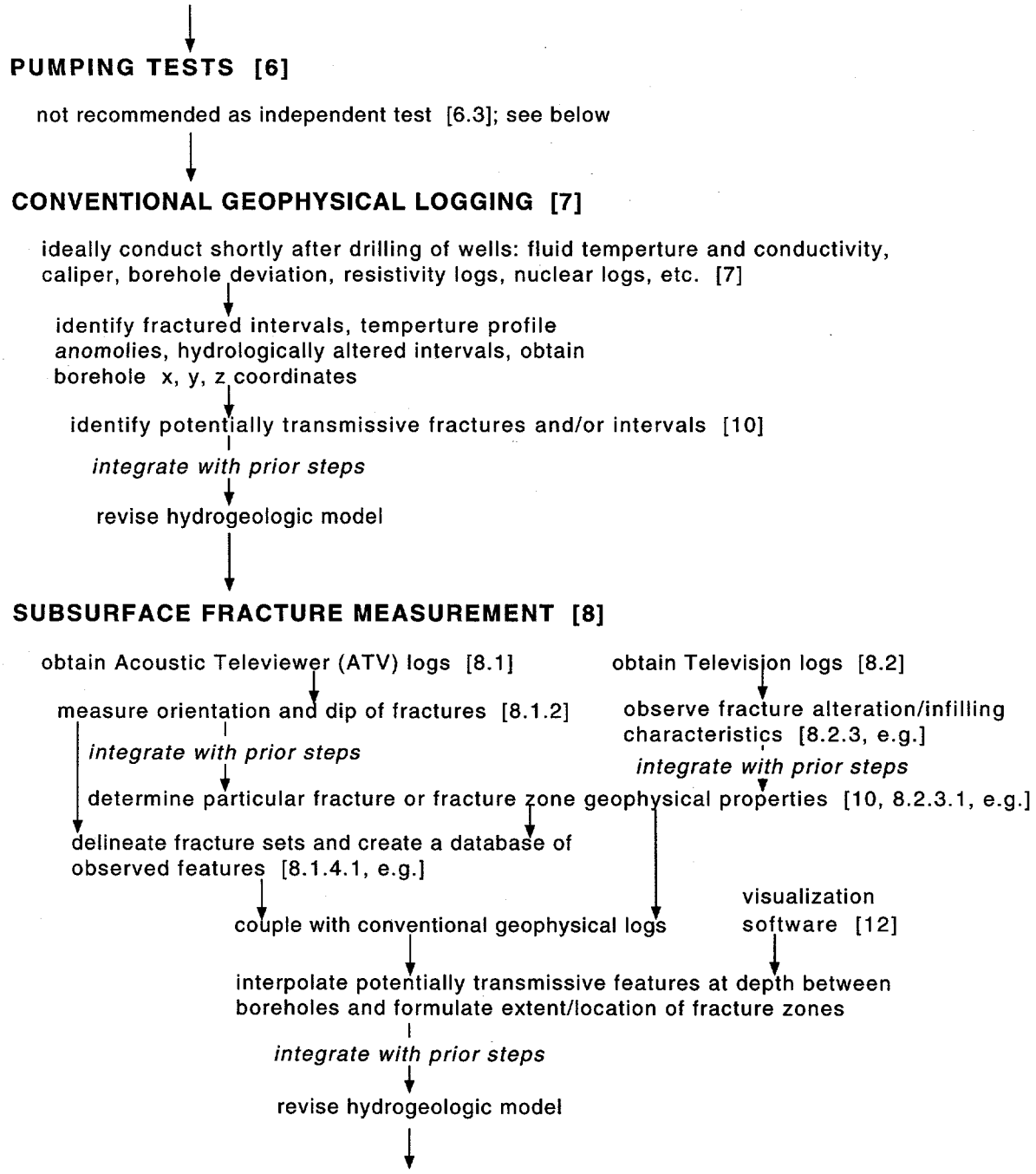

Figure 13.1 continued.

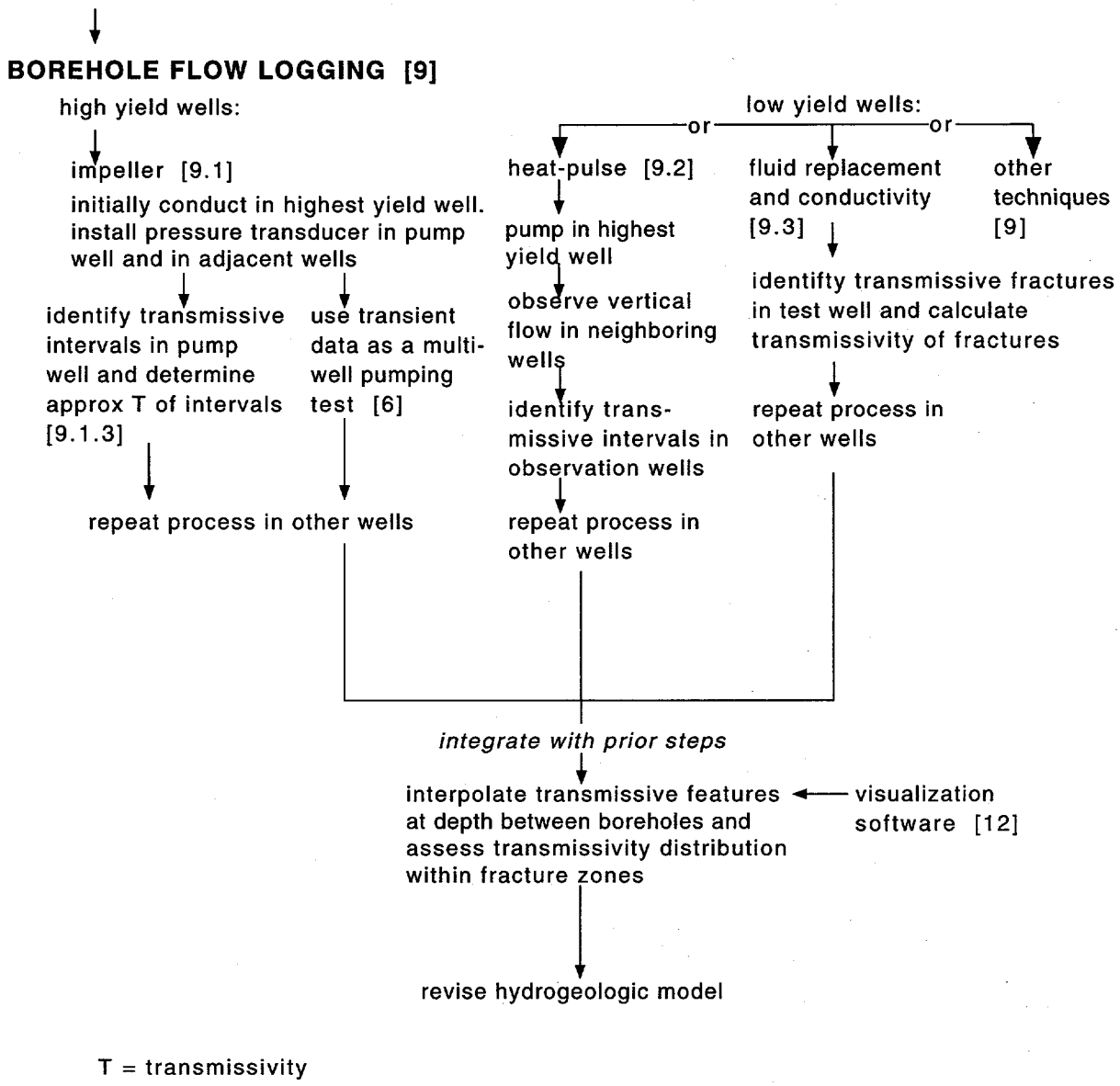

Figure 13.1 continued.

References

Barker, J. A., 1988. A generalized radial flow model for hydraulic tests in fractured rock, *Water Resources Research*, 24(10), 1796-1804.

Barton, C., 1988. Development of in-situ stress measurement techniques for deep drillholes, Ph.D. Thesis, Stanford University.

Barton, C. C., and E. Larsen, 1985. Fractal geometry of two-dimensional fracture networks at Yucca Mountain, southwest Nevada, in: O. Stephannson (Editor), *Fundamentals of rock joints: Proceedings of the International Symposium on Fundamentals of Rock Joints*, Bjorkliden, Sweden, pp. 77-84.

Barton, N. R., and V. Choubey, 1977. The shear strength of rock joints in theory and practice, *Rock Mechanics*, 10, 1-54.

Bateman, P. C., A. J. Busacca, D. E. Marchand, and W. N. Sawka, 1982. *Geologic map of the Raymond quadrangle, Madera and Mariposa counties, California, Map GQ-1555*. United States Geological Survey.

Bateman, P. C., and W. N. Sawka, 1981. Raymond quadrangle, Madera and Mariposa counties, California-analytic data, U. S. Geological Survey Professional Paper #1214, U. S. Geological Survey, Washington, D. C.

Billings, M. P., 1972. *Structural Geology*, Prentice-Hall, Inc., Englewood Cliffs, New Jersey, 606 pp.

Bourdet, D. P., and A. C. Gringarten, 1980. *Determination of fissured volume and block size in fractured reservoirs by type-curve analysis*, in SPE 55th Annual Technical Conference and Exhibition, Dallas, TX.

Buckley, B. K., R. J. DeLuca, and P. J. McGlew, 1985. *Hazardous waste investigations in fractured bedrock: a case study*, in The second annual eastern regional ground water conference, Portland, Maine, pp. 416-425.

Butler, J. J., Jr., and W. Liu, 1993. Pumping tests in nonuniform aquifers: the radially asymmetric case, *Water Resources Research*, 29(2), 259-269.

Carlsson, A., and T. Olsson, 1981. *Hydraulic properties of a fractured granitic rock mass at Forsmark, Sweden*, Paris, 228 pp.

Chernyshev, S. N., and W. R. Dearman, 1991. *Rock Fractures*, Butterworth-Heinemann, London, 272 pp.

Cohen, A. J. B., 1993. Hydrogeologic characterization of a fractured granitic rock aquifer, Raymond, California, M.Sc. Thesis, University of California, Lawrence Berkeley Laboratory, LBL-34838, Berkeley, 97 pp.

Committee on Ground Water Cleanup Alternatives, 1994. *Alternatives for Ground Water Cleanup*, National Academy Press, Washington, D.C., 315 pp.

Cook, P., 1995. Analysis of Hydraulic Connectivity in Fractured Granite, M.Sc. Thesis, University of California, Lawrence Berkeley National Laboratory report in press, Berkeley, 70 pp.

Crowder, R., F. Paillet, and A. Hess, 1994. *High resolution flowmeter logging - a unique combination of borehole geophysics and hydraulics: part I - flowmeter techniques and equipment development*, in Symposium on the Application of Geophysics to Engineering and Environmental Problems. Environmental and Engineering Geophysical Society, Englewood, CO, Boston, Mass, pp. 361-380.

Davison, C. C., W. S. Keys, and F. L. Paillet, 1982. Use of borehole-geophysical logs and hydrologic tests to characterize crystalline rock for nuclear-waste storage, Whiteshell Nuclear Research Establishment, Manitoba, and Chalk River Nuclear Laboratory, Ontario, Canada, ONWI-418, U. S. Department of Commerce, Springfield, VA.

Di Nitto, R. G., W. R. Norman, and M. M. Hanley, 1982. *An approach to investigating groundwater contaminant movement in bedrock aquifers: case histories*, in National Conference on Management of Uncontrolled Hazardous Waste Sites. Hazardous Materials Control Research Institute, Washington, D. C., pp. 111-117.

Dott, R. H., Jr., and R. L. Batten, 1988. *Evolution of the Earth*, McGraw-Hill, Inc., New York, 643 pp.

Earlougher, R. C. J., 1977. *Advances in well test analysis*, Society of Petroleum Engineers of AIME, Dallas, TX, 264 pp.

EPA, 1989. Evaluation of ground-water extraction remedies, Volume 3: general site data base reports, EPA/540/2-89/054, U. S. Environmental Protection Agency, Washington, D.C.

Fortin, R. L., 1988. *Control and remediation of volatile organic chemical migration in fractured bedrock*, in HWHM 88: Hazardous wastes and hazardous materials, 5th national conference, Las Vegas, Nevada, pp. 29-33.

Freifeld, B., K. Karasaki, R. Solbau, and A. Cohen, 1995. *Reactive Transport Studies at the Raymond Field Site*, in Proceedings of the Sixth Annual International Conference on High Level Radioactive Waste Management, Las Vegas, Nevada, pp. 91-93.

Gale, J. E., 1982. Assessing the permeability characteristics of fractured rock, in: T.N. Narasimhan (Editor), *Geologic Society of America, Special paper 189*, pp. 163-181.

Grossenbacher, K. A., K. Karasaki, and D. Bahat, 1995. *Characterizing fracture networks at curved surfaces and irregularly shaped outcrops*, in AGU Fall Meeting, San Francisco, CA.

Hale, F. V., and C. F. Tsang, 1988. A code to compute borehole fluid conductivity profiles with multiple feed points, LBL-24928, Lawrence Berkeley Laboratory, Berkeley, CA.

Hantush, M. S., 1966. Analysis of data from pumping tests in anisotropic aquifer, *Journal of Geophysical Research*, 71(2), 421-426.

Hantush, M. S., and R. G. Thomas, 1966. A method for analyzing a drawdown test in anisotropic aquifers, *Water Resources Research*, 2(2), 281-285.

Hess, A. E., 1986. Identifying hydraulically conductive fractures with a slow-velocity borehole flowmeter, *Canadian Geotechnical Journal*, 23(1), 69-78.

Hess, A. E., and F. L. Paillet, 1990. *Applications of the thermal-pulse flowmeter in the hydraulic characterization of fractured rocks*, in American Society for Testing and Materials, pp. 99-112.

Hsieh, P. A. et al., 1993. Methods of characterizing fluid movement and chemical transport in fractured rock, in: J.T. Chaney and J.C. Hepburn (Editors), *Field Trip Guidebook for Northeastern United States*, Geological Society of America, Annual Meeting, October 25-28. Geological Society of America, Boston, Massachusetts.

Huber, N. K., 1987. The geologic story of Yosemite National Park, U. S. Geological Survey Bulletin 1595, 64 pp.

Jones, J. W., E. S. Simpson, S. P. Neuman, and W. S. Keys, 1986. Field and theoretical investigations of fractured crystalline rock near Oracle, Arizona, NUREG/CR-3736, Division of Radiation Programs and Earth Sciences, Office of Nuclear Regulatory Research, U. S. Nuclear Regulatory Commission, Washington, D.C.

Karasaki, K., 1987. Well test analysis in fractured media, Ph.D. Thesis, University of California, Berkeley, CA, 239 pp.

Karasaki, K., B. Freifeld, and C. Davison, 1994. *A characterization study of fractured rock*, in Proceedings of the Fifth Annual International Conference on High Level Radioactive Waste Management, Las Vegas, Nevada.

Katz, A. R., 1993. Cameras shed light on down-hole troubles, *Ground Water Age*, 28(2).

Keely, J. F., 1989. Performance evaluations of pump-and-treat remediations, EPA/540/4-89/005, U. S. Environmental Protection Agency, Washington, D. C.

Kerfoot, W. B., 1986. *Monitoring well construction, and recommended procedures for direct ground-water measurements using a heat-pulse flowmeter*, in Symposium on Field Methods for Ground-Water Contamination Studies and Their Standardization. American Society for Testing and Materials, Philadelphia, PA, pp. 146-161.

Keys, W. S., 1990. Borehole geophysics applied to ground-water investigations, *Techniques of Water-Resources Investigations of the United States Geological Survey*. U. S. Geologic Survey, Denver, CO, pp. bk 2, chp. E2.

Kruseman, G. P., and N. A. de Ridder, 1990. *Analysis and evaluation of pumping test data*, International Institute for Land Reclamation and Improvement, Wageningen, The Netherlands, 367 pp.

Lattman, D. H., and R. H. Matzke, 1961. Geological significance of fracture traces, *Photogrammetric Engineering*, 27, 435-438.

Lockwood, J. P., and J. G. Moore, 1979. Regional deformation of the Sierra Nevada, California, on conjugate microfault sets, *Journal of Geophysical Research*, 84(B11), 6041-6049.

Long, J. C. S., J. S. Remer, C. R. Wilson, and P. A. Witherspoon, 1982. Porous media equivalents for networks of discontinuous fractures, *Water Resources Research*, 18(3), 645-658.

Mackay, D. M., and J. A. Cherry, 1989. Groundwater contamination: Pump-and-treat remediation, *Environmental Science and Technology*, 23(6), 630-636.

Marsily, G., de, 1986. *Quantitative Hydrogeology*, Academic Press, Inc., San Diego, California, 440 pp.

Martel, R., 1988. Groundwater contamination by organic compounds in Ville Mercier: new developments, Report to the NATO/CCMS pilot study of remedial action and technologies for contaminated land and groundwater, Bilthoven, The Netherlands.

Martel, S. J., D. D. Pollard, and P. Segall, 1988. Development of simple strike-slip fault zones, Mount Abbot quadrangle, Sierra Nevada, California, *Geological Society of America Bulletin*, 100, 1451-1465.

Matthews, C. S., and D. G. Russell, 1967. *Pressure Buildup and Flow Tests in Wells*, Society of Petroleum Engineers of AIME, Dallas, TX, 167 pp.

McGlew, P. J., and J. E. Thomas, Jr., 1984. *Determining contaminant migration pathways in fractured bedrock*, in The 5th National Conference on Management of Uncontrolled Hazardous Waste Sites. Hazardous Materials Control Research Institute, Washington, D. C., pp. 150-157.

Molz, F. J., and S. C. Young, 1993. Development and application of borehole flowmeters for environmental assessment, *The Log Analyst*, 1-11.

Nolet, G. (Editor), 1987. Seismic Tomography, with applications in global seismology and exploration geophysics. R. Reidel Publishing Company, Holland, 386 pp.

Norris, R. M., and R. W. Webb, 1976. *Geology of California*, John Wiley & Sons, New York, 365 pp.

Novakowski, K. S., 1990. Analysis of aquifer tests conducted in fractured rock: a review of the physical background and design of a computer program for generating type curves, *Ground Water*, 28(1), 99-107.

Paillet, F., R. Crowder, and A. Hess, 1994. *High resolution flowmeter logging - a unique combination of borehole geophysics and hydraulics: part II - borehole applications with the heat-pulse flowmeter*, in Symposium on the Application of Geophysics to Engineering and Environmental Problems (SAGEEP '94). Environmental and Engineering Geophysical Society, Englewood, CO, Boston, Mass, pp. 381-404.

Paillet, F., and R. Duncanson, 1994. Comparison of drilling reports and detailed geophysical analysis of ground-water production in bedrock wells, *Ground Water*, 32(2), 200-206.

Paillet, F. L., 1991. Use of geophysical well logs in evaluating crystalline rocks for siting of radioactive-waste repositories, *The Log Analyst*(March-April), 85-107.

Paillet, F. L., A. E. Hess, C. H. Cheng, and E. Hardin, 1987. Characterization of fracture permeability with high-resolution vertical flow measurements during borehole pumping, *Ground Water*, 25(1), 28-40.

Paillet, F. L., W. S. Keys, and A. E. Hess, 1985. *Effects of lithology on televiewer-log quality and fracture interpretation*, in Society of Professional Well Log Analysts 26th Annual Logging Symposium. Society of Professional Well Log Analysts, Dallas, TX, pp. JJJ1-JJJ31.

Papadapulos, I. S., and H. H. Cooper, Jr, 1967. Drawdown in a well of large diameter, *Water Resources Research*, 3(1), 241-244.

Papadopulos, I. S., 1965. *Nonsteady flow to a well in an infinite anisotropic aquifer*, in Intern. Assoc. Sci. Hydrol., Dubrovnik Symposium on the Hydrology of fractured rocks, pp. 21-31.

Pedler, W. H., M. J. Barvenik, C. F. Tsang, and F. V. Hale, 1990. *Determination of bedrock hydraulic conductivity and hydrochemistry using a wellbore fluid logging method*, in National Well Water Association's Outdoor Action Conference, Las Vegas, NV.

Peterson, J. E., 1986. The application of algebraic reconstruction techniques to geophysical problems, Ph.D. Thesis, University of California, Lawrence Berkeley Laboratory, LBL-21498, 188 pp.

Priest, S. D., 1993. *Discontinuity analysis for rock engineering*, St Edmundsbury Press Ltd, Great Britain, 473 pp.

Priest, S. D., and J. A. Hudson, 1976. Discontinuity Spacing in Rock, *International Journal of Rock Mechanics and Mining Science and Geomechanics Abstracts*, 13, 135-148.

Rehfeldt, K. R., P. Hufschmied, L. W. Gelhar, and M. E. Schaefer, 1989. Measuring hydraulic conductivity with the borehole flowmeter, EN-6511, Electric Power Research Institute, Palo Alto, California.

Segall, P., and D. D. Pollard, 1983a. Joint formation in granitic rock of the Sierra Nevada, *Geological Society of America Bulletin*, 94, 563-575.

Segall, P., and D. D. Pollard, 1983b. Nucleation and growth of strike slip faults in granite, *Journal of Geophysical Research*, 88, 555-568.

Streltsova, T. D., and R. M. McKinley, 1984. Effect of flow time duration on buildup pattern for reservoirs with heterogeneous properties, *Society of Petroleum Engineers Journal*, 24(3), 294-306.

Thapa, B. B., 1994. Analysis of in-situ rock joint strength using digital borehole scanner images, Ph.D. Thesis, University of California, Berkeley, 152 pp.

Tsang, C. F., P. Hufschmied, and F. V. Hale, 1990. Determination of fracture inflow parameters with a borehole fluid conductivity logging method, *Water Resources Research*, 26(4), 561-578.

Tsang, C. F., Y. W. Tsang, and F. V. Hale, 1991. Tracer transport in fractures - analysis of field data based on variable-aperture channel model, *Water Resources Research*, 27(12), 3095-3106.

Vasco, D. W., J. E. Peterson, and E. L. Major, 1995. A simultaneous inversion of seismic traveltimes and amplitudes for velocity and attenuation, *Geophysics*, in press.

Warren, J. F., and P. J. Root, 1963. The behavior of naturally fractured reservoirs, *Society of Petroleum Engineers Journal, AIME*, 228, 245-255.

Williams, J. H., and R. W. Conger, 1990. Preliminary delineation of contaminated water-bearing fractures intersected by open-hole bedrock wells, *Ground Water Monitoring Review*, 10(4), 118-126.

Zemanek, J., R. L. Caldwell, E. E. Glenn, Jr., S. V. Holcomb, L. J. Norton, and A. J. D. Straus, 1969. The borehole televiewer - a new logging concept for fracture location and other types of borehole inspection, *Journal of Petroleum Technology*, 21(6), 762-774.